859

TECHNICAL NOTES

NATIONAL ADVISORY COMMITTEE FOR AERONAUTICS

No. 859

ON THE DISTRIBUTION OF STRESS IN A THIN PLATE ELASTICALLY SUPPORTED ALONG TWO EDGES AT LOADS BEYOND THE STABILITY LIMIT

By Louis G. Dunn
California Institute of Technology

Washington
October 1942

NATIONAL ADVISORY COMMITTEE FOR AERONAUTICS

TECHNICAL NOTE NO. 859

ON THE DISTRIBUTION OF STRESS IN A THIN PLATE ELASTICALLY SUPPORTED ALONG TWO EDGES AT LOADS BEYOND THE STABILITY LIMIT

By Louis G. Dunn

SUMMARY

This report presents the results of an investigation on the distribution of stress in a plate elastically supported along two edges and subjected to compressive loads in a direction parallel to the elastically supported edges.

In section I methods are developed for calculating:

1. The compression stresses at the median surface in directions parallel and perpendicular to the applied load.

2. Bending stresses

3. Combined bending and compression stresses

4. The effective width of sheet acting with each stringer

Section II presents the results of a limited number of tests on:

1. The wave form of the buckled plate with increasing stringer stress

2. Compression tests on 24S-T dural sheet and 24S-T alclad sheet

A comparison between the assumed wave form and the experimentally determined wave forms given in reference 4 is indicated in section I. The calculated strains have been compared with the measured strains of reference 4. The discrepancies between theory and experiment are discussed in sections I and II.

INTRODUCTION

A considerable amount of theoretical and experimental work has been done on the stress distribution in thin plates at loads beyond the stability limit, as is evidenced by the references included at the end of this report. The two important factors which enter into the theoretical calculations are the amplitude and the wave form of the buckled plate as a function of the ratio of the edge stress to the buckling stress. Several approximate expressions for the amplitude have been derived. (See references 1, 2, and 5.) Calculations of the exact wave form after buckling are extremely complicated even for simple cases; for example, a circular plate with a simply supported edge and subjected to a uniform compression load in the plane of the plate (reference 6). For this reason, in the case of rectangular plates, it is customary to assume that the wave form after buckling remains constant and equal to that at buckling.

The majority of investigators have assumed a wave form which satisfies the boundary conditions of simple support along all four edges. This type of edge support is very seldom realized in airplane construction since the edges parallel to the applied load are usually supported by some form of stiffener; that is, the edges are elastically supported.

For the practical usage of thin plates the distribution of the median fiber stress and the bending stress is of importance. The first is important in the effective width calculations and the latter in the calculations of the maximum stresses for permanent deformations. Since these stresses are functions of the plate curvature, it is desirable to have a reasonably close approximation of the correct wave form. The condition of simple support along the edges requires zero bending moment at the edges; however in the actual case the bending moments along the elastically supported edges are different from zero. Also, the maximum compression stress at the median surface occurs at these edges, so that for the effects of combined bending and compression stresses it is important that the elastic support along the edges be considered.

In the present report a theoretical calculation has been carried out in which the influence of the elastic support has been taken into account. No attempt was made

to calculate the exact wave form after buckling; it was assumed that it remains constant and equal to that at buckling. The deviation of the experimentally obtained wave form from the assumed one is shown in section II to be quite small at relatively high stringer stresses. Since the amplitude also checks the experimental values closely, it seems reasonable to assume that the calculated stresses will be in good agreement with the actual values.

This investigation, conducted at the California Institute of Technology, was sponsored by, and conducted with financial assistance from the National Advisory Committee for Aeronautics.

The author wishes to acknowledge his appreciation for the advice given by Dr. Theodor von Kármán during the preparation of this paper and to thank Dr. Hsue-Shen Tsien for his willing cooperation, and Mr. Alfred Slater for his assistance.

I- THEORETICAL DISCUSSION OF THE PROBLEM

For a plate subjected to a uniform compression load along two edges and elastically supported along the edges parallel to the load (fig. 1b), the influence of the elastic support on the wave form at buckling, and on the buckling stress has been considered in reference 5. For symmetrical elastic supports the wave form at buckling is given by

$$w = [A \cosh \alpha y + B \cos \beta y] \sin \phi x \qquad (1)$$

where:

$$\alpha = \sqrt{\frac{m^2\pi^2}{a^2} + \sqrt{\frac{m^2\pi^2}{a^2}\frac{\sigma_c t}{D}}}$$

$$\beta = \sqrt{-\frac{m^2\pi^2}{a^2} + \sqrt{\frac{m^2\pi^2}{a^2}\frac{\sigma_c t}{D}}}$$

$$\phi = \frac{m\pi}{a}$$

$$D = \frac{Et^3}{12(1-\nu^2)}$$

σ_c buckling stress, pounds per square inch

ν Poisson's ratio

m number of half waves

t plate thickness, inches

a plate length, inches

b plate width, inches

If it is again assumed that the wave form after buckling remains the same as at buckling, the distribution of compression and bending stresses can be calculated. Since the boundary conditions at the edges are given in terms of displacement of the median surface of the plate, it is convenient to deal with displacements rather than stress. For the plate the following assumptions are made:

(a) The plate under consideration is one of the panels of a continuous plate attached to stiffening elements of equal flexural and torsional rigidity, spaced a distance b apart. (See figure 1a.)

(b) The length of the plate is large in comparison to its width b, so that its behavior is not influenced by length.

Then the boundary conditions along the elastically supported edges are:

$$u + \epsilon_{st}\, x = 0 \quad \text{at } y = \pm\frac{b}{2} \tag{2}$$

$$v = 0 \quad \text{at } y = \pm\frac{b}{2} \tag{3}$$

$$w = 0 \quad \text{at } y = \pm\frac{b}{2} \tag{4}$$

and in the x direction

$$w = 0 \quad \text{at} \quad x = \frac{a}{m} \tag{5}$$

$$u = -\epsilon_{st}\frac{a}{m} \quad \text{at} \quad x = \frac{a}{m} \tag{5'}$$

where u and v are the displacements of the median plane of the plate, in directions parallel and normal to the load respectively, and ϵ_{st} is the compressive strain in the stiffeners. In applying expressions (1) through (5') to describe the deformations of the buckled plate, the

conditions of zero curvature and constant displacement at the nodal points $x = a/m$ of the buckle are satisfied. The conditions along the edge $y = b/2$ depend upon the torsional and flexural rigidity of the stiffening element as well as the method of attachment. The influence of the torsional rigidity is taken into account to some extent by the assumed wave form. Since the plate under consideration is a panel from a continuous plate, the v component is zero at the edges $y = \pm b/2$ by virtue of the continuity of the plate in the y direction. This condition is probably closely realized in actual structures such as wings where the sheet is continuous around the wing, or where the sheet is riveted to heavy fore and aft spars.

General expressions for the displacements u and v can be determined from the equations of equilibrium

$$\frac{\partial \sigma_x}{\partial x} + \frac{\partial \tau_{xy}}{\partial y} = 0$$

$$\frac{\partial \sigma_y}{\partial y} + \frac{\partial \tau_{xy}}{\partial x} = 0 \tag{6}$$

and of strain

$$\epsilon_x = \frac{\partial u}{\partial x} + \frac{1}{2}\left(\frac{\partial w}{\partial x}\right)^2 = \frac{1}{E}\left(\sigma_x - \nu\sigma_y\right)$$

$$\epsilon_y = \frac{\partial v}{\partial y} + \frac{1}{2}\left(\frac{\partial w}{\partial y}\right)^2 = \frac{1}{E}\left(\sigma_y - \nu\sigma_x\right)$$

$$\gamma_{xy} = \frac{\partial u}{\partial y} + \frac{\partial v}{\partial x} + \frac{\partial w}{\partial x}\frac{\partial w}{\partial y} = \frac{2(1 + \nu)}{E}\tau_{xy} \tag{7}$$

By substituting the relations of equations (7) into equations (6) the following two equations connecting u, v and w are obtained:

$$\frac{\partial^2 u}{\partial x^2} + \frac{\partial^2 u}{\partial y^2} + \frac{1 + \nu}{1 - \nu}\frac{\partial}{\partial x}\left(\frac{\partial u}{\partial x} + \frac{\partial v}{\partial y}\right) + \frac{1}{1 - \nu}\frac{\partial}{\partial x}\left[\left(\frac{\partial w}{\partial x}\right)^2 + \left(\frac{\partial w}{\partial y}\right)^2\right] + \frac{\partial w}{\partial x}\frac{\partial^2 w}{\partial y^2} - \frac{\partial w}{\partial y}\frac{\partial^2 w}{\partial x \partial y} = 0 \tag{8}$$

$$\frac{\partial^2 v}{\partial y^2} + \frac{\partial^2 v}{\partial x^2} + \frac{1+\nu}{1-\nu}\frac{\partial}{\partial y}\left(\frac{\partial u}{\partial x} + \frac{\partial v}{\partial y}\right) + \frac{1}{1-\nu}\frac{\partial}{\partial y}\left[\left(\frac{\partial w}{\partial x}\right)^2 + \left(\frac{\partial w}{\partial y}\right)^2\right] + \frac{\partial^2 w}{\partial x^2}\frac{\partial w}{\partial y} - \frac{\partial w}{\partial x}\frac{\partial^2 w}{\partial x \partial y} = 0 \qquad (9)$$

Substituting expression (1) for w, equations (8) and (9) become

$$\frac{\partial^2 u}{\partial x^2} + \frac{\partial^2 u}{\partial y^2} + \frac{1+\nu}{1-\nu}\frac{\partial}{\partial x}\left(\frac{\partial u}{\partial x} + \frac{\partial v}{\partial y}\right) = -\sin 2\phi x(k_1' \cosh 2\alpha y + k_2' \cos 2\beta y + k_3' \sinh \alpha y \sin \beta y + k_4' \cosh \alpha y \cos \beta y + k_5') \qquad (10)$$

$$\frac{\partial^2 v}{\partial y^2} + \frac{\partial^2 v}{\partial x^2} + \frac{1+\nu}{1-\nu}\frac{\partial}{\partial y}\left(\frac{\partial u}{\partial x} + \frac{\partial v}{\partial y}\right) = -\cos 2\phi x[k_1 \sinh 2\alpha y + k_2 \cosh \alpha y \sin \beta y + k_3 \sinh \alpha y \cos \beta y + k_4 \sin 2\beta y] - [k_5 \sinh 2\alpha y + k_6 \cosh \alpha y \sin \beta y + k_7 \sinh \alpha y \cos \beta y + k_8 \sin 2\beta y] \qquad (11)$$

where $k_1' = \frac{\phi A^2}{2(1-\nu)}(\phi^2 + \beta^2)$ $\quad k_2' = \frac{-\phi B^2}{2(1-\nu)}(\phi^2 + \beta^2)$

$k_3' = -AB\alpha\beta\phi\left(\frac{1+\nu}{1-\nu}\right)$ $\quad k_4' = -AB\phi^3\left(\frac{1+\nu}{1-\nu}\right)$ $\quad k_5' = \frac{-\phi[A^2(\phi^2 + \nu\alpha^2) + B^2(\phi^2 - \nu\beta^2)]}{2(1-\nu)}$

$k_1 = \frac{-A^2\alpha}{2(1-\nu)}(\phi^2 + \beta^2)$ $\quad k_2 = \frac{AB\beta}{(1-\nu)}(\phi^2 + \beta^2)$ $\quad k_3 = \frac{AB\alpha}{(1-\nu)}(\phi^2 + \beta^2)$

$k_4 = \frac{-B^2\beta}{2(1-\nu)}(\phi^2 + \beta^2)$ $\quad k_5 = \frac{A^2\alpha}{2(1-\nu)}(\alpha^2 + \nu\phi^2)$ $\quad k_6 = \frac{-AB\beta}{(1-\nu)}(\alpha^2 + \nu\phi^2)$

$k_7 = \frac{-AB\alpha}{(1-\nu)}(\beta^2 - \nu\phi^2)$ $\quad k_8 = \frac{B^2\beta}{2(1-\nu)}(\beta^2 - \nu\phi^2)$

By inspection of equations (10) and (11) it is apparent that the particular integrals can be written with undetermined coefficients in the form:

$$u = \sin 2\phi x[M_1 \cosh 2\alpha y + M_2 \cos 2\beta y + M_3 \sinh \alpha y \sin \beta y + M_4 \cosh \alpha y \cos \beta y + M_5] \quad (12)$$

$$v = \cos 2\phi x[N_1 \sinh 2\alpha y + N_2 \sin 2\beta y + N_3 \cosh \alpha y \sin \beta y + N_4 \sinh \alpha y \cos \beta y] + N_5 \sinh 2\alpha y + N_6 \sin 2\beta y + N_7 \cosh \alpha y \sin \beta y + N_8 \sinh \alpha y \cos \beta y \quad (13)$$

The coefficients M and N are determined by direct substitution in equations (10) and (11), and are as follows:

$$M_1 = \frac{-A^2\phi}{16} \qquad M_2 = \frac{-B^2\phi}{16} \qquad M_3 = \frac{2AB\phi^3\alpha\beta(1+\nu)}{(\alpha^2+\beta^2)^2}$$

$$M_4 = \frac{-2AB\phi^5(1+\nu)}{(\alpha^2+\beta^2)^2} \qquad M_5 = \frac{-A^2(\phi^2+\nu\alpha^2) - B^2(\phi^2-\nu\beta^2)}{16\phi}$$

$$N_1 = \frac{A^2\alpha}{16} \qquad N_2 = \frac{-B^2\beta}{16} \qquad N_3 = \frac{-AB\beta}{(\alpha^2+\beta^2)^2}[4\phi^4 + (\alpha^2+\phi^2)(\beta^2+\nu\phi^2)]$$

$$N_4 = \frac{AB\alpha}{(\alpha^2+\beta^2)^2}[4\phi^4 + (\beta^2-\phi^2)(\alpha^2-\nu\phi^2)] \qquad N_5 = \frac{-A^2(\alpha^2+\nu\phi^2)}{16\alpha}$$

$$N_6 = \frac{-B^2(\nu\phi^2-\beta^2)}{16\beta} \qquad N_7 = \frac{-AB\beta(\nu\phi^2-\alpha^2)}{4(\phi^2+\beta^2)}$$

$$N_8 = \frac{-AB\alpha(\nu\phi^2+\beta^2)}{4(\phi^2+\beta^2)}$$

The particular solution of the differential equations (10) and (11) gives the primary displacements u and v due to bending. The complementary solution of the homoge-

neous differential equations (that is, the equations obtained by equating the right-hand side of equations (10) and (11) to zero) gives the induced displacements due to bending.

In view of the boundary condition (5') the appropriate complementary solution can be shown to be of the form

$$u = \left[(C_1' + C_2') \cosh 2\phi y + C_2' 2\phi y \sinh 2\phi y\right] \sin 2\phi x - \epsilon_{st} x$$

$$v = \left[\left(\frac{2 - 2\nu}{1 + \nu} C_2' - C_1'\right) \sinh 2\phi y - C_2' 2\phi y \cosh 2\phi y\right] \cos 2\phi x + e'_y y$$

The general expressions for the displacements u and v can now be written as

$$u = \left[(C_1' + C_2') \cosh 2\phi y + C_2' 2\phi y \sinh 2\phi y + M_1 \cosh 2\alpha y + M_2 \cos 2\beta y + M_3 \sinh \alpha y \sin \beta y + M_4 \cosh \alpha y \cos \beta y + M_5\right] \sin 2\phi x - \epsilon_{st} x \qquad (14)$$

$$v = \left[\left(\frac{2 - 2\nu}{1 + \nu} C_2' - C_1'\right) \sinh 2\phi y - C_2' 2\phi y \cosh 2\phi y + N_1 \sinh 2\alpha y + N_2 \sin 2\beta y + N_3 \cosh \alpha y \sin \beta y + N_4 \sinh \alpha y \cos \beta y\right] \cos 2\phi x + N_5 \sinh 2\alpha y + N_6 \sin 2\beta y + N_7 \cosh \alpha y \sin \beta y + N_8 \sinh \alpha y \cos \beta y + e'_y y \qquad (15)$$

Since the boundary conditions indicated by expressions (2) and (3) must be satisfied for all values of x, it is necessary that the terms of expressions (14) and (15) included in the square brackets, vanish when $y = \pm b/2$. In addition, the boundary condition (3) requires that the remaining terms of expression (15) vanish when $y = \pm b/2$. From these conditions the constants C_1' and C_2', and e_y' can be determined, their respective values being

$$C_1' = \frac{1}{\cosh \phi b}\left[\frac{F_1 \sinh \phi b + F_2 \cosh \phi b}{\frac{3-\nu}{1+\nu}\sinh \phi b \cosh \phi b - \phi b}(\cosh \phi b + \phi b \sinh \phi b) - F_1\right]$$

$$C_2' = -\frac{F_1 \sinh \phi b + F_2 \cosh \phi b}{\frac{3-\nu}{1+\nu}\sinh \phi b \cosh \phi b - \phi b}$$

$$e'_y = -\frac{2}{b}\left[N_5 \sinh \alpha b + N_6 \sin \beta b + N_7 \cosh \frac{\alpha b}{2} \sin \frac{\beta b}{2} + N_8 \sinh \frac{\alpha b}{2} \cos \frac{\beta b}{2}\right]$$

where

$$F_1 = M_1 \cosh \alpha b + M_2 \cos \beta b + M_3 \sinh \frac{\alpha b}{2} \sin \frac{\beta b}{2} + M_4 \cosh \frac{\alpha b}{2} \cos \frac{\beta b}{2} + M_5$$

$$F_2 = N_1 \sinh \alpha b + N_2 \sin \beta b + N_3 \cosh \frac{\alpha b}{2} \sin \frac{\beta b}{2} + N_4 \sinh \frac{\alpha b}{2} \cos \frac{\beta b}{2}$$

The constants appearing in the expressions for u and v are now all evaluated in terms of the quantities, A, B, α, β, and ϕ. Therefore, the stress at any point on the median surface of the plate in the directions x and y can be calculated in terms of these quantities from the following expressions:

$$\sigma_x = \frac{E_s}{1-\nu^2}\left[\epsilon_x + \nu \epsilon_y\right] = \frac{E_s}{1-\nu^2}\left[\frac{\partial u}{\partial x} + \nu \frac{\partial v}{\partial y} + \frac{1}{2}\left(\frac{\partial w}{\partial x}\right)^2 + \frac{1}{2}\nu\left(\frac{\partial w}{\partial y}\right)^2\right] \tag{16}$$

where E_s is Young's modulus for sheet

$$\sigma_y = \frac{E_s}{1-\nu^2}[\epsilon_y + \nu\epsilon_x] = \frac{E_s}{1-\nu^2}\left[\frac{\partial v}{\partial y} + \nu\frac{\partial u}{\partial x} + \frac{1}{2}\left(\frac{\partial w}{\partial y}\right)^2 + \frac{1}{2}\nu\left(\frac{\partial w}{\partial x}\right)^2\right] \quad (17)$$

Substituting in equations (16) and (17) the values of u, v, and w given by expressions (1), (14), and (15) gives

$$\sigma_x = \frac{E_s}{1-\nu^2}\left[(F_4' + F_5')\cos 2\phi x + F_6' + F_7'\cos^2\phi x + F_8\sin^2\phi x - \epsilon_{st} + \nu e'_y\right] \quad (18)$$

$$\sigma_y = \frac{E_s}{1-\nu^2}\left[(\nu F_4' + \frac{1}{\nu}F_5')\cos 2\phi x + \frac{1}{\nu}F_6' + \nu F_7'\cos^2\phi x + \frac{1}{\nu}F_8'\sin^2\phi x + e'_y - \nu\epsilon_{st}\right] \quad (19)$$

where:

$$F_4' = \Big[(C_1' + C_2')\cosh 2\phi y + C_2' 2\phi y \sinh 2\phi y + M_1\cosh 2\alpha y + M_2\cos 2\beta y + M_3\sinh\alpha y\sin\beta y + M_4\cosh\alpha y\cos\beta y + M_5\Big]2\phi$$

$$F_5' = \nu\Big[\left(\frac{2-2\nu}{1+\nu}C_2' - C_1'\right)2\phi\cosh 2\phi y - C_2'(4\phi^2 y\sinh 2\phi y + 2\phi\cosh 2\phi y) + N_1 2\alpha\cosh 2\alpha y + N_2 2\beta\cos 2\beta y + N_3(\alpha\sinh\alpha y\sin\beta y + \beta\cosh\alpha y\cos\beta y) + N_4(\alpha\cosh\alpha y\cos\beta y - \beta\sinh\alpha y\sin\beta y)\Big]$$

$$F_6' = \nu[N_5 2\alpha\cosh 2\alpha y + N_6 2\beta\cos 2\beta y + N_7(\alpha\sinh\alpha y\sin\beta y + \beta\cosh\alpha y\cos\beta y) + N_8(\alpha\cosh\alpha y\cos\beta y - \beta\sinh\alpha y\sin\beta y)]$$

$$F_7' = \frac{1}{2}(A\cosh\alpha y + B\cos\beta y)^2\phi^2$$

$$F_8' = \frac{1}{2}\nu(A\alpha\sinh\alpha y - B\beta\sin\beta y)^2$$

Before any numerical calculations of the stresses σ_x and σ_y can be carried out it is necessary to first evaluate the quantities A, B, α, β, and ϕ. The constants A and B can be evaluated from the boundary condition of expression (4) and the condition that at $y = 0$ and $x = \frac{a}{2m}$, the deflection w is equal to the maximum amplitude w_o. From these conditions the following values for A and B are obtained:

$$A = w_o \left[\frac{\cos \frac{\beta b}{2}}{\cos \frac{\beta b}{2} - \cosh \frac{\alpha b}{2}} \right] \tag{20}$$

$$B = -w_o \left[\frac{\cosh \frac{\alpha b}{2}}{\cos \frac{\beta b}{2} - \cosh \frac{\alpha b}{2}} \right] \tag{21}$$

To evaluate the maximum amplitude, w_o, another boundary condition is necessary. At the point $y = 0$ and $x = a/m$ an empirical expression for the stress at the median fiber of the form $\sigma_x = \sigma_{cr}\left(\frac{\sigma_{cr}}{\sigma_{st}}\right)^{1/2}$ appears to be in fair agreement with the experimental evidence of reference 4. The comparison is shown in figure 1c.

In the expressions for α, β, and ϕ the only unknown quantity for a given panel is the half-wave length λ. It is therefore desirable to determine a general expression for λ. When dealing with a plate of large a/b ratio, the wave length of a buckle will not be influenced by the plate length, but only by the plate width and the elastic support along the edges $y = \pm b/2$. Hence, for large a/b ratios, the ratio of the half-wave length to the plate width can be calculated as a function of the parameter μ, where

$$\mu = \frac{bD}{C} = \frac{Et^3 b}{12(1-\nu^2)C}$$

The method of calculating μ is given in reference 5.

The critical buckling stress of the sheet between stringers was shown in reference 5 to be given by the transcendental equation

$$\sqrt{\theta\psi - \theta^2}\,\tan\frac{1}{2}\sqrt{\theta\psi-\theta^2} + \sqrt{\theta\psi+\theta^2}\,\tanh\frac{1}{2}\sqrt{\theta\psi+\theta^2} + \frac{2\psi\mu}{\theta} = 0 \tag{22}$$

where:

Glenn 3-27-47

$$\psi = \frac{\sigma_{cr}\, b^2 t}{D} = \frac{12(1-\nu^2)b^2\sigma_{cr}}{Et^2}$$

$$\theta = \frac{\pi b}{\lambda}$$

For large values of the ratio a/b the quantity ψ is a constant for a given value of μ and the value of b/λ is given by the expression

$$\frac{d\psi}{d\theta} = 0$$

or

$$\frac{\theta\psi - 2\theta^2}{\sqrt{\theta\psi-\theta^2}}\tan\frac{1}{2}\sqrt{\theta\psi-\theta^2} + \frac{1}{2}(\theta\psi - 2\theta^2)\sec^2\frac{1}{2}\sqrt{\theta\psi-\theta^2}$$

$$+ \frac{\theta\psi+2\theta^2}{\sqrt{\theta\psi+\theta^2}}\tanh\frac{1}{2}\sqrt{\theta\psi+\theta^2} + \frac{1}{2}(\theta\psi+2\theta^2)\operatorname{sech}^2\frac{1}{2}\sqrt{\theta\psi+\theta^2}$$

$$- \frac{4\psi\mu}{\theta} = 0 \tag{23}$$

From equations (22) and (23), the value of b/λ or λ/b and the values of ψ as functions of μ can be determined and are shown in figure 2. It should be emphasized that these values of ψ are the minimum values corresponding to given values of μ.

Now observing that,

$$\alpha b = \sqrt{\theta^2+\theta\psi}, \qquad \beta b = \sqrt{\theta\psi-\theta^2}, \qquad \phi b = \frac{\pi b}{\lambda}$$

it is seen that the coefficients M and N appearing in the expressions for u and v can be determined as functions of μ if the coefficients are multiplied by b/w_o^2. For example

$$M_1 = \frac{A^2\phi}{16} = \frac{w_o^2\phi}{16}\left[\frac{\cos\frac{\beta b}{2}}{\cos\frac{\beta b}{2} - \cosh\frac{\alpha b}{2}}\right]^2 \tag{24a}$$

$$\frac{M_1 b}{w_o^2} = \frac{\phi b}{16}\left[\frac{\cos\frac{\beta b}{2}}{\cos\frac{\beta b}{2} - \cosh\frac{\alpha b}{2}}\right]^2 \tag{24b}$$

and since ϕb, αb and βb are all known for a given value of μ, the quantity $\frac{M_1 b}{w_o^2}$ can be determined as a function of μ. All coefficients have been evaluated in this form and are shown in figures 3 to 6. The constants C_1' and C_2' can be evaluated in the same manner.

In order to simplify the necessary calculations it is desirable to write the functions F_4', F_5' and so forth, in such a form, that they can be evaluated as functions of the parameter μ. It can be seen that if these functions are multiplied by $\frac{b^2}{w_o^2}$ the expressions (18) and (19) can be written in the form

$$\left.\begin{aligned}\sigma_x &= \frac{E_s w_o^2}{(1-\nu^2)b^2}\left[(F_4 + F_5)\cos 2\phi x + F_6 + F_7\cos^2\phi x + F_8\sin^2\phi x + \nu e'_y\right] - \frac{E_s\epsilon_{st}}{1-\nu^2}\\ \sigma_y &= \frac{E_s w_o^2}{(1-\nu^2)b^2}\left[(\nu F_4 + \frac{1}{\nu}F_5)\cos 2\phi x + \frac{1}{\nu}F_6 + \nu F_7\cos^2\phi x + \frac{1}{\nu}F_8\sin^2\phi x + e_y\right] - \frac{\nu E_s\epsilon_{st}}{1-\nu^2}\end{aligned}\right\} \tag{25}$$

where

$$e_y = \frac{b^2 e'_y}{w_o^2} \qquad F_4 = \frac{b^2 F_4'}{w_o^2} \qquad F_5 = \frac{b^2 F_5'}{w_o^2} \qquad \text{and so forth.}$$

The functions F_4, F_5, F_6, F_7, and F_8 can now be evaluated for various values of y as functions of the parameter μ and are shown in figures 8 to 12 inclusive. The constant e_y is independent of y and is shown in figure 7 as a function of μ.

The amplitude w_o can now be evaluated from the condition that at $y = 0$ and $x = a/m$ the stress $\sigma_x = \sigma_{cr}\left(\frac{\sigma_{cr}}{\sigma_{st}}\right)^{1/2}$. Writing for ϵ_{st} its equivalent $\frac{\sigma_{st}}{E_{st}}$ and noting that E in equation (25) applies to the sheet, the value of $\frac{w_o}{b}$ is obtained as follows:

$$\sigma_x = -\sigma_{cr}\left(\frac{\sigma_{cr}}{\sigma_{st}}\right)^{1/2} = \frac{E_s w_o^2}{(1-\nu^2)b^2}\left[F_4 + F_5 + F_6 + F_7 + \nu e_y\right]_{y=0} - \frac{E_s \sigma_{st}}{(1-\nu^2)E_{st}}$$

or

$$\frac{w_o}{b} = \sqrt{\frac{1}{F_9}}\sqrt{\frac{\sigma_{st}}{E_{st}} - (1-\nu^2)\frac{\sigma_{cr}}{E_s}\sqrt{\frac{\sigma_{cr}}{\sigma_{st}}}} \tag{26}$$

where:

σ_{st} stringer stress, pounds per square inch

E_{st} Young's modulus for the stringer, pounds per square inch

E_s Young's modulus for the sheet, pounds per square inch

$$F_9 = \left[F_4 + F_5 + F_6 + F_7 + \nu e_y\right]_{y=0}$$

The expression for F_9 can be evaluated as a function of the parameter μ and is shown in figure 13. Substituting equations (25) and (26) gives

$$\sigma_x = \frac{E_s}{(1-\nu^2)F_9}\left(\frac{\sigma_{st}}{E_{st}} - \frac{(1-\nu^2)\sigma_{cr}\sqrt{\frac{\sigma_{cr}}{\sigma_{st}}}}{E_s}\right)\left[(F_4 + F_5)\cos 2\phi x + F_6 + F_7\cos^2\phi x + F_8\sin^2\phi x + \nu e_y\right] - \frac{E_s\sigma_{st}}{(1-\nu^2)E_{st}} \tag{27}$$

$$\sigma_y = \frac{E_s}{(1-\nu^2)F_9}\left(\frac{\sigma_{st}}{E_{st}} - \frac{(1-\nu^2)\sigma_{cr}\sqrt{\frac{\sigma_{cr}}{\sigma_{st}}}}{E_s}\right)\left[(\nu F_4 + \frac{1}{\nu}F_5)\cos 2\phi x + \frac{1}{\nu}F_6 + \nu F_7\cos^2\phi x + \frac{1}{\nu}F_8\sin^2\phi x + e_y\right] - \frac{\nu E_s\sigma_{st}}{(1-\nu^2)E_{st}} \tag{28}$$

The actual load carried by the plate for a given stringer stress and also the effective width can now be calculated. The total load carried by the plate is given by

$$P = 2t\int_0^{b/2} \sigma_x \, dy$$

and the effective width is by definition

$$2 w_e t \sigma_{st} = 2t\int_0^{b/2} \sigma_x \, dy$$

or the ratio of the effective width to the plate width is

$$\frac{w_e}{b} = \frac{1}{\sigma_{st} b}\int_0^{b/2} \sigma_x \, dy \tag{29}$$

Substituting for σ_x the expression (18) and integrating gives

$$\int_0^{b/2} \sigma_x \, dy = \frac{E_s}{1-\nu^2}\left[F_{10}' \cos 2\phi x + F_{11}' + F_{12}' \cos^2 \phi x + F_{13}' \sin^2 \phi x - \frac{\epsilon_{st} b}{2} + \nu v_y' \frac{b}{2}\right]$$

where:

$$F_{10}' = (1-\nu)\left(C_1' + \frac{2\nu C_2'}{1+\nu}\right)\sinh \phi b + \phi b C_2'(1-\nu) \cosh \phi b + \left(\frac{M_1\phi}{\alpha} + \nu N_1\right) \sinh \alpha b + \left(\frac{M_2\phi}{\beta} + \nu N_2\right) \sin \beta b + \left[\frac{2\phi}{\alpha^2 + \beta^2}(\alpha M_3 + \beta M_4) + \nu N_3\right] \cosh \frac{\alpha b}{2} \sin \frac{\beta b}{2} + \left[\frac{2\phi}{\alpha^2 + \beta^2}(\alpha M_4 - \beta M_3) + \nu N_4\right] \sinh \frac{\alpha b}{2} \cos \frac{\beta b}{2} + \phi b M_5$$

$$F_{11}' = \nu\left[N_5 \sinh \alpha b + N_6 \sin \beta b + N_7 \cosh \frac{\alpha b}{2} \sin \frac{\beta b}{2} + N_8 \sinh \frac{\alpha b}{2} \cos \frac{\beta b}{2}\right]$$

$$F_{12}' = \frac{\phi^2}{2}\left[\frac{b}{4}(A^2 + B^2) + \frac{A^2}{4\alpha} \sinh \alpha b + \frac{B^2}{4\beta} \sin \beta b + \frac{2AB}{\alpha^2 + \beta^2}\left(\alpha \sinh \frac{\alpha b}{2} \cos \frac{\beta b}{2} + \beta \cosh \frac{\alpha b}{2} \sin \frac{\beta b}{2}\right)\right]$$

$$F_{13}' = \frac{\nu}{2}\left[\frac{b}{4}(B^2\beta^2 - A^2\alpha^2) + \frac{A^2\alpha}{4} \sinh \alpha b - \frac{B^2\beta}{4} \sin \beta b - \frac{2AB\alpha\beta}{\alpha^2 + \beta^2}\left(\alpha \cosh \frac{\alpha b}{2} \sin \frac{\beta b}{2} - \beta \sinh \frac{\alpha b}{2} \cos \frac{\beta b}{2}\right)\right]$$

If the expressions for F_{10}', F_{11}', and so forth, are multiplied by $\frac{b}{w_o^2}$ the above equation can be written in the form

$$\int_0^{b/2} \sigma_x \, dy = \frac{E_s w_o^2}{(1-\nu^2) b}\left[F_{10} \cos 2\phi x + F_{11} + F_{12} \cos^2 \phi x + F_{13} \sin^2 \phi x + \frac{\nu e_y}{2}\right] - \frac{E_s \epsilon_{st}}{2(1-\nu^2)}$$

where $e_y = \frac{b^2}{w_o^2} e'_y$, $F_{11} = \frac{b}{w_o^2} F_{11}'$, and so forth.

Substituting the above expression in equation (29)(noting that σ_{st} is negative and $F_{11} = -\frac{\nu e_y}{2}$) and the value for $\frac{w_o}{b}$ from equation (26), gives

$$\frac{w_e}{b} = -\left[\frac{E_s}{(1-\nu^2)E_{st}} - \left(\frac{\sigma_{cr}}{\sigma_{st}}\right)^{3/2}\right] \frac{1}{F_9}\left[F_{10} \cos 2\phi x + F_{12} \cos^2 \phi x + F_{13} \sin^2 \phi x\right] + \frac{E_s}{2(1-\nu^2)E_{st}} \qquad (30)$$

As indicated by equation (27), the distribution of the stress across the plate also varies in a lengthwise direction. The total load carried by the plate is given by the stress distribution at the nodal lines. For example, if a stiffened plate is tested in compression, the total load on the plate as measured in the test, is that which exists at the head of the test machine, namely, at a nodal line. The variation of the transverse stress distribution between nodal lines is balanced by induced shear stresses at the stringer, and does not influence the total load carried by the plate. However, the compression stress in the stringer will be influenced to some extent by the lengthwise variation of the plate stress; that is, the total load in any transverse cross section of a stiffened panel being constant, any variation in the sheet load must be transferred to the stringer. This means that the compression stress in the stringer will be influenced by the lengthwise variation of the plate stress. The extent to which the stringer stress will vary between nodal points of the plate, will depend on the ratio of the stringer cross-section area to the plate cross-section area.

The transverse stress distributions at the nodal lines and at the maximum amplitude positions have been calculated in terms of the ratio σ_x/σ_{cr} for $\mu = 0$ and $\mu = \infty$, and are shown in figure 14. Although at the nodal points a considerable difference in stress intensity occurs at certain values of y, in going from $\mu = 0$ to $\mu = \infty$, this difference occurs only over a narrow region so that the total load carried by the plate is not greatly affected by the elastic support along the edges. At a stringer stress of 10 times the plate buckling stress, the simply supported plate carries 19.5 percent less load than the one with clamped edges.

The distribution of the σ_x stresses at $x = \frac{a}{2m}$ is influenced to some extent by the induced transverse stresses. As shown in figure 14, at the center of the buckle the stress changes to tension for the edge condition $\mu = 0$; whereas, for $\mu = \infty$ there is no appreciable change. However, in the latter case the edge stress is considerably reduced; whereas, the edge stress for $\mu = 0$ changes only slightly. This transverse stress distribution is primarily of interest in the calculations of the maximum combined stresses, for the maximum bending stresses occur along the line $x = \frac{a}{2m}$.

As previously pointed out the distribution of stress

at the nodal lines gives the actual load carried by the plate and any variation of the stress distribution between the nodal lines is balanced by shearing stresses at the stringer. Therefore, the effective width of sheet acting with each stringer would be given by equation (30), when $\phi x = 1, 2, 4,$ and so forth, or

$$\frac{w_e}{b} = \frac{1}{2(1-\nu^2)} \frac{E_s}{E_{st}} - \left[\frac{E_s}{(1-\nu^2)E_{st}} - \left(\frac{\sigma_{cr}}{\sigma_{st}}\right)^{3/2} \right] \frac{F_{14}}{F_8} \qquad (31)$$

where

$$F_{14} = F_{10} + F_{12}$$

The values of F_{14}, for various values of μ, are shown in figure 15. If the calculated effective width is to be compared with experimental results, further consideration must be given to the method in which the experimental results are obtained. From the previous discussion it is obvious that the compression stress in the stringer is not constant along its length but is a minimum at the nodal lines of the plate, and a maximum at the maximum amplitude of the plate. To obtain the experimental values of effective width, it is only necessary to measure the stringer stress corresponding to a given total panel load. The load carried by the plate alone can then be determined, and by the definition of the effective width, its value becomes immediately calculable. However, if the stringer stress is not constant along its length, the effective width thus determined would be a function of the position at which the stringer stress is measured. The experimental results given in reference 5 were obtained by averaging the measured strains, employing from 8 to 18 gages mounted as shown in figure 10, of reference 5. It is likely that the average of these measurements closely represents the average strain in the stringers. Hence, the experimental results thus obtained should be compared with the calculated effective width corresponding to the integrated mean value of the plate load between nodal lines, rather than the load existing at the nodal lines. The effective width based on this integrated mean value of the load can be obtained immediately from the integrated mean value of equation (30), that is,

$$\left(\frac{w_e}{b}\right)_{mean} = \frac{m}{a}\int_0^{m/a}\left\{\frac{1}{2(1-\nu^2)}\frac{E_s}{E_{st}} - \frac{1}{F_9}\left[\frac{E_s}{(1-\nu^2)E_{st}} - \left(\frac{\sigma_{cr}}{\sigma_{st}}\right)^{3/2}\right]\left[F_{10}\cos 2\phi x + F_{12}\cos^2\phi x + F_{13}\sin^2\phi x\right]\right\}dx$$

$$= \frac{1}{2(1-\nu^2)}\frac{E_s}{E_{st}} - \frac{F_{15}}{F_9}\left[\frac{E_s}{(1-\nu^2)E_{st}} - \left(\frac{\sigma_{cr}}{\sigma_{st}}\right)^{3/2}\right] \quad (32)$$

where $$F_{15} = \frac{F_{12} + F_{13}}{2}$$

The value of F_{15}, as a function of μ, is indicated in figure 16. Assuming Young's moduli to be the same for the plate and stringer the mean effective width curves for the two limiting conditions, that is, $\mu = 0$ and $\mu = \infty$, are shown in figure 17. The effective width values given by equation (32) are slightly lower than those given by equation (31), the maximum difference being of the order of 6 percent.

In calculating the effective width for any plate-stringer combination, it should be kept in mind that the torsional rigidity of the stringer varies as σ_{st} increases. Since both F_9 and F_{15} are functions of μ it is necessary to correct these quantities for the change in torsional rigidity of the stringer as σ_{st} increases. Equation (25) of reference 5 can be written in the form

$$E_{st} C_{BT}\frac{d^4\Phi}{dx^4} + (\sigma_x I_p - C)\frac{d^2\Phi}{dx^2} - K_\mu \sin\frac{m\pi x}{a} = 0 \quad (33)$$

where

E_{st} Young's modulus for the stringer

C_{BT} torsion bending constant (references 11 and 12)*

σ_x axial compressive stress in the stringer

I_p polar moment of inertia of the stringer section about the axis of twist

*See appendix A, for example.

C torsional rigidity of the stringer

$K_\mu \sin \frac{m\pi x}{a}$ moment transferred by the buckled plate to the stringer

Φ unit torsional deflection of the stringer

Neglecting end effects, a solution of the above equation can be written in the form

$$\Phi = A \sin \frac{m\pi x}{a}$$

from which

$$A = \frac{K}{E_{st} C_{BT}\left(\frac{m\pi}{a}\right)^4 + (C - \sigma_x I_p)\left(\frac{m\pi}{a}\right)^2} \tag{34}$$

Since the amplitude A is a measure of the torsional stiffness of the stringer the ratio

$$\frac{C_r}{C} = \frac{A_o}{A} = \frac{E_{st} C_{BT}\left(\frac{m\pi}{a}\right)^2 + (C - \sigma_x I_p)}{E_{st} C_{BT}\left(\frac{m\pi}{a}\right)^2 + C} \tag{35}$$

would be a measure of the change of the torsional stiffness of the stringer, where C_r is the reduced torsional stiffness of the stringer and A_o corresponds to A when $\sigma_x = 0$. This equation then allows a calculation of the variation in torsional rigidity of the stringer with increasing stress.

The experimental values of effective width for a number of panels have been compared with the results given by equation (32) and are shown in figures 18 and 18a. The curves are the calculated values corrected for the change in torsional stiffness of the stringer with increasing stress, and taking into account any difference between E_s and E_{st}. As indicated by this comparison, the calculated results do not compare favorably with the experimental results. This is particularly true for the torsionally weak stringer. Although the correction for reduced torsional stiffness of the stringer recognizes a change in wave form of the plate with increasing stress, it is felt that the magnitude of this correction does not fully compensate for the actual changes in wave form which may occur. It is believed that this is the principal cause of the deviation of the calculated values. It should also be

noted that the derived equations are only valid below the proportional limit. It has been proposed in literature on the subject of effective width, that above the proportional limit it is only necessary to replace E_s by $\bar{E}_s$ where $\bar{E}_s$ is the secant modulus. This is a fallacy, for only that portion of the sheet subjected to stresses above the proportional limit is affected by the change in E. The distribution of stress in that portion of the sheet subjected to stresses below the proportional limit remains unchanged. Above the proportional limit it is necessary to make a point-by-point correction for the reduced value of E. It will be appreciated that a blanket application of the secant modulus will reduce the stresses throughout the entire sheet and thereby incorrectly reduce the effective width. In figures 19 and 20, a point-by-point correction is illustrated for the J-section panel with .040-24S-T alclad sheet. The method consists essentially of a calculation of the strain ϵ_x', at the median fiber in the x direction, where

$$\epsilon_x' = \frac{\epsilon_x + \nu\epsilon_y}{1 - \nu^2} \qquad (36)$$

The working expression for ϵ_x' was obtained directly from equations (16) and (18). This strain distribution was then plotted and the corresponding stress in the sheet obtained from the stress-strain curves of figures 36. Of course, using the stress-strain curve obtained from a unidirectional load is not strictly correct. However, if σ_y is small in comparison to σ_x the method should at least approximate the correct stress distribution. A study of these curves indicates that the reduced E, above the proportional limit, is not sufficient to account for the discrepancies of the effective width calculations indicated in figures 18 and 19. Of course, the above method does not consider the effects of the induced bending stresses. The dimensions of the stringers are shown in figure 42, and the stress-strain properties in figures 36 to 40. (The data on the J-section was supplied by the Lockheed Aircraft Corporation)

The x components of the bending stress are computed as follows:

$$\sigma_{xB} = \frac{EZ}{1-\nu^2}\frac{M_x}{D} \qquad (37)$$

where Z is measured from the median surface of the plate. Substituting for Z its maximum value $t/2$ and for M_x the expression

$$M_x = - D\left(\frac{\partial^2 w}{\partial x^2} + \nu \frac{\partial^2 w}{\partial y^2}\right)$$

equation (37) becomes

$$\sigma_{xB} = - \frac{E_s t}{2(1-\nu^2)}\left(\frac{\partial^2 w}{\partial x^2} + \nu \frac{\partial^2 w}{\partial y^2}\right) \tag{38}$$

Substituting the expression (1) for w, equation (38) can be written in the form

$$\sigma_{xB} = -\left[\frac{E_s F_{16}}{2(1-\nu^2)} \frac{1}{\sqrt{F_9}} \left(\frac{t}{b}\right) \sqrt{\frac{\sigma_{st}}{E_{st}} - \frac{(1-\nu^2)}{E_s} \sigma_{cr} \sqrt{\frac{\sigma_{cr}}{\sigma_{st}}}}\right] \sin \phi x \tag{39}$$

where

$$F_{16} = \frac{b^2}{w_o}\left[A(\nu\alpha^2 - \phi^2) \cosh \alpha y - B(\nu\beta^2 + \phi^2) \cos \beta y\right]$$

The function F_{16} has been evaluated as a function of μ for a number of values of y, as indicated in figure 21. If both sides of expression (34) are divided by σ_{cr}, it can be written in the form

$$\frac{\sigma_{xB}}{\sigma_{cr}} = -\left\{\frac{E_s F_{17}}{2(1-\nu^2)} \frac{1}{\sqrt{F_9}} \left(\frac{t}{b}\right) \frac{1}{\sqrt{\sigma_{cr}}} \sqrt{\frac{\sigma_{st}}{\sigma_{cr} E_{st}} - \frac{(1-\nu^2)}{E_s} \sqrt{\frac{\sigma_{cr}}{\sigma_{st}}}}\right\} \sin \phi x$$

Noting that,

$$\sigma_{cr} = \frac{\psi^2 E_s t^2}{12(1-\nu^2) b^2}$$

the above equation can be written as

$$\frac{\sigma_{xB}}{\sigma_{cr}} = \left\{- \frac{1.732}{\sqrt{1-\nu^2}} \frac{\sqrt{E_s}}{\psi} \frac{F_{17}}{\sqrt{F_9}} \sqrt{\frac{\sigma_{st}}{\sigma_{cr} E_{st}} - \frac{(1-\nu^2)}{E_s} \sqrt{\frac{\sigma_{cr}}{\sigma_{st}}}}\right\} \sin \phi x \tag{40}$$

This ratio assumes its maximum value when $\sin \phi x = 1$. Hence $\left(\frac{\sigma_{xB}}{\sigma_{cr}}\right)_{max}$ occurs along the line $x = \frac{a}{2m}$, and is given by the bracketed portion of equation (35).

The sum of this maximum bending stress distribution and the compression stress distribution given by expression (27) gives the maximum compression stress distribution in the x direction. Taking $\frac{\sigma_{st}}{\sigma_{cr}} = 10$ and $E_{st} = E_s$, the maximum stress distribution has been plotted for $\mu = 0.5$ and $\mu = \infty$, and is shown in figure 22. As seen from this figure, for the case of simply supported edges the maximum compression stress does not appreciably exceed the stringer stress over the entire panel width. The value of $\mu = 0.5$ corresponds to a stringer of high torsional rigidity and in this case, at the edges $y = \pm\frac{b}{2}$, the maximum compression stress exceeds the stringer stress by approximately 27 percent. This increase in the maximum plate compressive stress over the stringer stress will not affect to any appreciable extent the load-carrying ability of the sheet.

The wave form of equation (1) was compared with the measured wave forms given in figures 27 and 28 of reference 4, as shown in figure 23 of this report. Both the transverse and longitudinal wave forms check closely with the measured ones. In order to make this comparison, the torsional rigidity of the stringers must be known. It was computed approximately by assuming the stringer rigidity to be the same as that of a rectangular plate having the same cross-section area and thickness as the stringer. By this method the torsional rigidity was found to be 630 inch-pounds per radian per inch. The corresponding value of μ was 0.198, the wave length was determined from figure 2 and the maximum amplitude from equation (26). The buckling stress of the sheet was computed and found to be 2500 pounds per square inch, which checks with the value indicated in figure 55 of reference 4.

In view of the good agreement between the calculated and measured wave forms, it is reasonable to expect also a good agreement between the calculated and measured strains. Calculating the strain by the equation

$$\epsilon_x = \frac{\partial u}{\partial x} + \frac{1}{2}\left(\frac{\partial w}{\partial x}\right)^2 = \frac{1}{F_9}\left[\frac{\sigma_{st}}{E_{st}} - \frac{(1-\nu^2)}{E_s}\sigma_{cr}\sqrt{\frac{\sigma_{cr}}{\sigma_{st}}}\right][F_4 \cos 2\phi x + F_7 \cos^2 \phi x] - \frac{\sigma_{st}}{E_{st}} \qquad (41)$$

the resulting values at $x = \frac{a}{m}$ and $\frac{a}{4m}$ are indicated in figures 24 and 25, where they are compared with the measured values given in figure 20 of reference 4. The measured and calculated strain distributions compare favorably. The transverse strain at the median fiber, at $x = \frac{0.125\ a}{m}$ has been calculated and is compared, in figure 25, with the observed value at $x = \frac{0.152\ a}{m}$. The agreement appears to be remarkably good.

II- EXPERIMENTAL RESULTS

Inasmuch as the wave form is one of the important factors in the theoretical calculations of the stress distribution in a buckled plate, it is desirable to have some knowledge regarding its variation with increasing load. A number of tests were conducted in which the wave form was measured for various increments of load. The measurements were obtained by means of a dial gage attached to a frame mounted on the bed of the testing machine. The results of these tests are shown in figures 26 to 33, where the deflections were plotted for various values of the ratio of the stringer strain ϵ_{st} to the sheet strain ϵ_c at buckling. The primary purpose of these tests was to determine qualitatively the amount of change in the wave form with increasing stringer stress. The wave forms plotted in figure 29 indicate that there is in some cases a considerable change in the wave form. The change in wave form as indicated by these curves is somewhat irregular: for example, the 0.025 sheet changed but slightly in wave form; whereas the change in the 0.040 sheet is more than in the 0.050 sheet. It seems there should be some degree of consistency in the amount of change in the wave form as the sheet thickness increases.

It is possible that the inconsistencies indicated by these results can be attributed to the influence of buckles in the adjacent sheet panels. It is difficult to estimate the influence on the compressive stress distribution due to the amount of change in wave form as indicated by the experiments. However, the indicated flattening of the wave will cause an increase in the y component of strain which, in turn causes a decrease in the x component of strain.

The compression stress-strain properties of the 24S-T sheet material used in the above tests are shown in figures 34 and 35. In addition, a number of compression tests were conducted on 24S-T alclad sheet; the curves for this material are shown in figure 36. The method employed in determining the compressive stress-strain properties was identical to that described in reference 7.

The stringer strain as a function of average stress is shown in figures 37 to 39 for the various panels tested. By average stress is meant the compressive load on the panel divided by its total cross-section area. The stress-strain properties of the stringers are shown in figures 40 and 41; the section dimensions are shown in figure 42.

Guggenheim Aeronautics Laboratory,
California Institute of Technology,
Pasadena, Calif., June 1941.

APPENDIX A

The value of the torsion-bending constant, C_{BT}, may be calculated either analytically or graphically. Considering a general section such as that shown in figure 43a, the value of C_{BT} is given by the expression

$$C_{BT} = \int_A w^2 dA - \frac{1}{A}\left[\int_A w\, dA\right]^2 \qquad (42)$$

where w is the circumferential warping and is given by the equation

$$w = \int_0^u r_t\, du$$

In the above expression the cross-sectional warping $r_n n$ has been neglected. Since n, at the most, is equal to $t/2$, the warping $r_n n$ will, in general, be small compared to the circumferential warping and may be neglected.

In evaluating the warping w, the following sign conventions have been adopted. A direction of rotation is chosen arbitrarily; then the circumferential coordinate u is taken positive in the direction of rotation. Also the positive sense of rotation indicates the positive direction of the tangent to the circumferential coordinate u. From the positive tangential direction, the positive normal n points to the right and a line drawn from O in the positive n direction indicates the positive r_n direction. The angle α is measured in the positive sense of rotation, that is, from +x to +y. As an illustration, consider the channel section shown in figure 43b and first calculate C_{Bt} about the point O.

Choose the origin of u at O; then,

From 1 to 2 $\quad r_t = 0$

From 2 to 3 $\quad r_t = \frac{a}{2}\, du$ is negative and $w = -\frac{au}{2}$

From 1 to 4 $\quad r_t = 0$

From 4 to 5 $\quad r_t = \frac{a}{2}\, du$ is positive and $w = \frac{au}{2}$

from which

$$\int_A wdA = -\frac{at}{2}\int_0^b udu + \frac{at}{2}\int_0^b udu = 0$$

hence

$$C_{BT} = \frac{a^2t}{4}\int_0^b u^2du + \frac{a^2t}{4}\int_0^b u^2du = \frac{a^2b^3t}{6}$$

Now let C_{BT} be calculated about the point O_1. Again, take the origin of u at 0; then,

From 1 to 2 $r_t = +c$ du is negative, and $w = -cu$

From 2 to 3 $r_t = +\frac{a}{2}$ du is negative, and $w = -\frac{au}{2} - \frac{ac}{2}$

From 1 to 4 $r_t = +c$ du is positive, and $w = cu$

From 4 to 5 $r_t = \frac{a}{2}$ du is positive, and $w = \frac{au}{2} + \frac{ac}{2}$

from which

$$\int_A wdA = 0$$

and

$$C_{BT} = 2\left\{c^2t\int_0^{a/2} u^2du + \frac{a^2t}{4}\int_0^b (u + c)^2\,du\right\} = \frac{a^2t}{12}\left\{c^2(a + 6b) + 2b^2(b + 3c)\right\}$$

The integral $\int_A wdA$ will not be zero if, for example, the origin of u is taken at point 2. However, the algebraic sum of the two integrals of equation (42) will always be constant for a given axis of rotation, that is, the expression for C_{BT} is invariant with respect to the origin of the circumferential coordinate u. The origin of the rectangular coordinates xy must, of course, be taken at the axis of rotation. Assume, for example, that the center of rotation of the section shown in figure 43c is at the point 0; then C_{BT} is evaluated as follows:

Take the origin of u at point 4; then from 4 to 3

$$r_t = r + d\cos\theta + b\sin\theta$$

and

$$w_{4-3} = \int_0^u r_t\,du = r\int_0^\theta (r + d\cos\theta + b\sin\theta)\,d\theta$$

From 3 to 2

$$r_t = r - d$$

and

$$w_{3-2} = w_{4-3}\Big|_{\theta=\pi} + \int_0^u (r - d)\,du = r^2\pi + 2rb + (r - d)u$$

From 2 to 1 $r_t = 0$

and $w_{2-1} = w_{3-2}\Big|_{u=b} = r^2\pi + b(3r - d)$

Hence

$$C_{BT} = \int_A w^2\,dA - \frac{1}{A}\left[\int_A w\,dA\right]^2 = tr^3\int_0^\pi [r\theta + d\sin\theta - b\cos\theta + b]^2\,d\theta + t\int_0^b [r^2\pi + 2rb + (r - d)u]^2\,du + t\int_0^a [r^2\pi + b(3r - d)]^2\,du - \frac{1}{A}\left\{r^2t\int_0^\pi [r\theta + d\sin\theta - b\cos\theta + b]\,d\theta + t\int_0^b [r^2\pi + 2rb + (r - d)u]\,du + t\,[r^2\pi + b(3r - d)]\,du\right\}^2$$

where A is the total cross-section area of the section. It can be seen, for example, that, if the origin of the circumferential coordinate u is taken at point 1, the resulting expression for C_{BT} would be considerably simplified, since the warping from 1 to 2 would be zero.

When a longitudinal stiffener is attached to a thin plate the rigidity of the plate requires that the axis of rotation lie in the plane of the plate. In computing C_{BT} for this condition, a number of values of C_{BT} corresponding to various positions in the plane of the plate were computed, and a curve was then plotted of C_{BT} as a function of position. The minimum value of C_{BT} was then used in computing the variation of torsional rigidity with increasing load.

REFERENCES

1. Marguerre, K., and Trefftz, E.: Über die Tragfähigkeit eines längsbelasteten Plattenstreifens nach Überschreiten der Beullast. Z.f.a.M.M., vol. 17, April 1937, pp. 85-100.

2. Marguerre, Karl: The Apparent Width of the Plate in Compression. T.M. No. 833, NACA, 1937.

3. von Kármán, Theodor, Sechler, Ernest E., and Donnell, L. H.: The Strength of Thin Plates in Compression. A.S.M.E. Trans., APM-54-5, vol. 54, no. 2, Jan. 30, 1932, pp. 53-57.

4. Ramberg, Walter, McPherson, Albert E., and Levy, Sam: Experimental Study of Deformation and of Effective Width in Axially Loaded Sheet-Stringer Panels. T.N. No. 684, NACA, 1939.

5. Dunn, Louis G.: An Investigation of Sheet Stiffener Panels Subjected to Compression Loads with Particular Reference to Torsionally Weak Stiffeners. T.N. No. 752, NACA, 1940.

6. Friedrichs, K. O., and Stoker, J. J.: The Non-linear Boundary Value Problem of the Buckled Plate. Proceedings of the National Academy of Sciences, vol. 25, 1939, pp. 535-540.

7. Aitchison, C. S., and Tuckerman, L. B.: The "Pack" Method for Compressive Tests of Thin Specimens of Materials Used in Thin-Wall Structures. Rep. No. 649, NACA, 1939.

8. Timoshenko, S.: Theory of Elastic Stability. McGraw-Hill Book Co., Inc., 1936.

9. Timoshenko, S.: Theory of Elasticity. 1st ed., McGraw-Hill Book Co, Inc., 1934.

10. Sechler, E. E.: Stress Distribution in Stiffened Panels under Compression. Jour. Aero. Sci., vol. 4, no. 8, June 1937, pp. 320-323.

11. Lundquist, Eugene E., and Fligg, Claude M.: A Theory for Primary Failure of Straight Centrally Loaded Columns. Rep. No. 582, NACA, 1937.

12. Kappus, Robert: Twisting Failure of Centrally Loaded Open-Section Columns in the Elastic Range. T.M. No. 851, NACA, 1938.

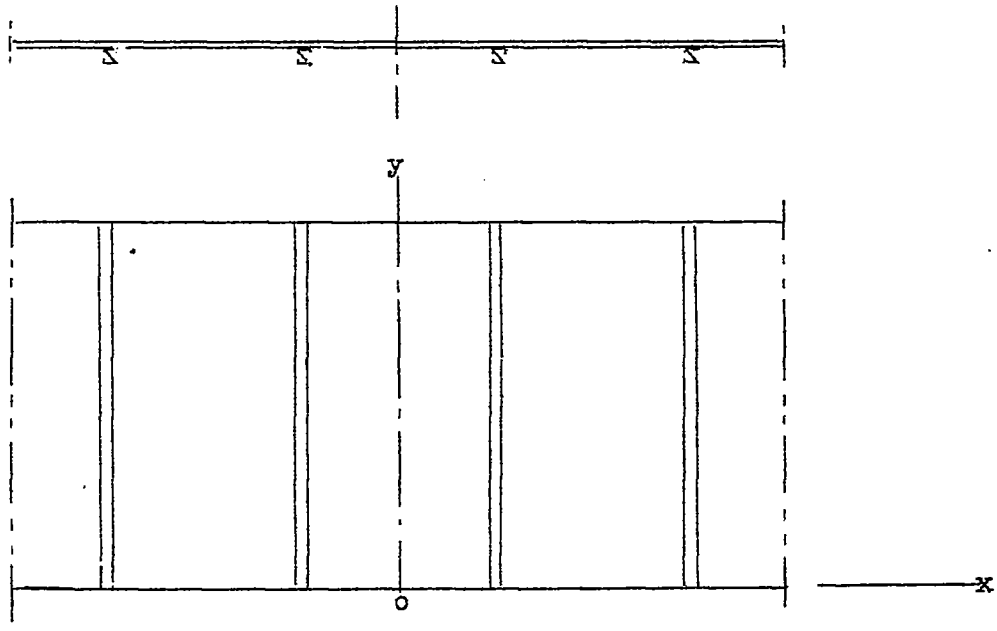

Figure 1a

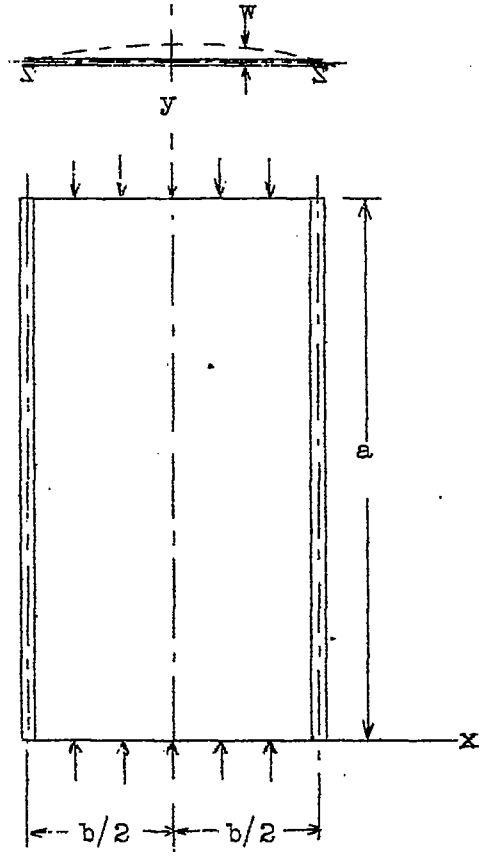

Figure 1b

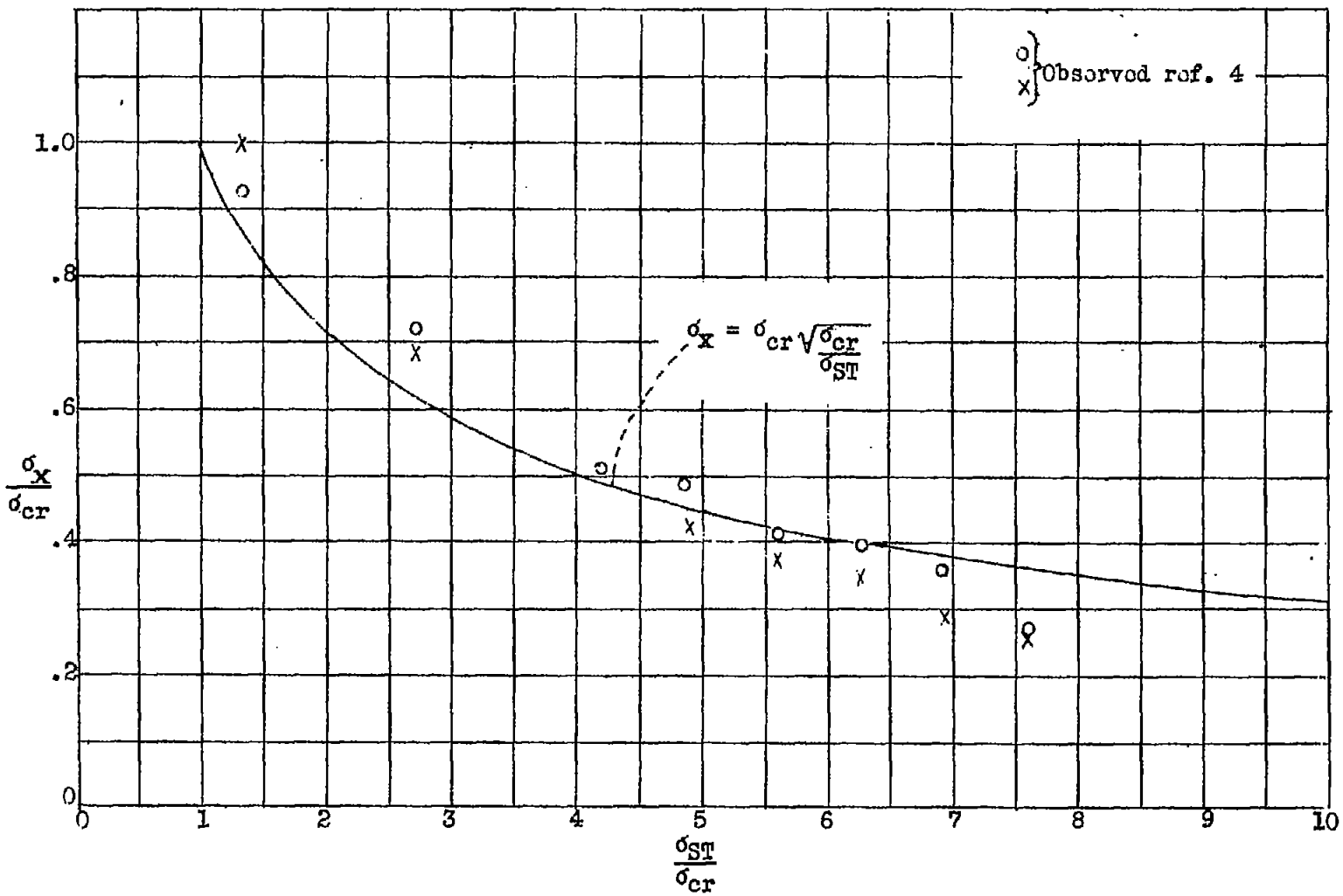

Figure 1c.- Variation of σ_x with σ_{ST} at y = 0, x = $\frac{a}{m}$

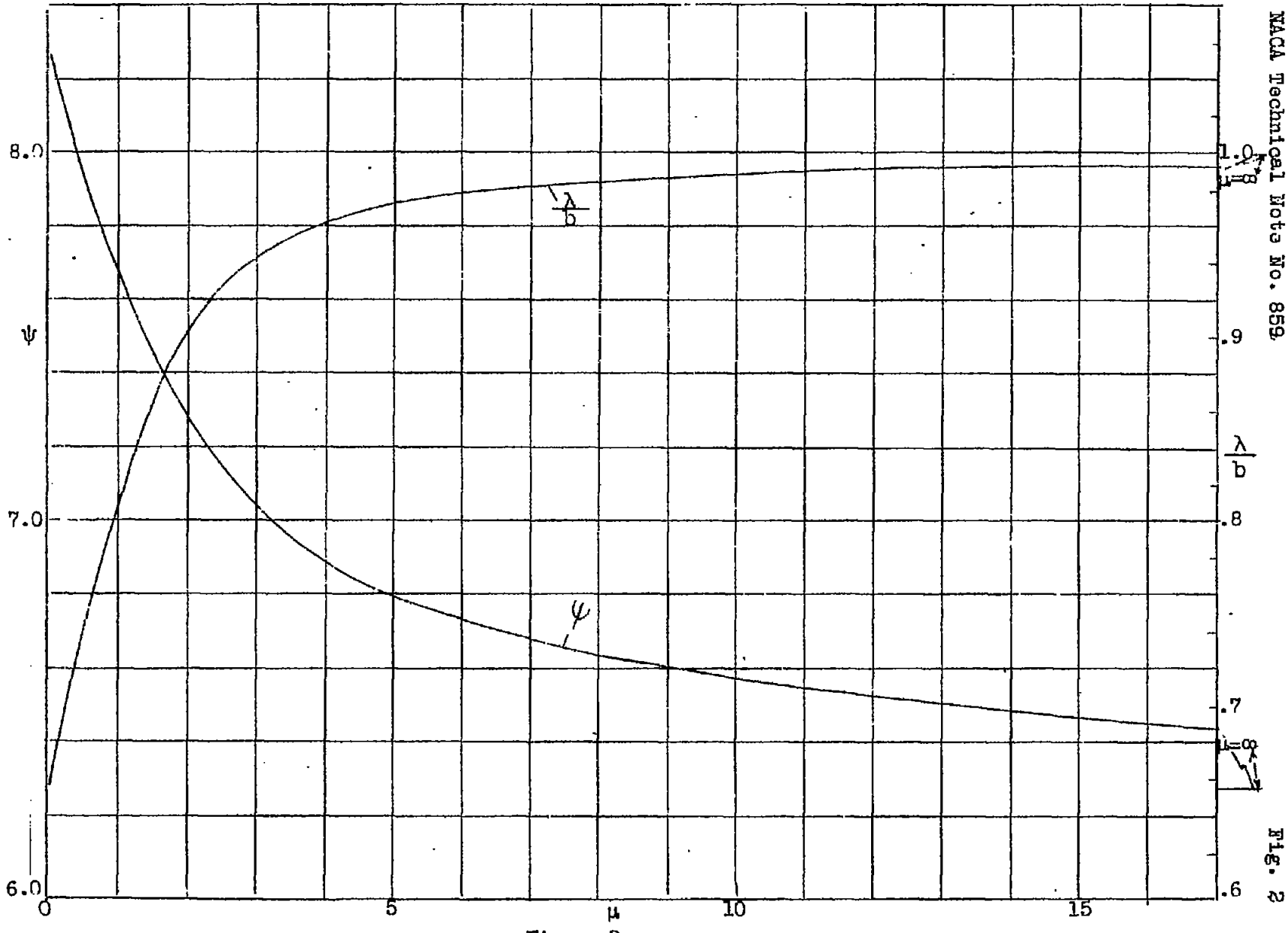

Figure 2

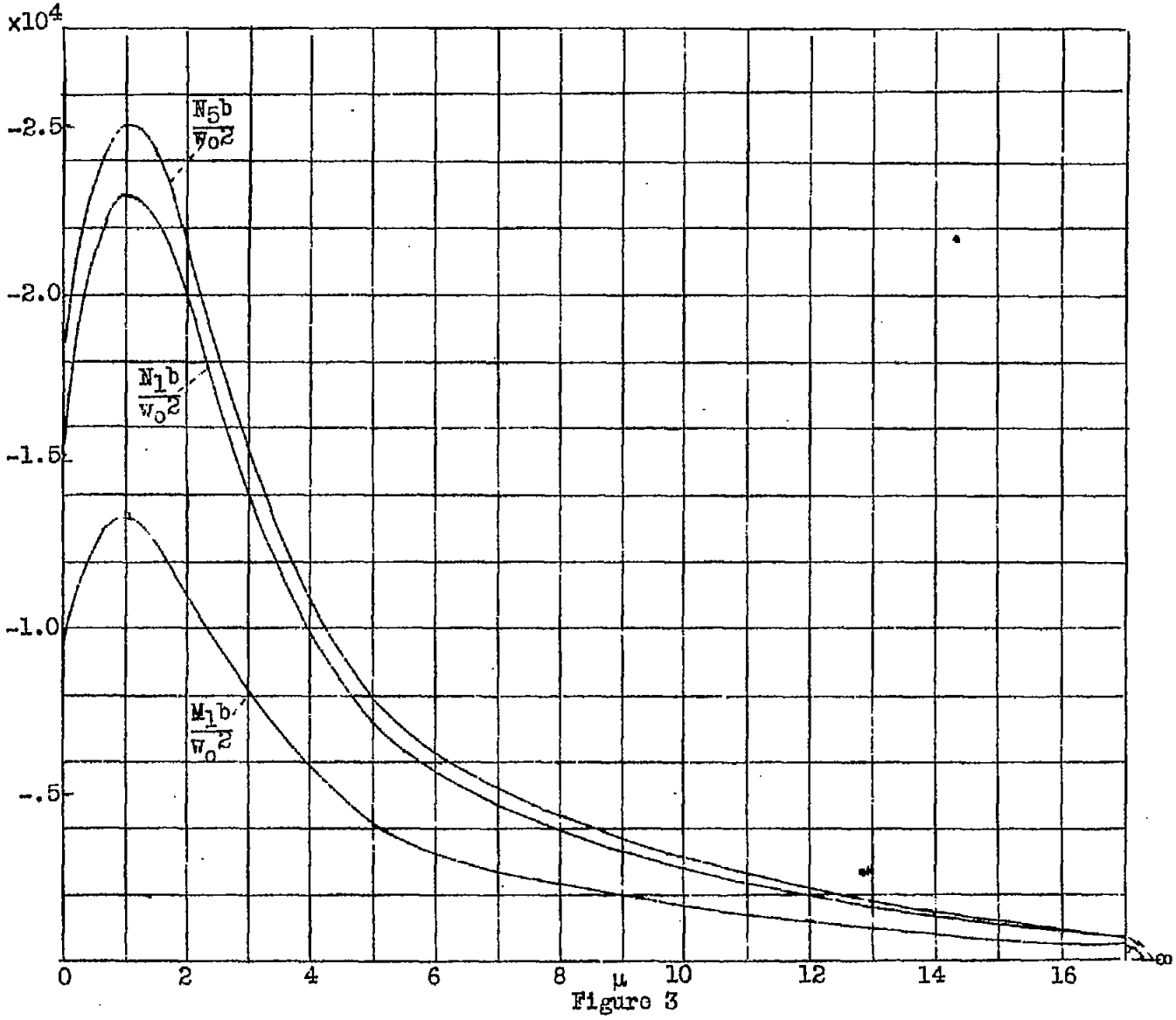

Figure 3

Fig. 3

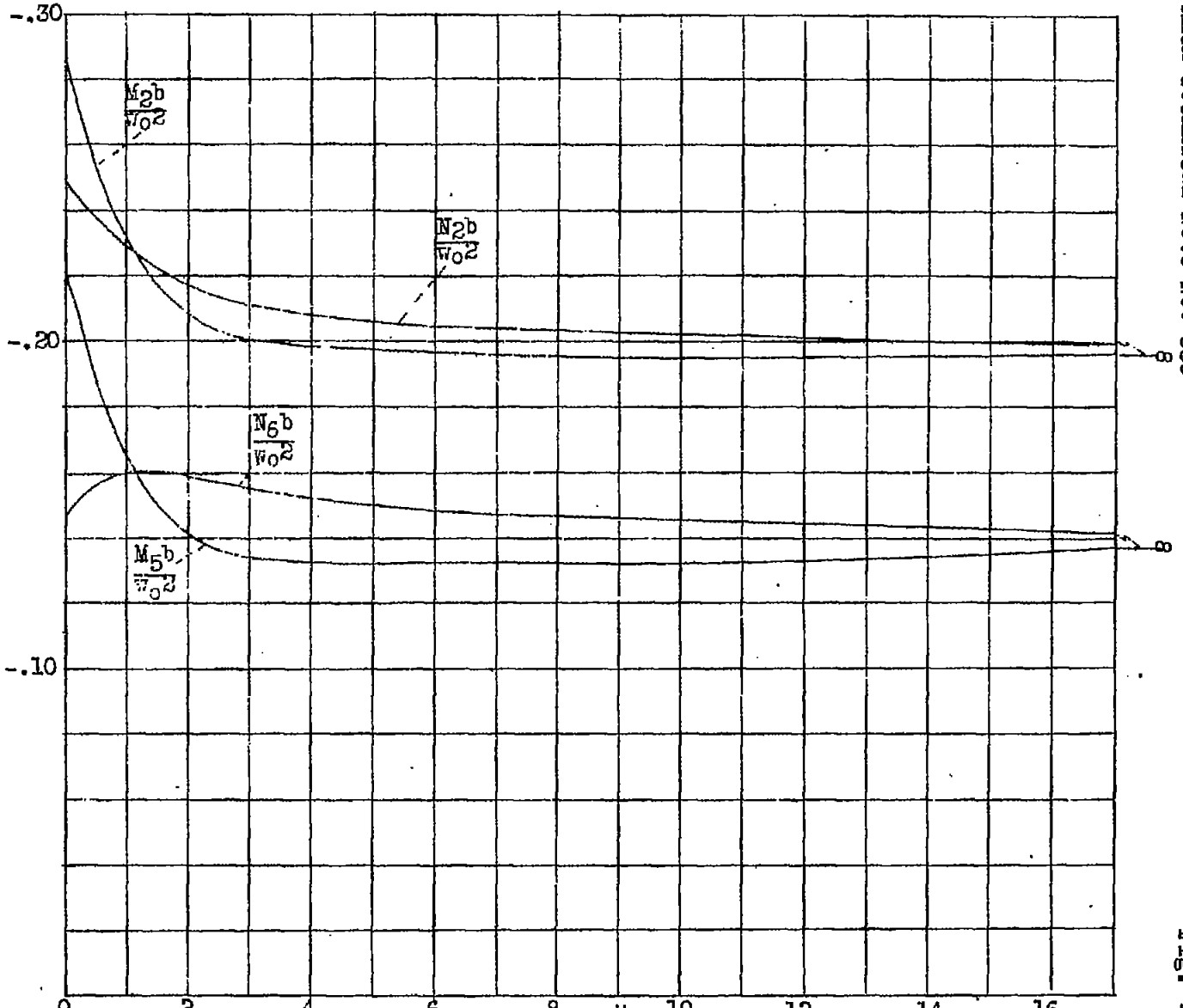

Figure 4

Fig. 4

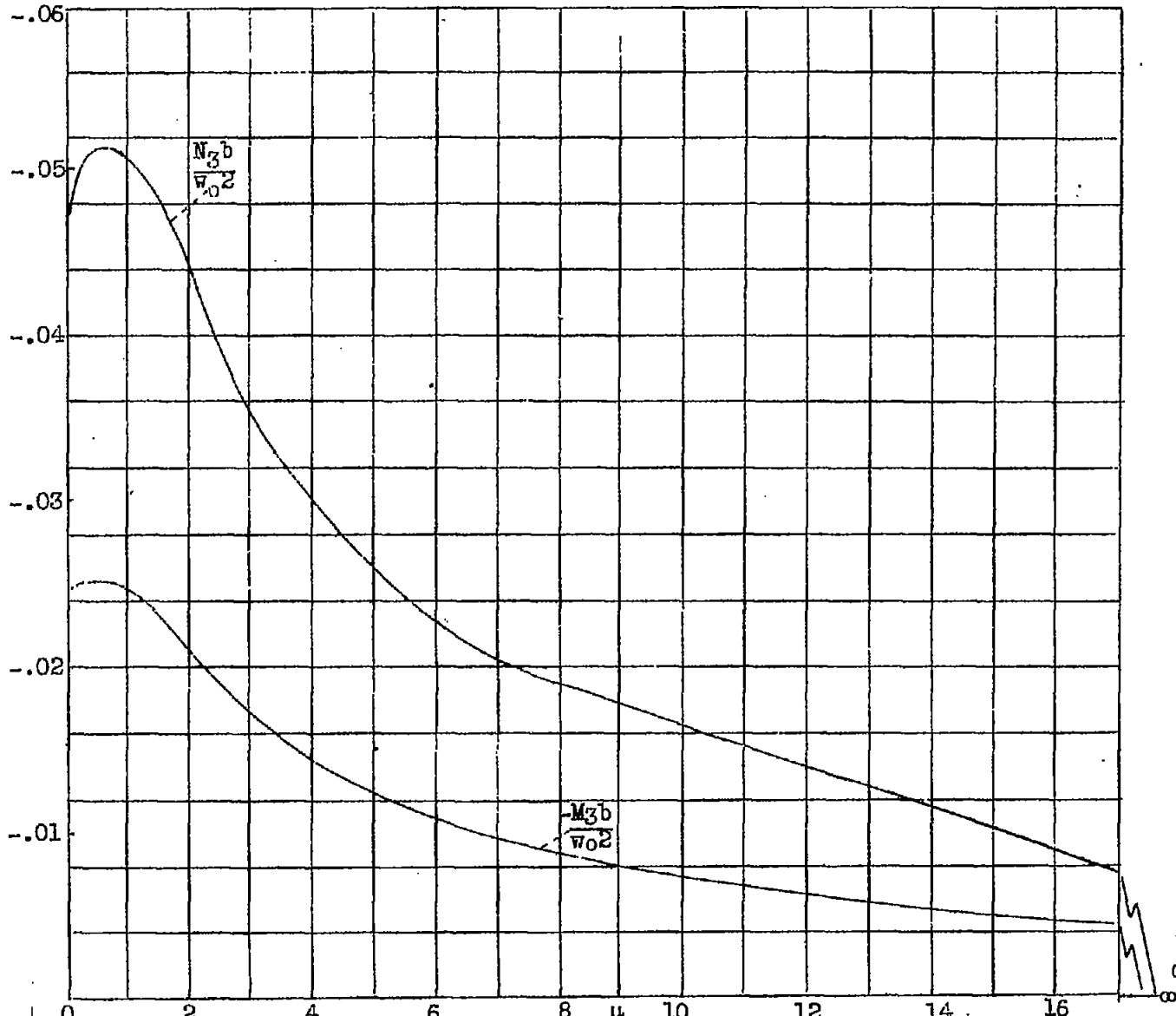

Figure 5

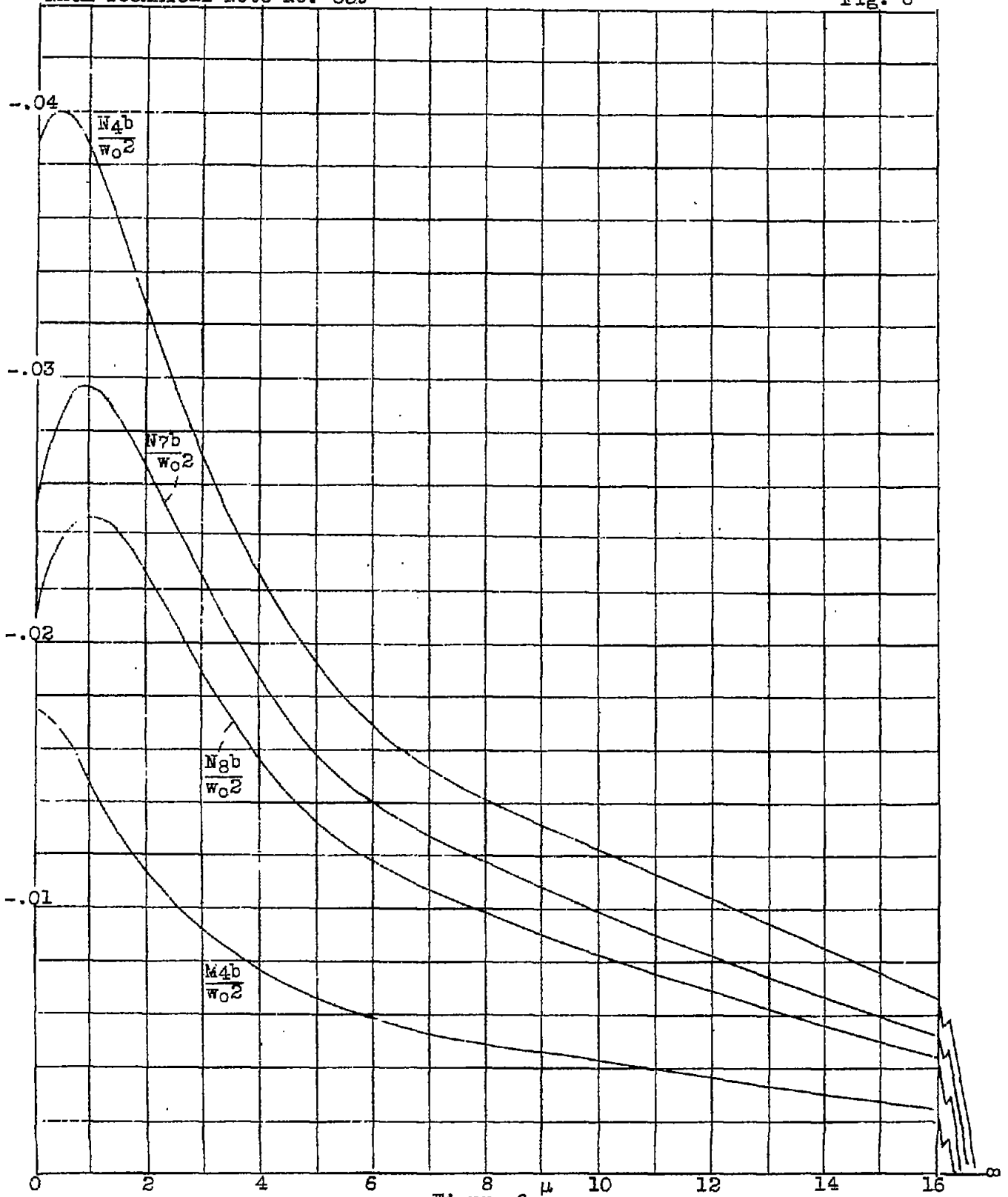
-.04
-.03
-.02
-.01
$\frac{N_4 b}{w_o 2}$
$\frac{N_7 b}{w_o 2}$
$\frac{N_8 b}{w_o 2}$
$\frac{M_4 b}{w_o 2}$
0
2
4
6
8
μ
10
12
14
16
∞

Figure 6

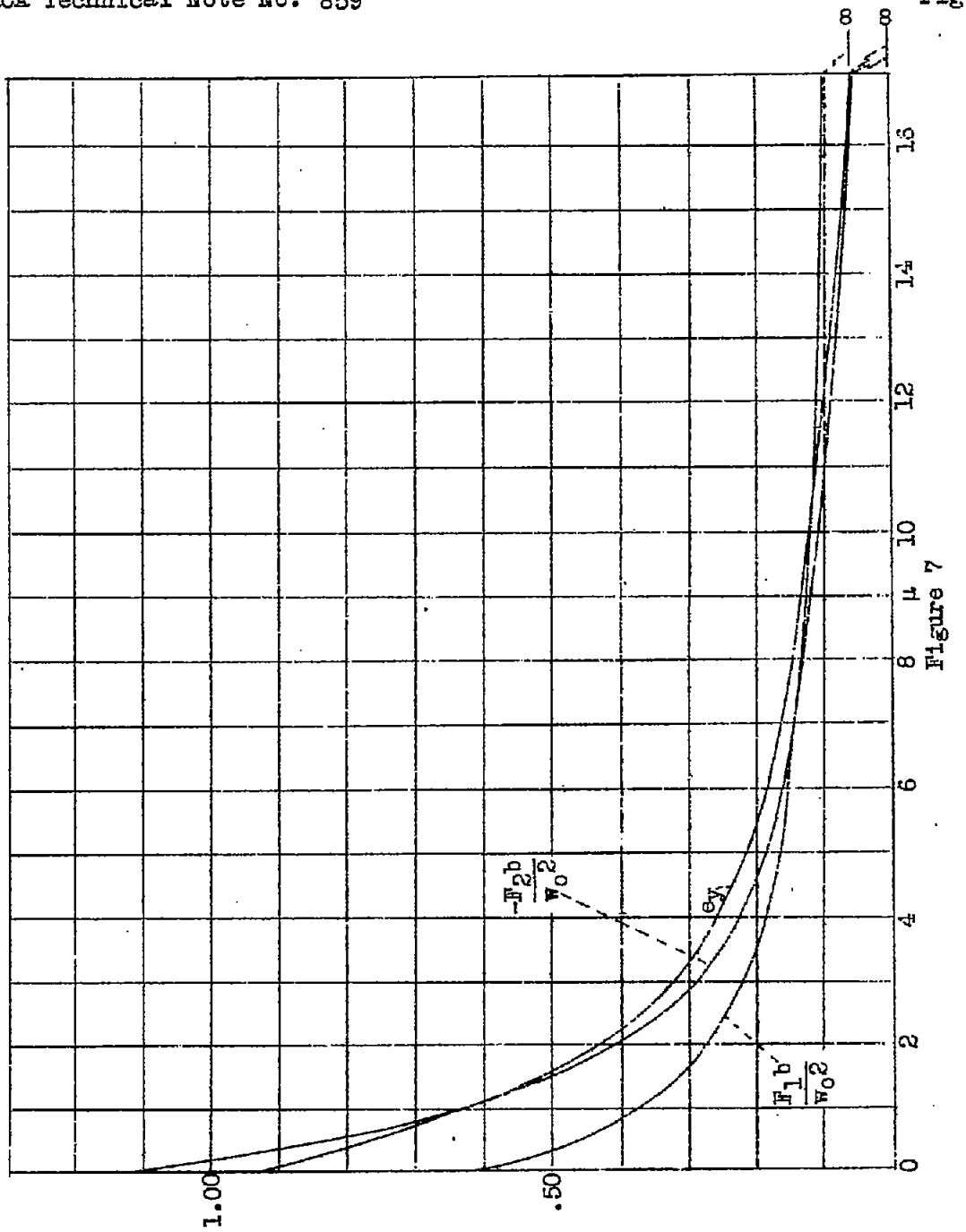

Figure 7

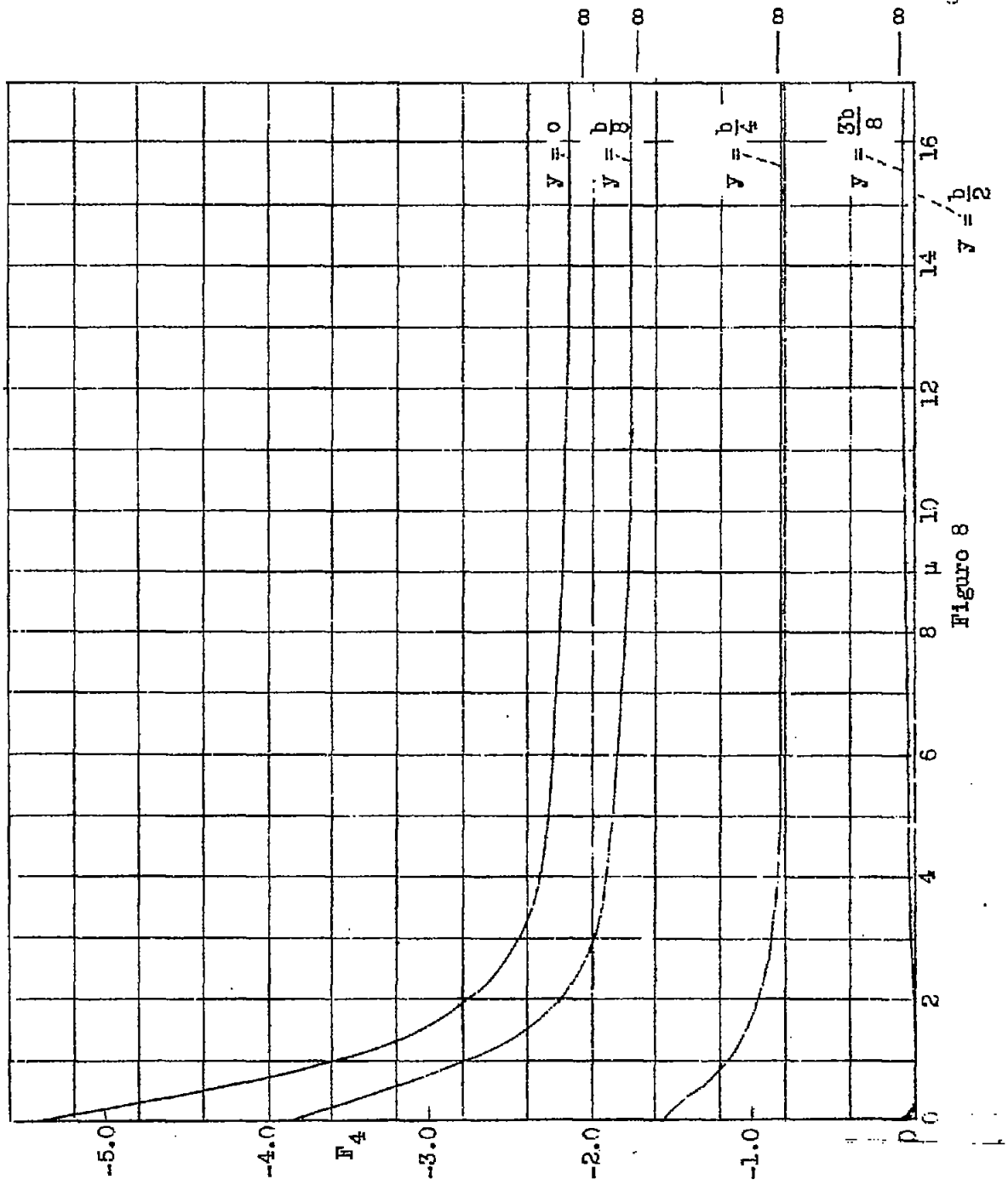

Figure 8

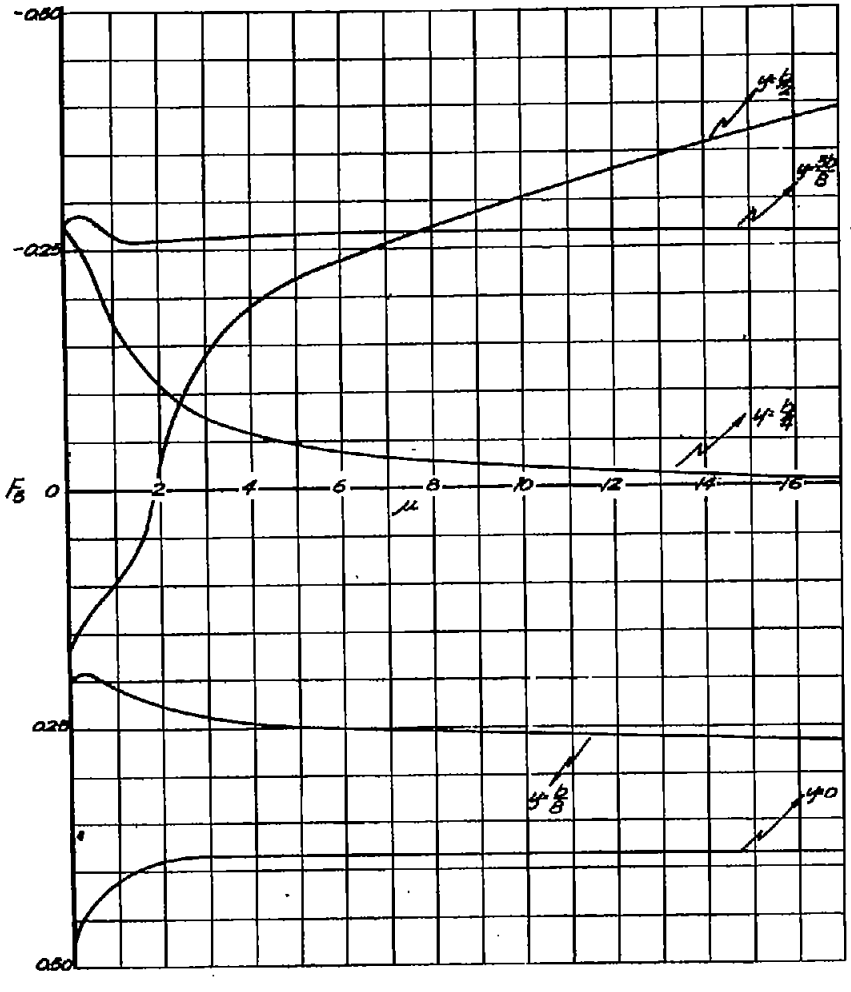

FIG. 9

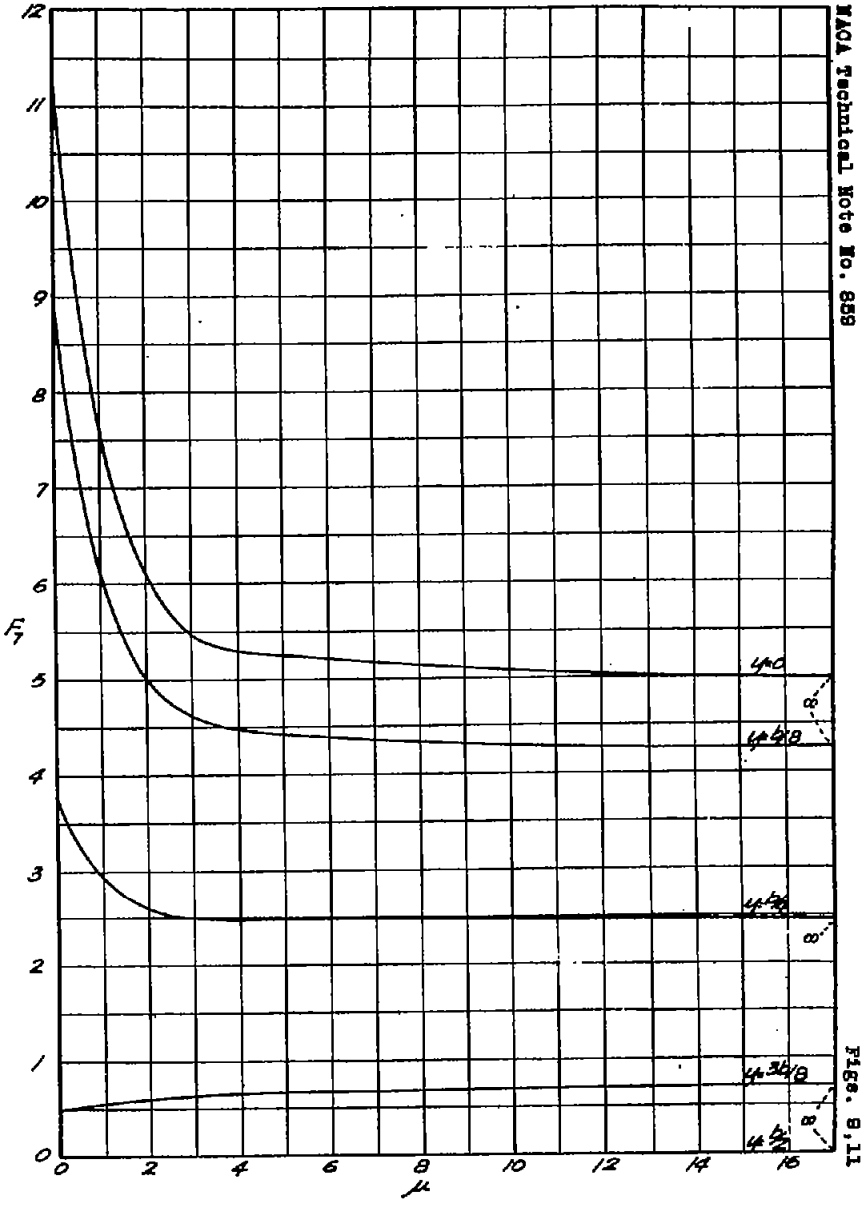

FIG. 11

FIGS. 8, 11

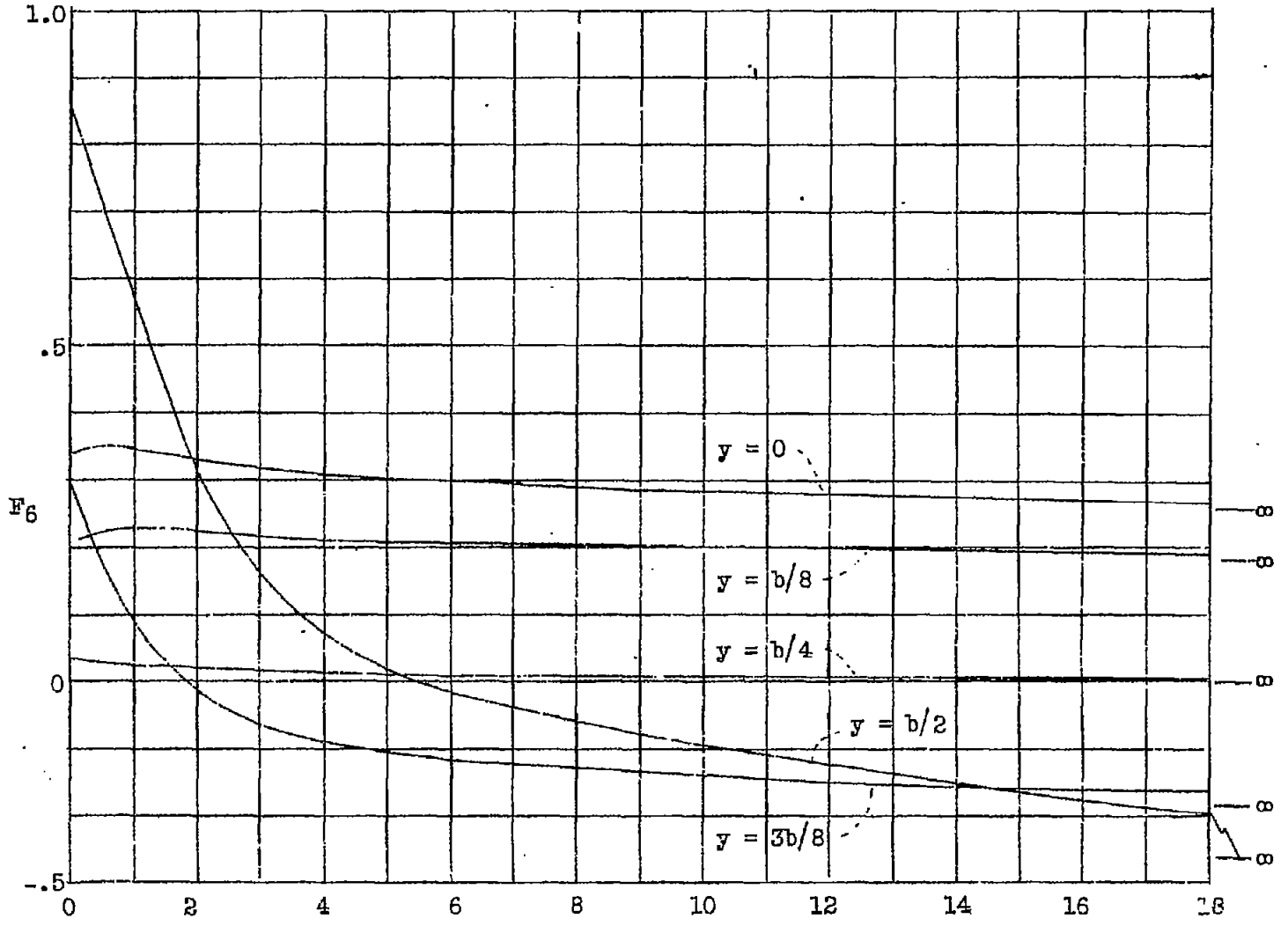

Figure 10

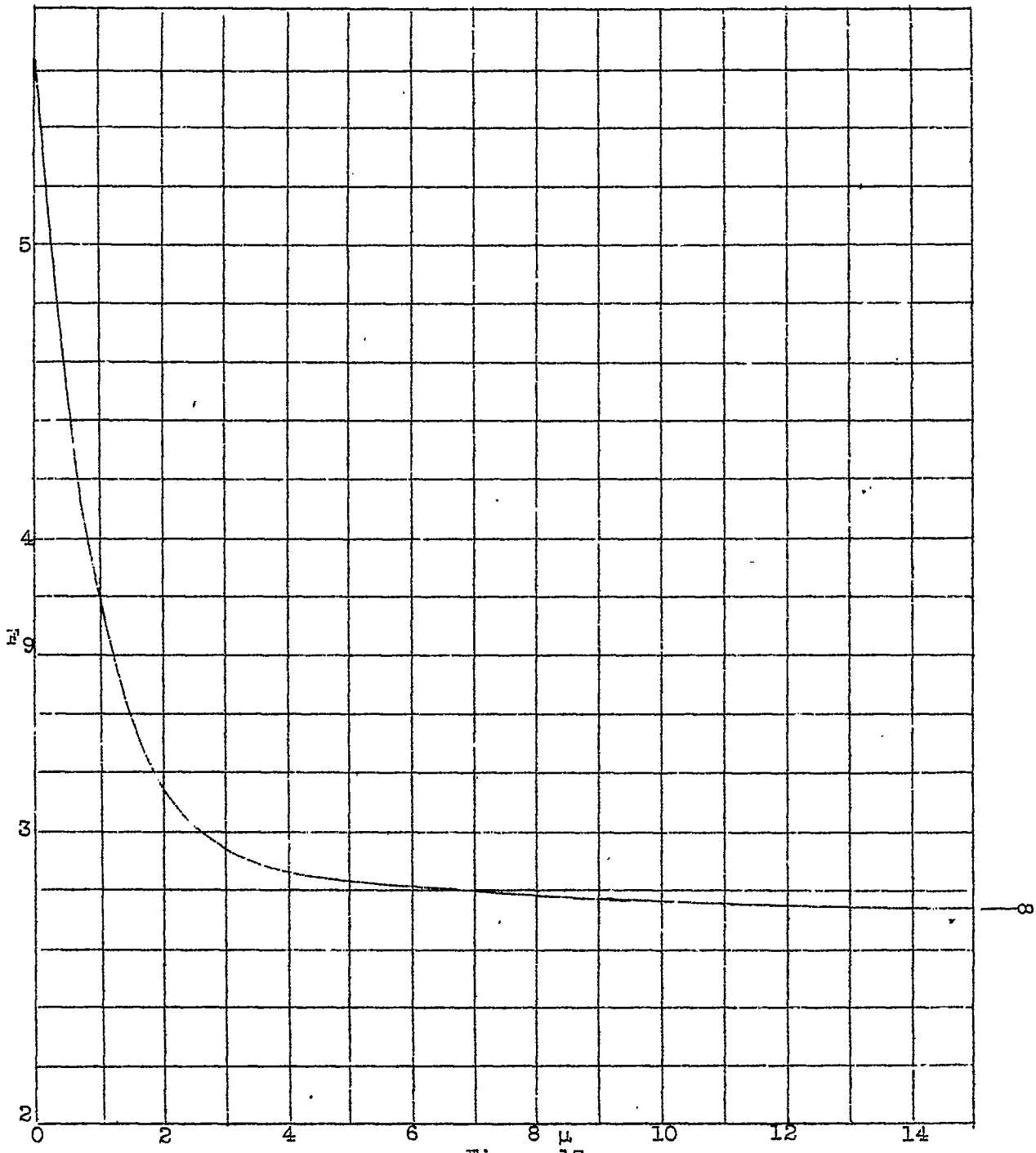

Figure 13

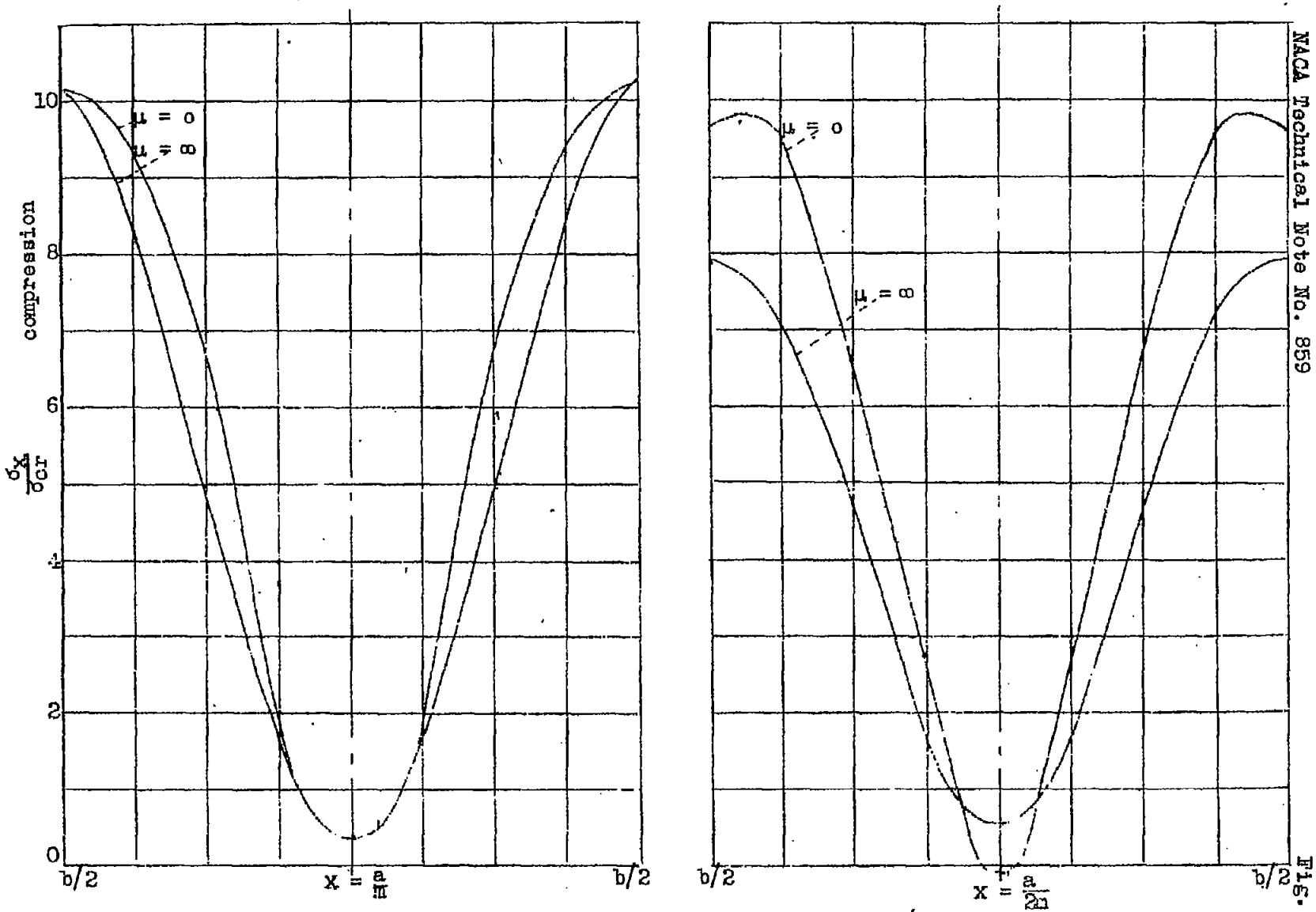

Figure 14.- Axial stress distribution for $\frac{\sigma_{ST}}{\sigma_{cr}} = 10$

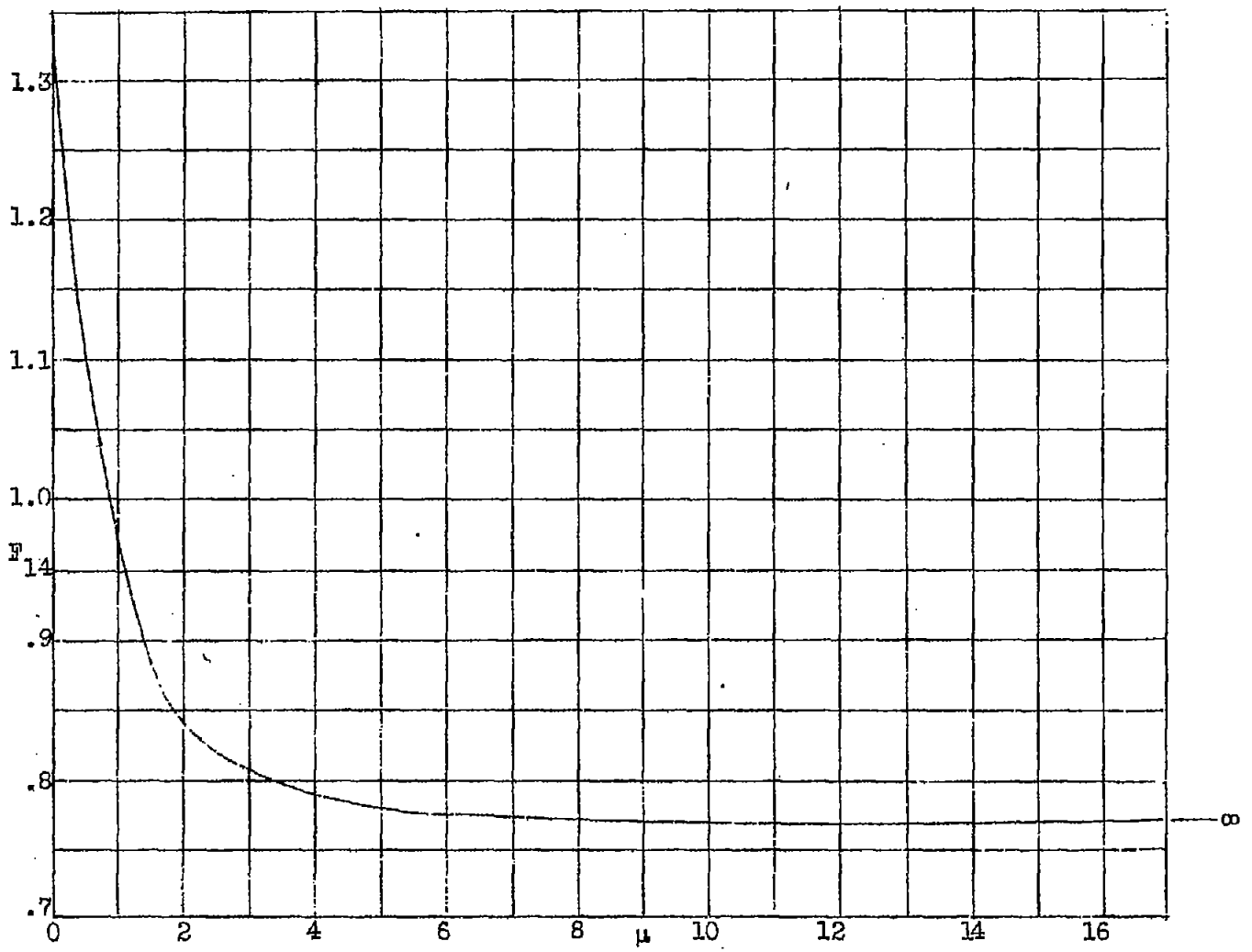

Figure 15

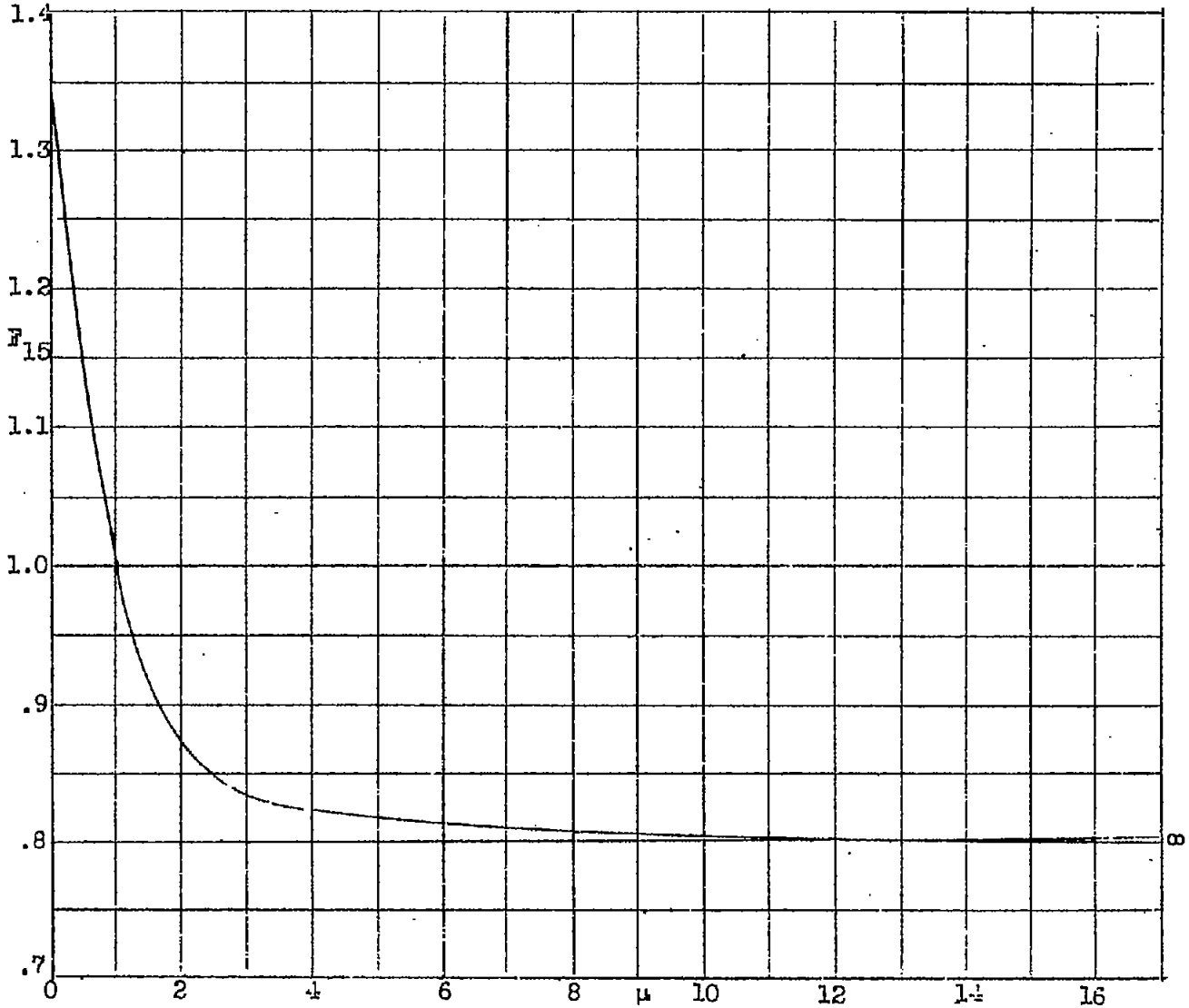

Figure 16

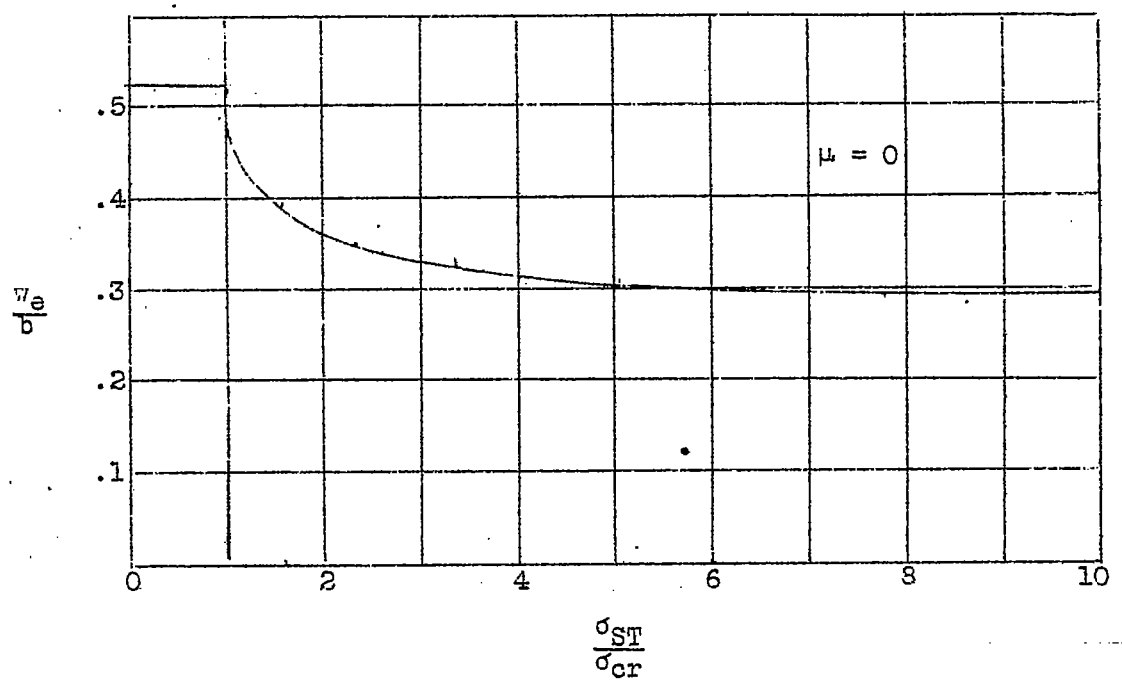

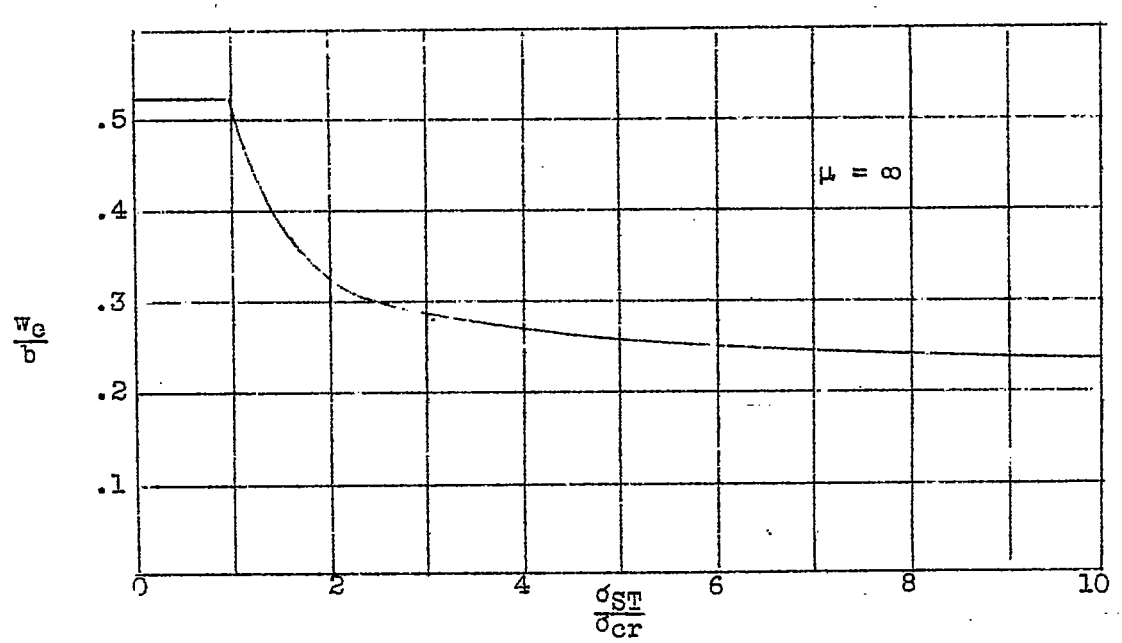

Figure 17.- Mean effective width as a function of $\frac{\sigma_{ST}}{\sigma_{cr}}$ $\left(E_S = E_{ST}\right)$

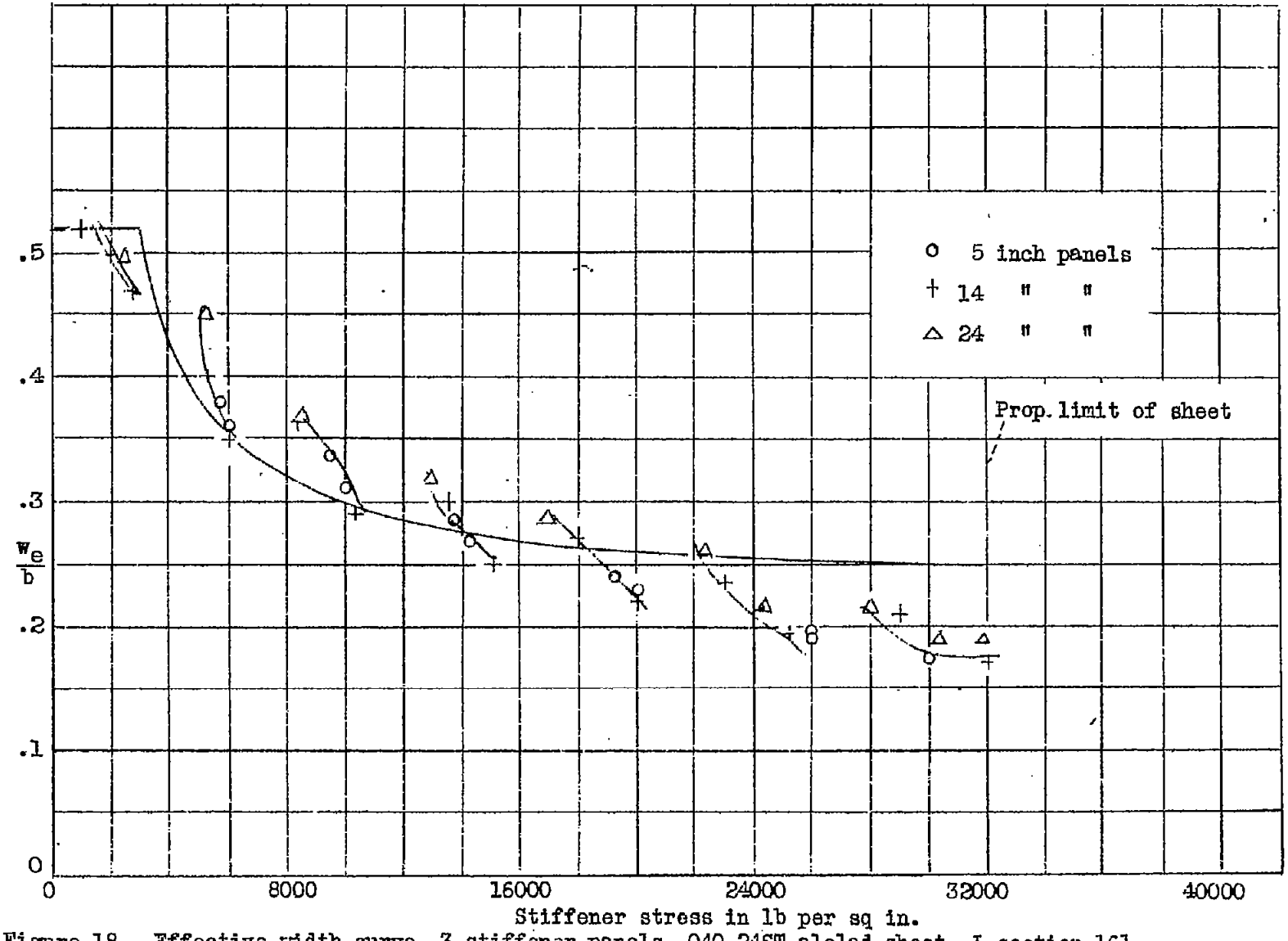

Figure 18.- Effective width curve, 3 stiffener panels, 040 24ST alclad sheet, J-section 161

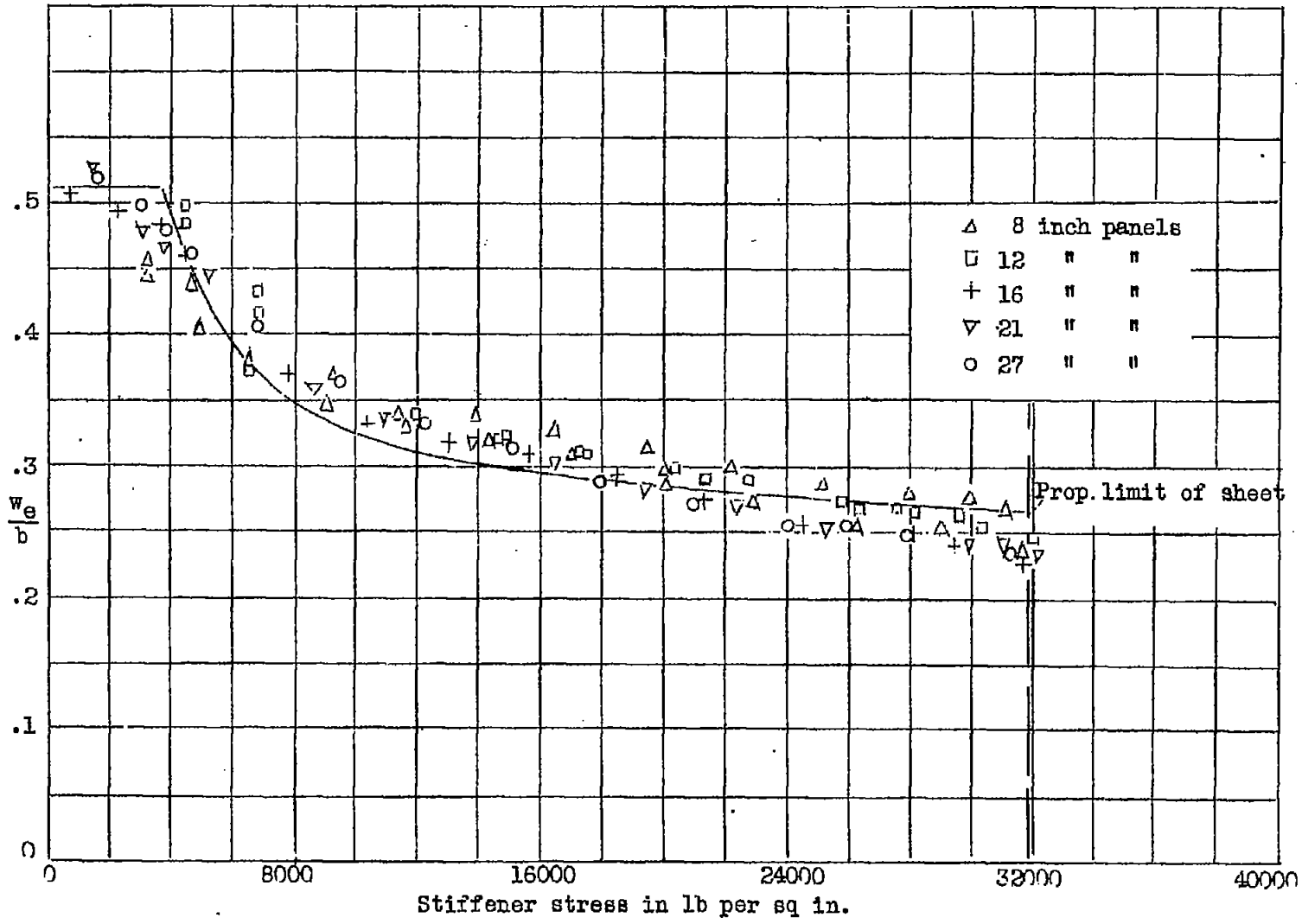

Figure 18a.- Effective width curve, 3 stiffener panels, .040 24ST alclad sheet, bulb angle #8477

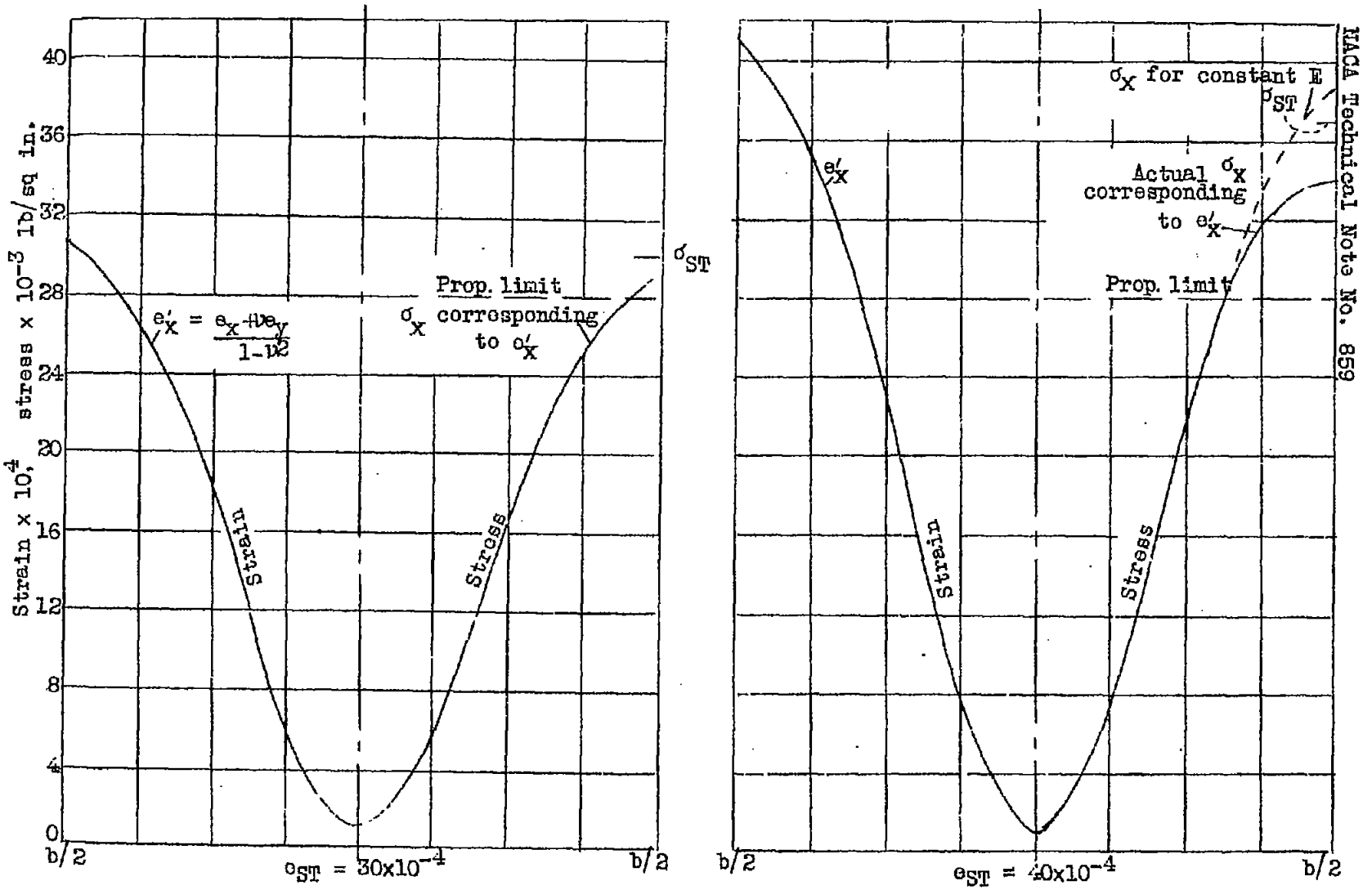

Figure 19.- Axial stress and strain distribution beyond proportional limit.

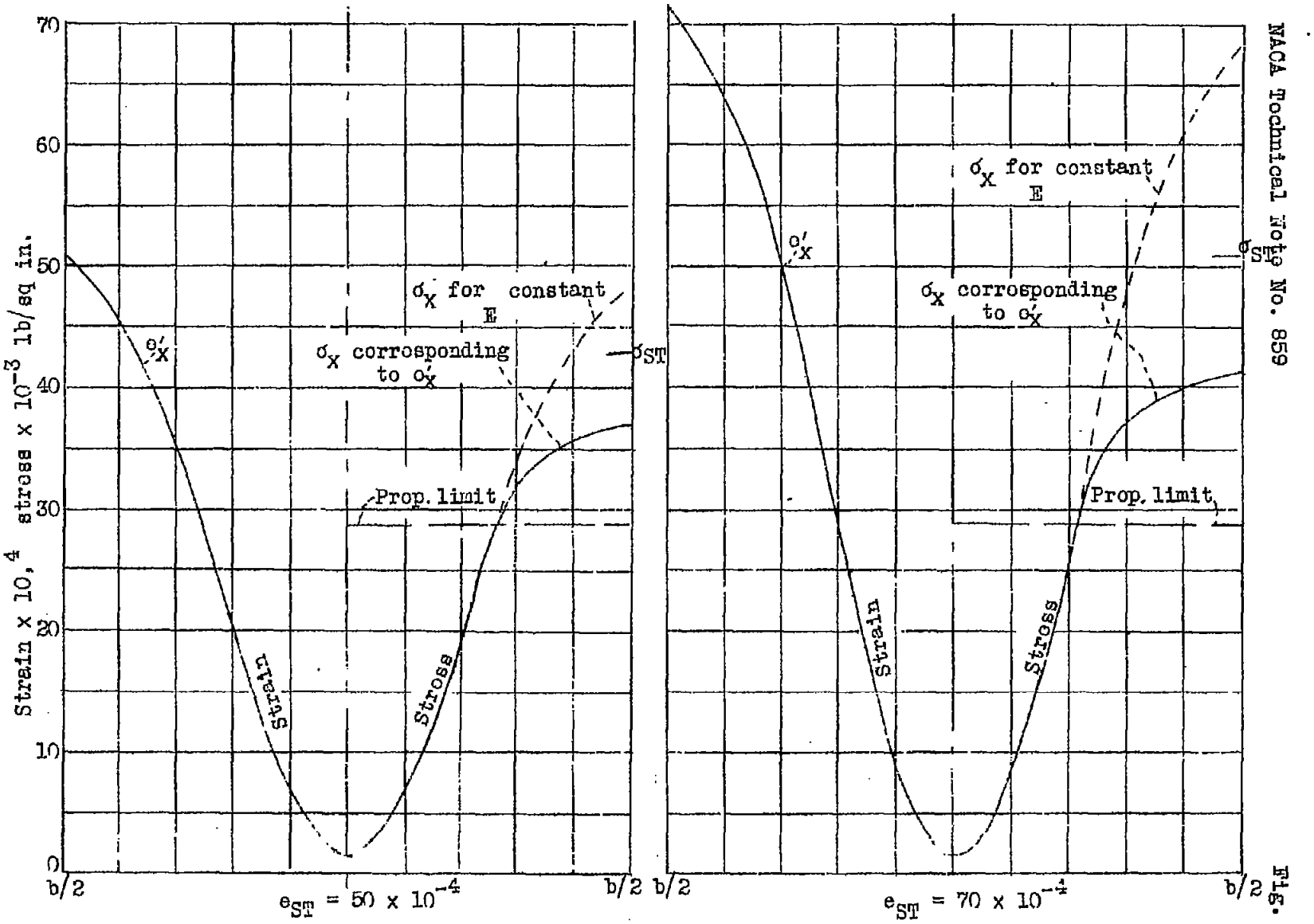

Figure 20.- Axial strain and stress distribution beyond proportional limit

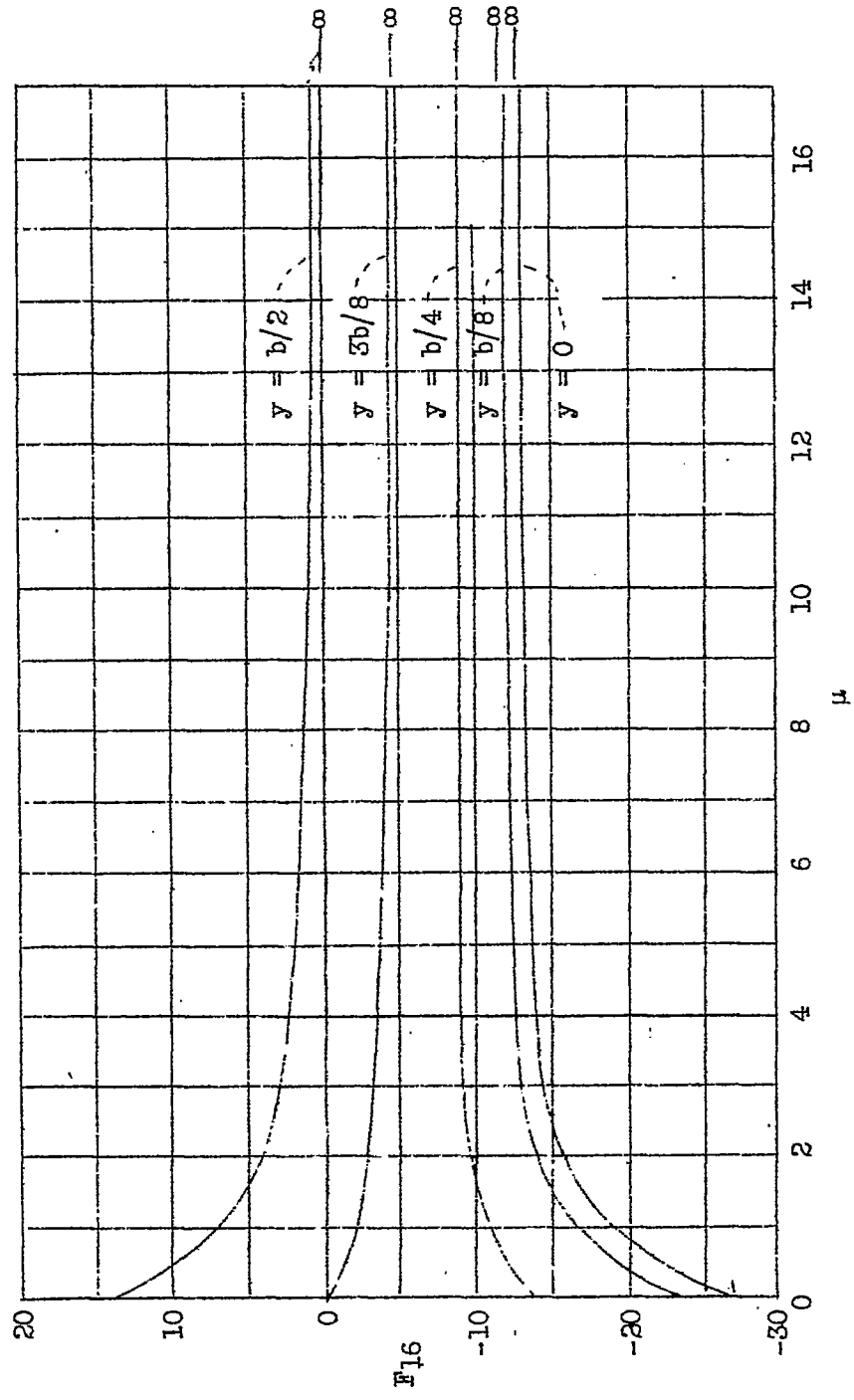

Figure 21

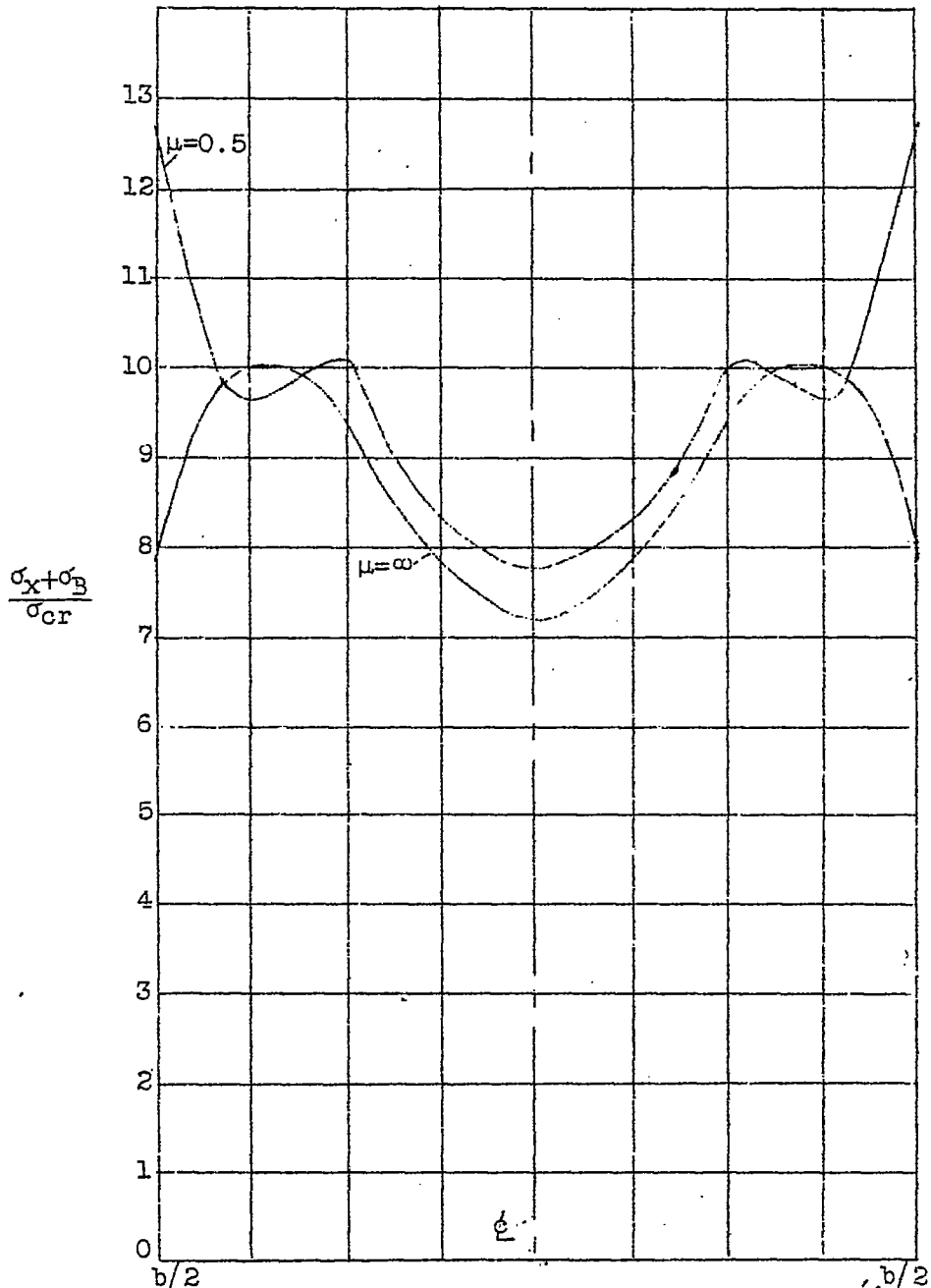

Figure 22.- Combined axial stress distribution at $x=\frac{a}{2m}\left(\frac{\sigma_{ST}^{b/2}}{\sigma_{cr}}=10\right)$

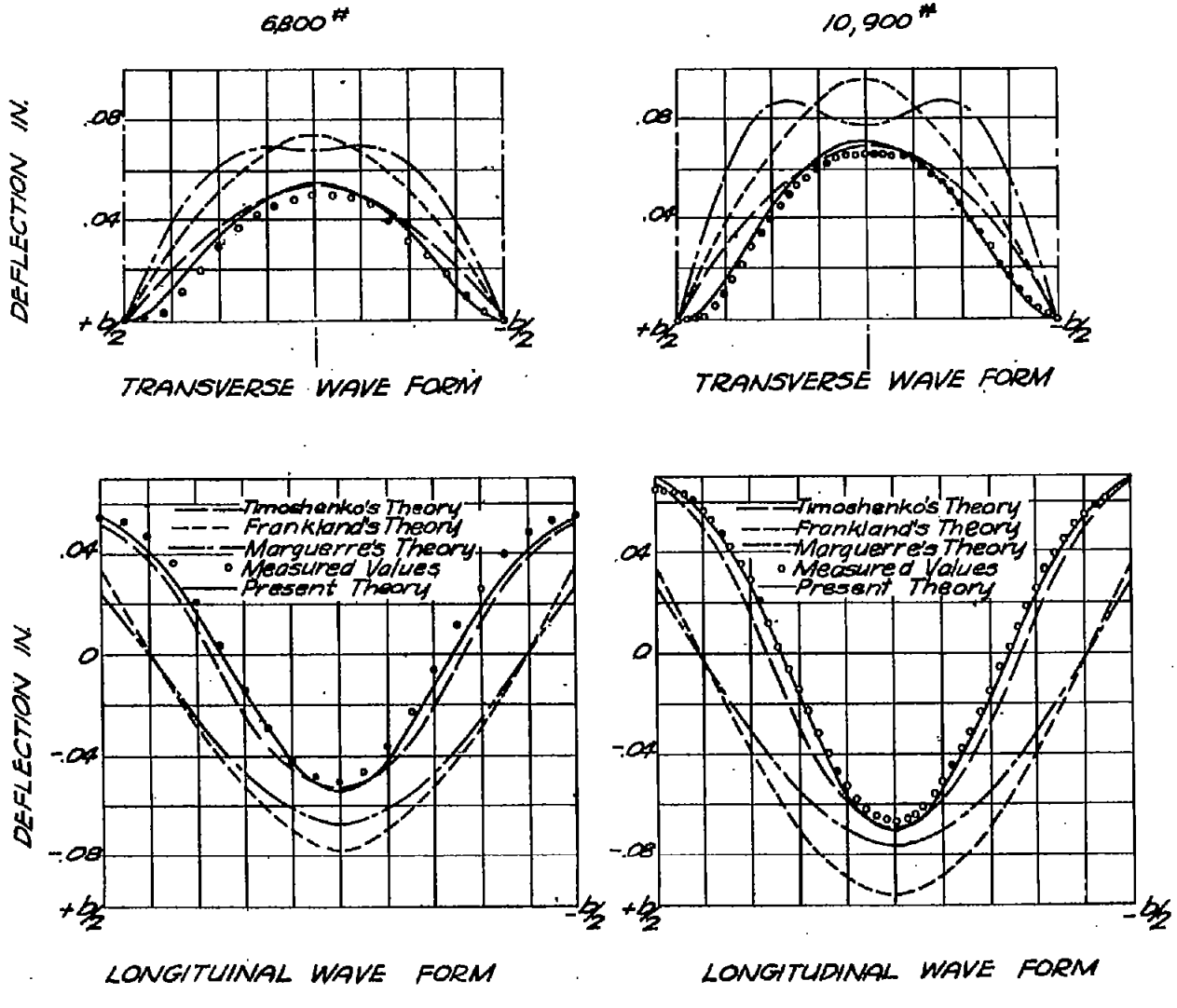

COMPARISON OF CALCULATED WAVE FORM WITH MEASURED VALUES GIVEN IN REF. 4

FIG. 23

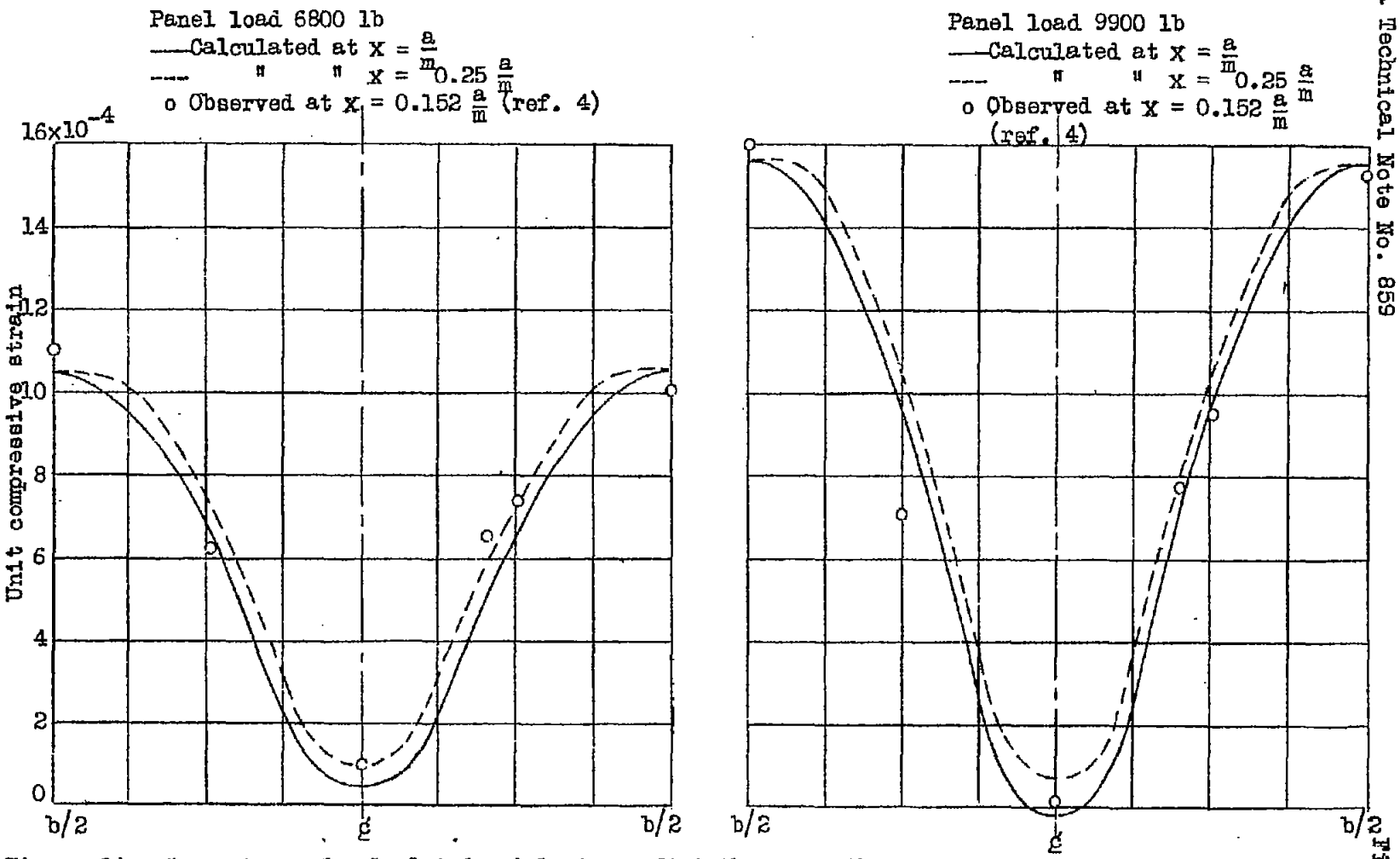

Figure 24.- Comparison of calculated axial strain distribution with experimental results given in reference 4.

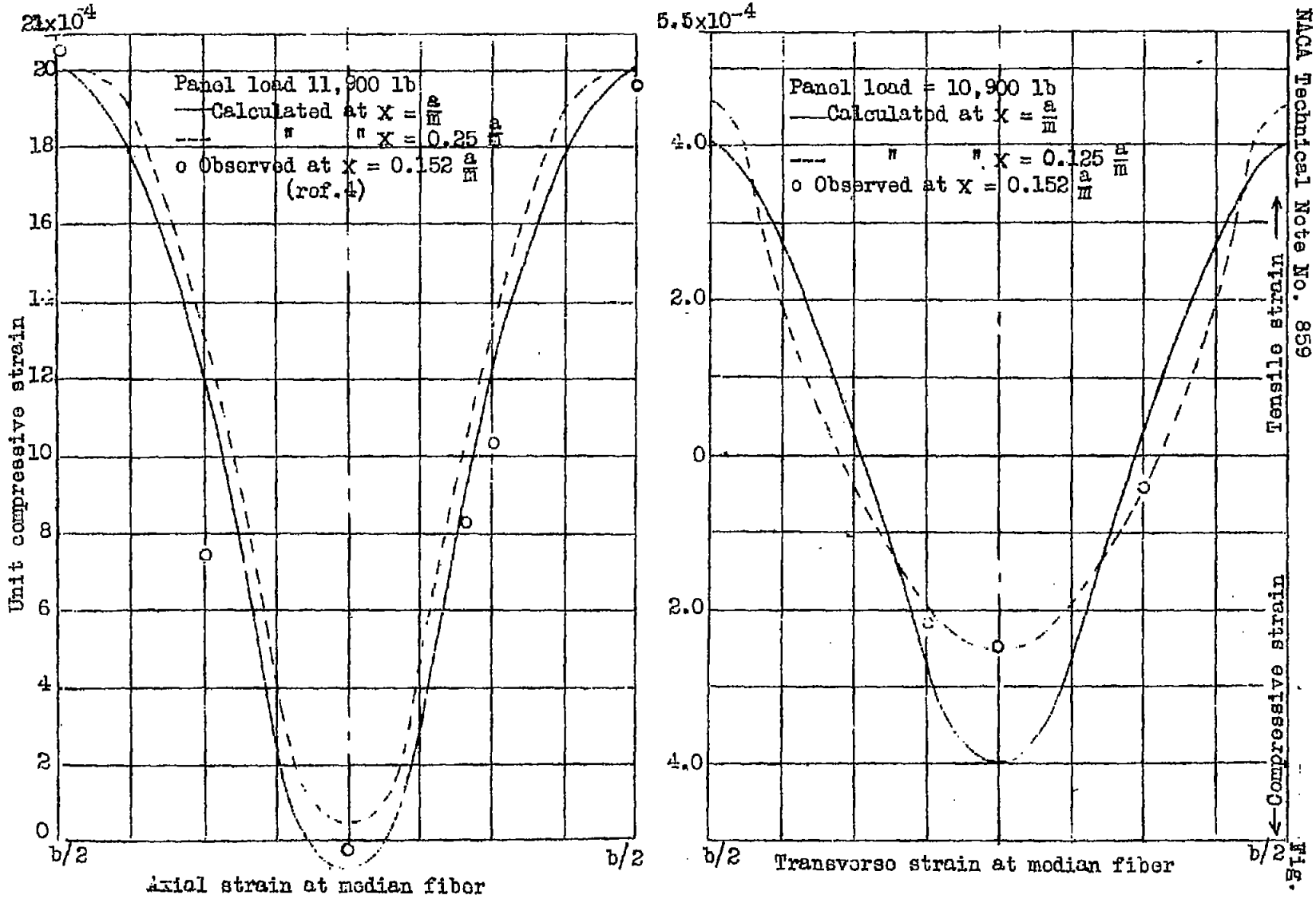

Fig. 25

Figure 25.- Comparison of calculated strain distribution with experimental results given in ref. 4.

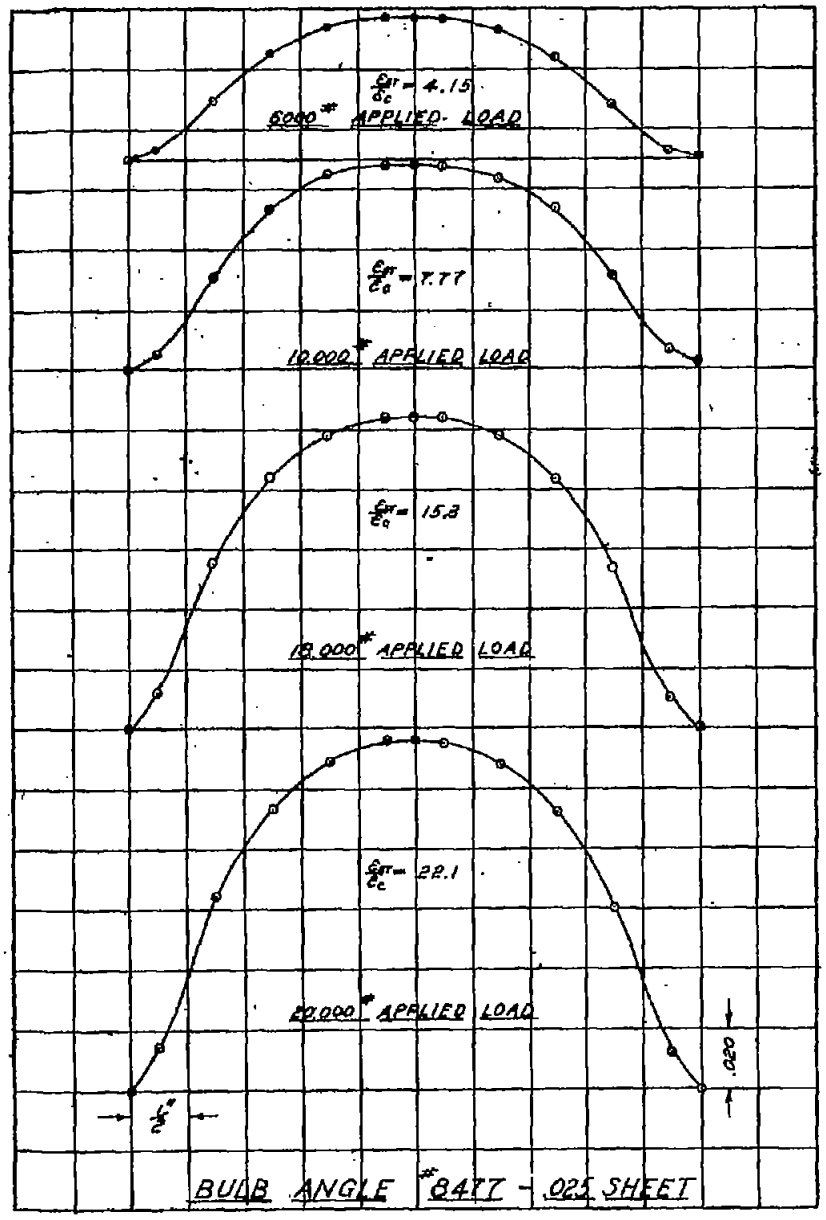
$\frac{\epsilon_{gr}}{\epsilon_c}$ = 4.15
5000# APPLIED LOAD
$\frac{\epsilon_{gr}}{\epsilon_c}$ = 7.77
10,000# APPLIED LOAD
$\frac{\epsilon_{gr}}{\epsilon_c}$ = 15.3
15,000# APPLIED LOAD
$\frac{\epsilon_{gr}}{\epsilon_c}$ = 22.1
20,000# APPLIED LOAD
.020
½"
BULB ANGLE #8477 - .025 SHEET

Fig. 26

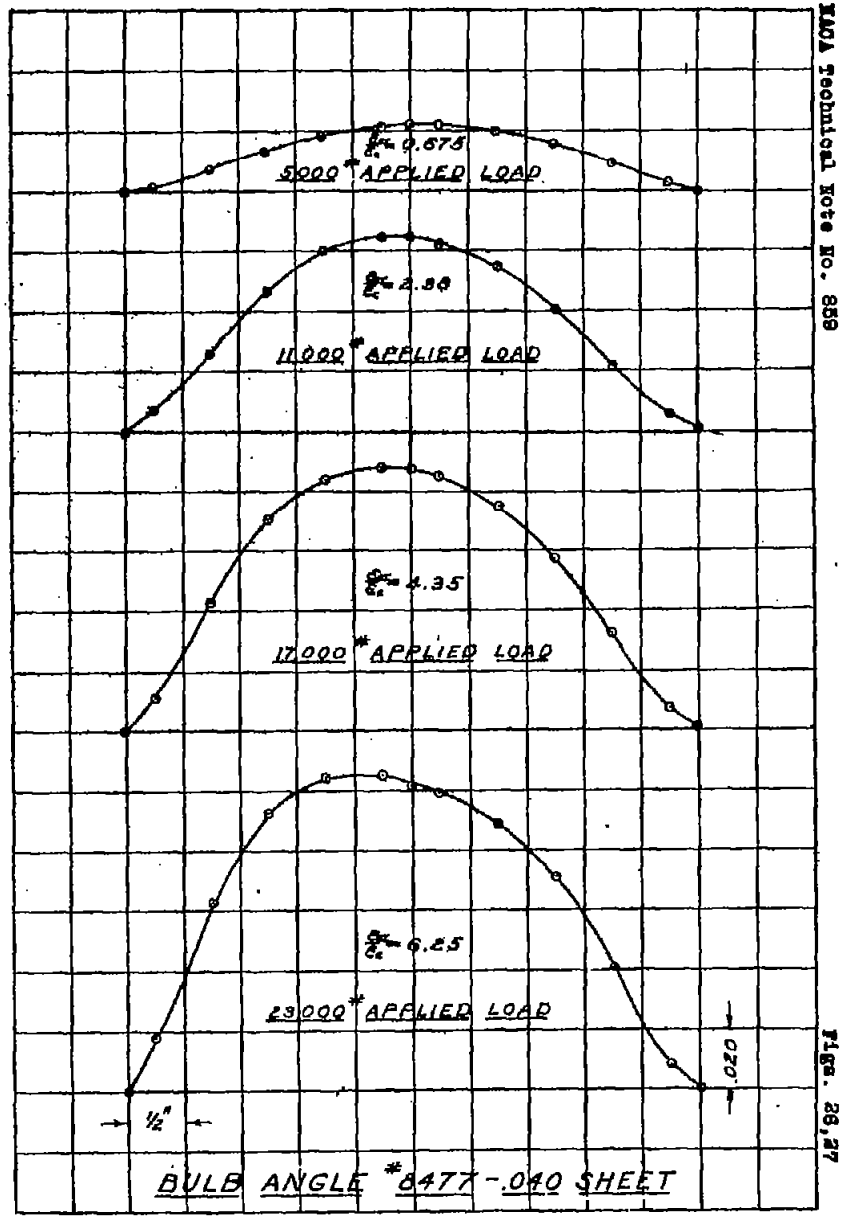
$\frac{\epsilon_{gr}}{\epsilon_c}$ = 0.675
5000# APPLIED LOAD
$\frac{\epsilon_{gr}}{\epsilon_c}$ = 2.30
11,000# APPLIED LOAD
$\frac{\epsilon_{gr}}{\epsilon_c}$ = 4.35
17,000# APPLIED LOAD
$\frac{\epsilon_{gr}}{\epsilon_c}$ = 6.25
23,000# APPLIED LOAD
.020
½"
BULB ANGLE #8477 - .040 SHEET

Fig. 27

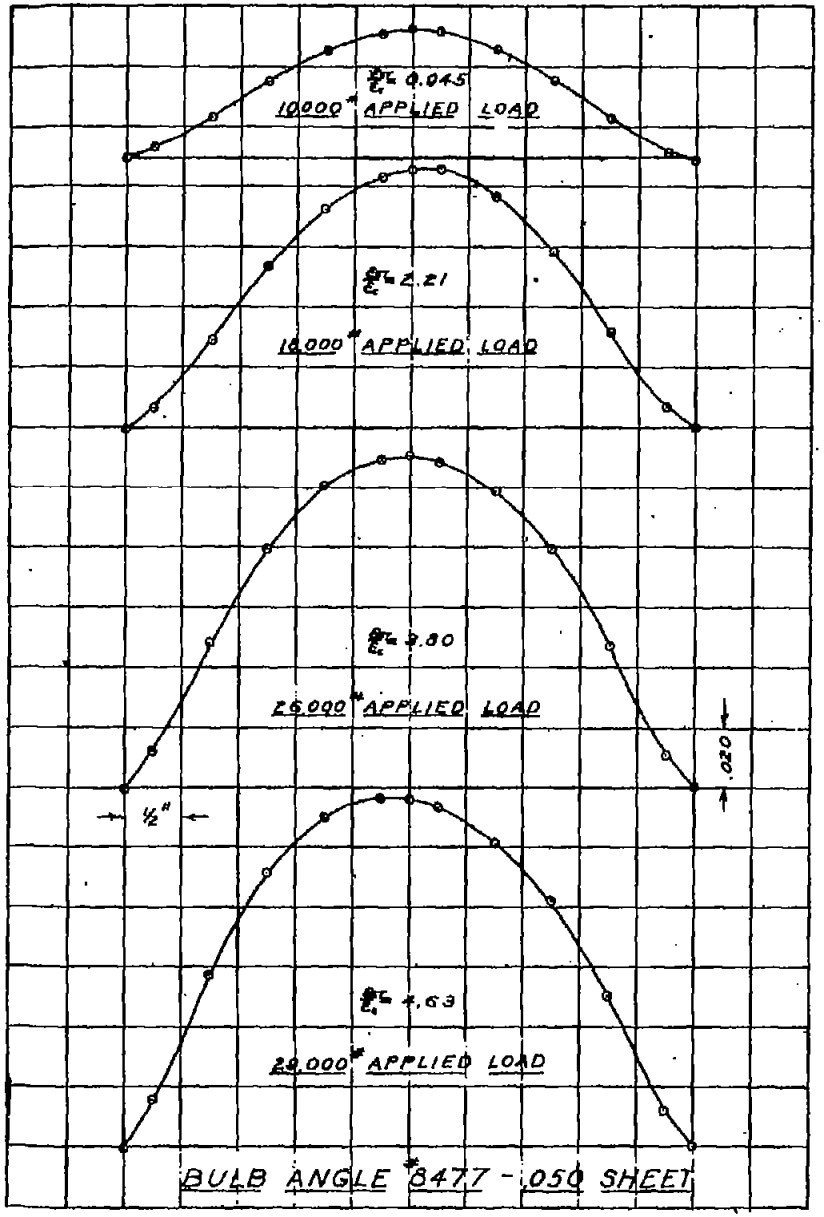
$\frac{\epsilon_T}{\epsilon_c}$ = 0.045
10000# APPLIED LOAD
$\frac{\epsilon_T}{\epsilon_c}$ = 2.21
16,000# APPLIED LOAD
$\frac{\epsilon_T}{\epsilon_c}$ = 3.80
26,000# APPLIED LOAD
.020
½"
$\frac{\epsilon_T}{\epsilon_c}$ = 4.63
29,000# APPLIED LOAD
BULB ANGLE #8477 - .050 SHEET

Fig. 28

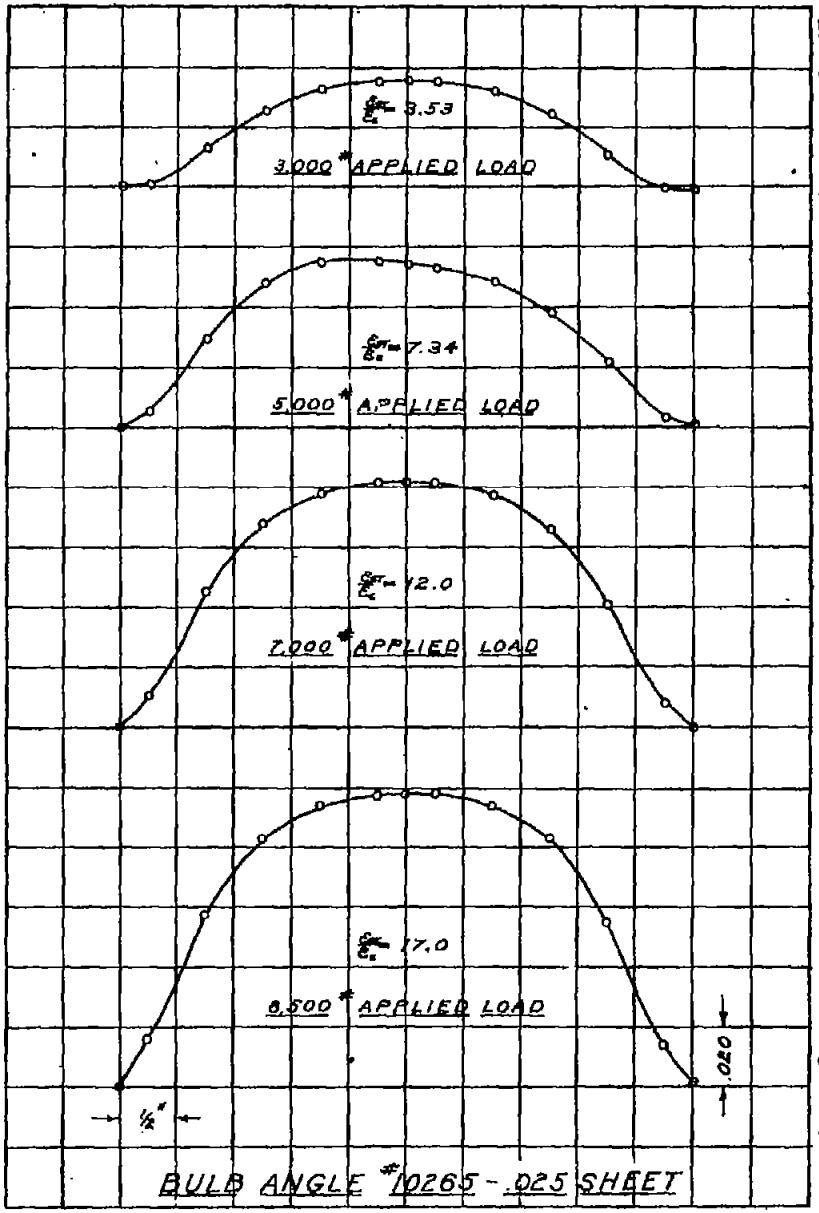
$\frac{\epsilon_T}{\epsilon_c}$ = 3.53
3,000# APPLIED LOAD
$\frac{\epsilon_T}{\epsilon_c}$ = 7.34
5,000# APPLIED LOAD
$\frac{\epsilon_T}{\epsilon_c}$ = 12.0
7,000# APPLIED LOAD
$\frac{\epsilon_T}{\epsilon_c}$ = 17.0
8,500# APPLIED LOAD
.070
½"
BULB ANGLE #10265 - .025 SHEET

Fig. 29

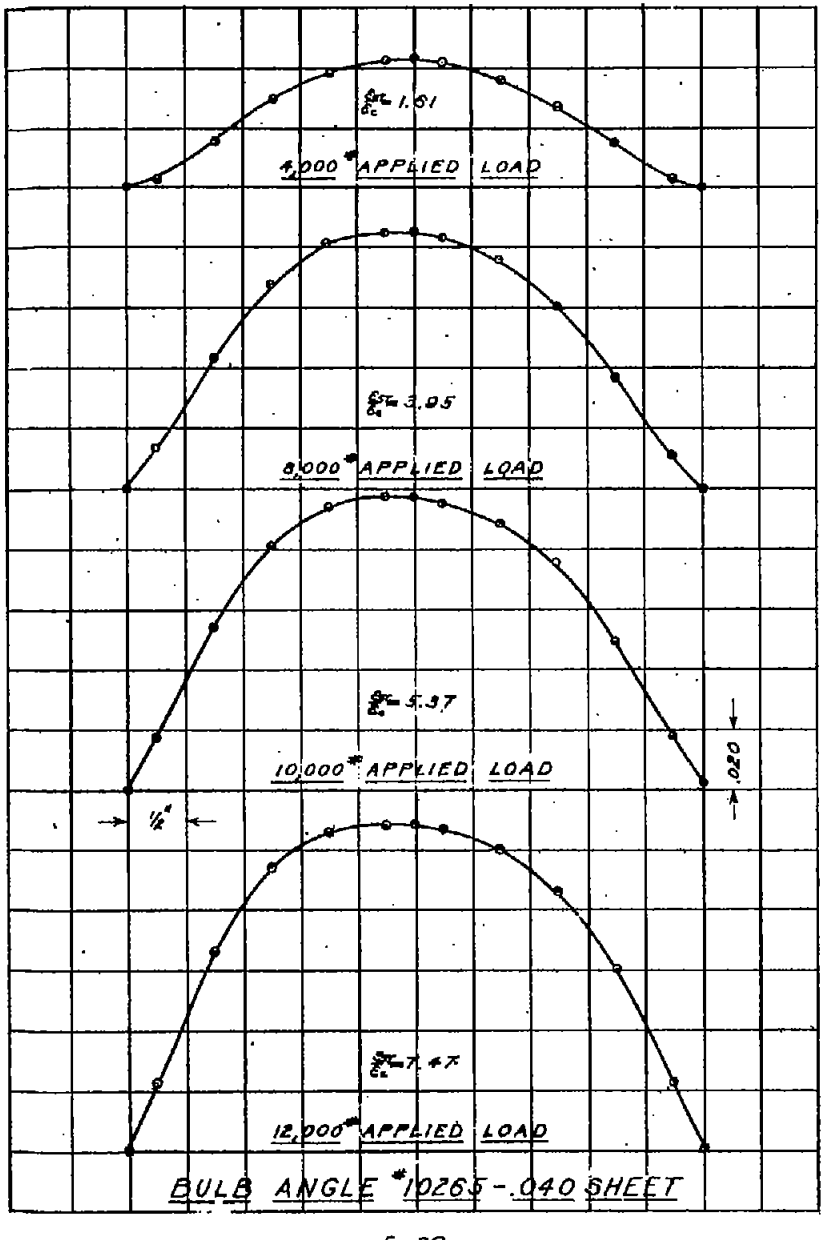
$\frac{\varepsilon_T}{\varepsilon_c}$ = 1.51
4,000 # APPLIED LOAD
$\frac{\varepsilon_T}{\varepsilon_c}$ = 3.05
8,000 # APPLIED LOAD
$\frac{\varepsilon_T}{\varepsilon_c}$ = 5.37
10,000 # APPLIED LOAD
$\frac{\varepsilon_T}{\varepsilon_c}$ = 7.47
12,000 # APPLIED LOAD
½"
.020
BULB ANGLE #10265 - .040 SHEET

Fig. 30

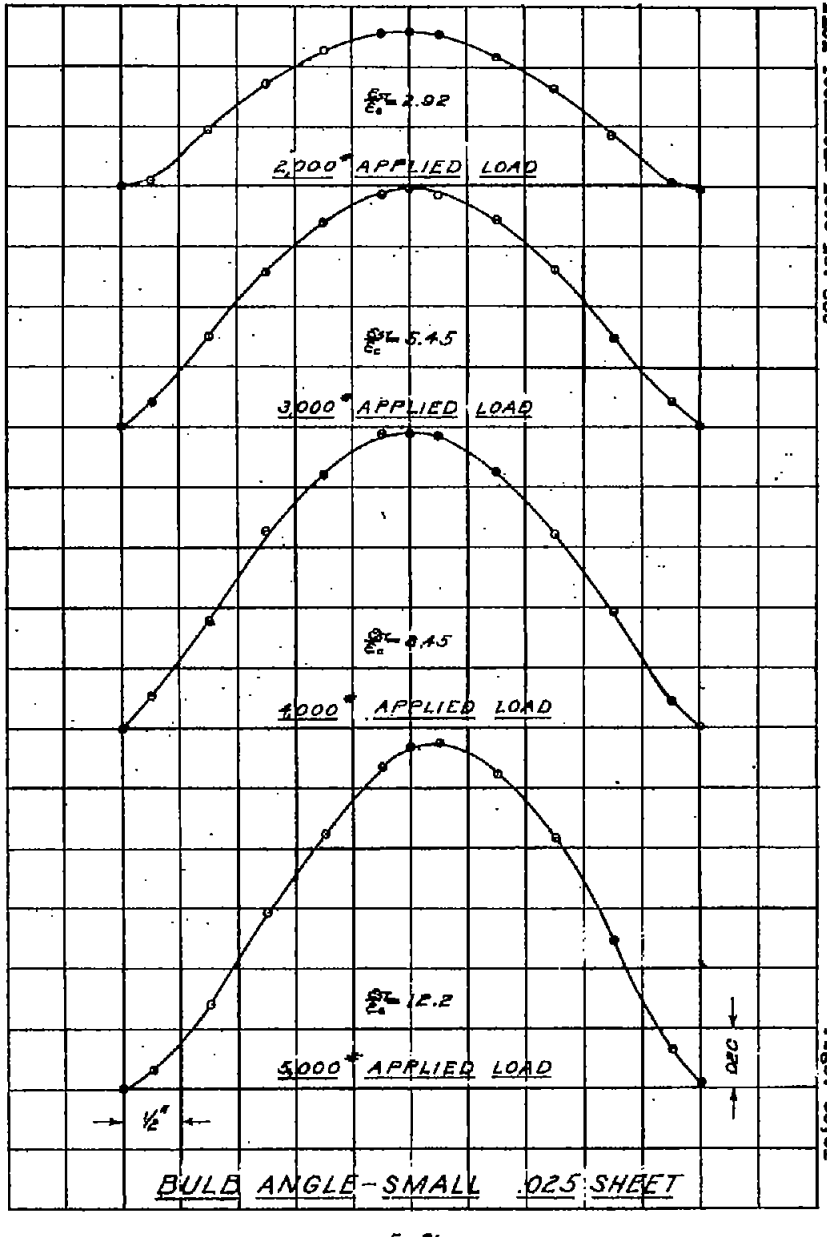
$\frac{\varepsilon_T}{\varepsilon_c}$ = 2.92
2,000 # APPLIED LOAD
$\frac{\varepsilon_T}{\varepsilon_c}$ = 5.45
3,000 # APPLIED LOAD
$\frac{\varepsilon_T}{\varepsilon_c}$ = 8.45
4,000 # APPLIED LOAD
$\frac{\varepsilon_T}{\varepsilon_c}$ = 12.2
5,000 # APPLIED LOAD
½"
.020
BULB ANGLE - SMALL .025 SHEET

Fig. 31

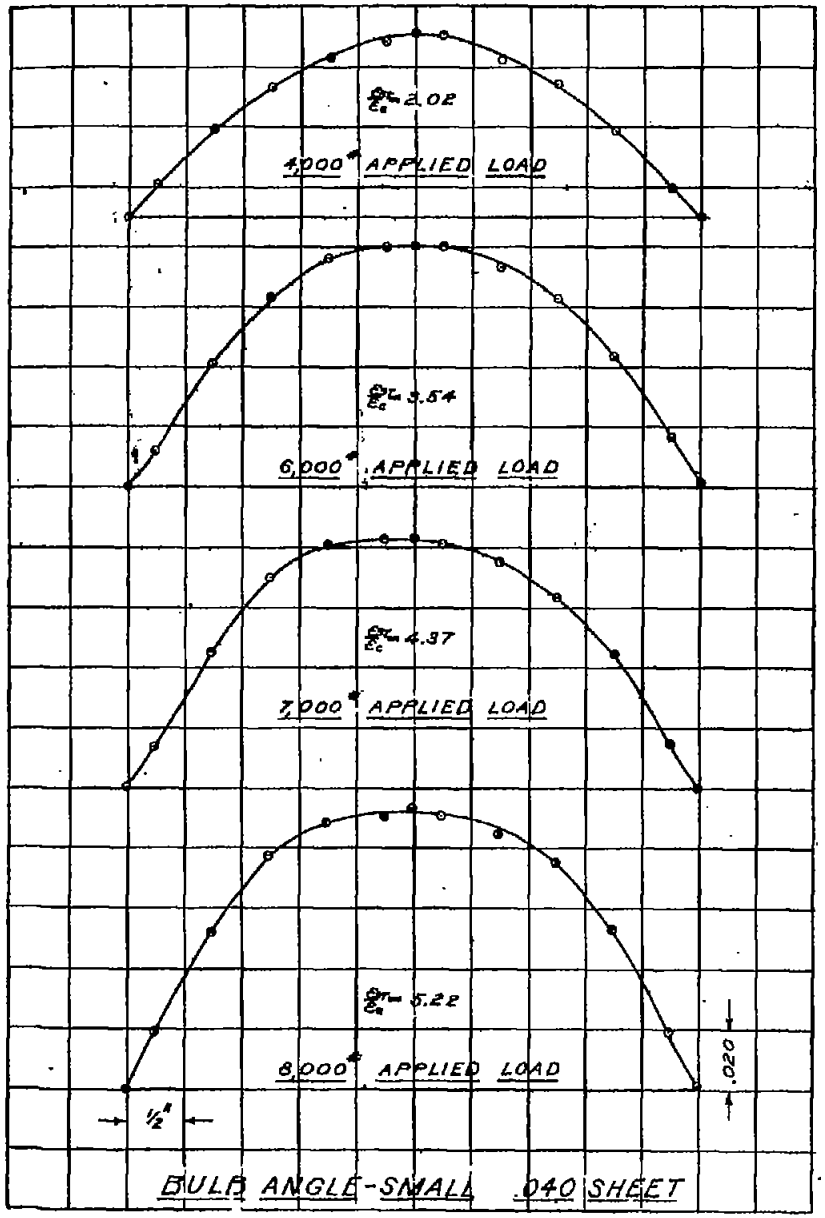
$\frac{\sigma_T}{\sigma_c}$= 2.02
4,000# APPLIED LOAD
$\frac{\sigma_T}{\sigma_c}$= 3.54
6,000# APPLIED LOAD
$\frac{\sigma_T}{\sigma_c}$= 4.37
7,000# APPLIED LOAD
$\frac{\sigma_T}{\sigma_c}$= 5.22
8,000# APPLIED LOAD
½"
.020
BULB ANGLE-SMALL .040 SHEET

Fig 32

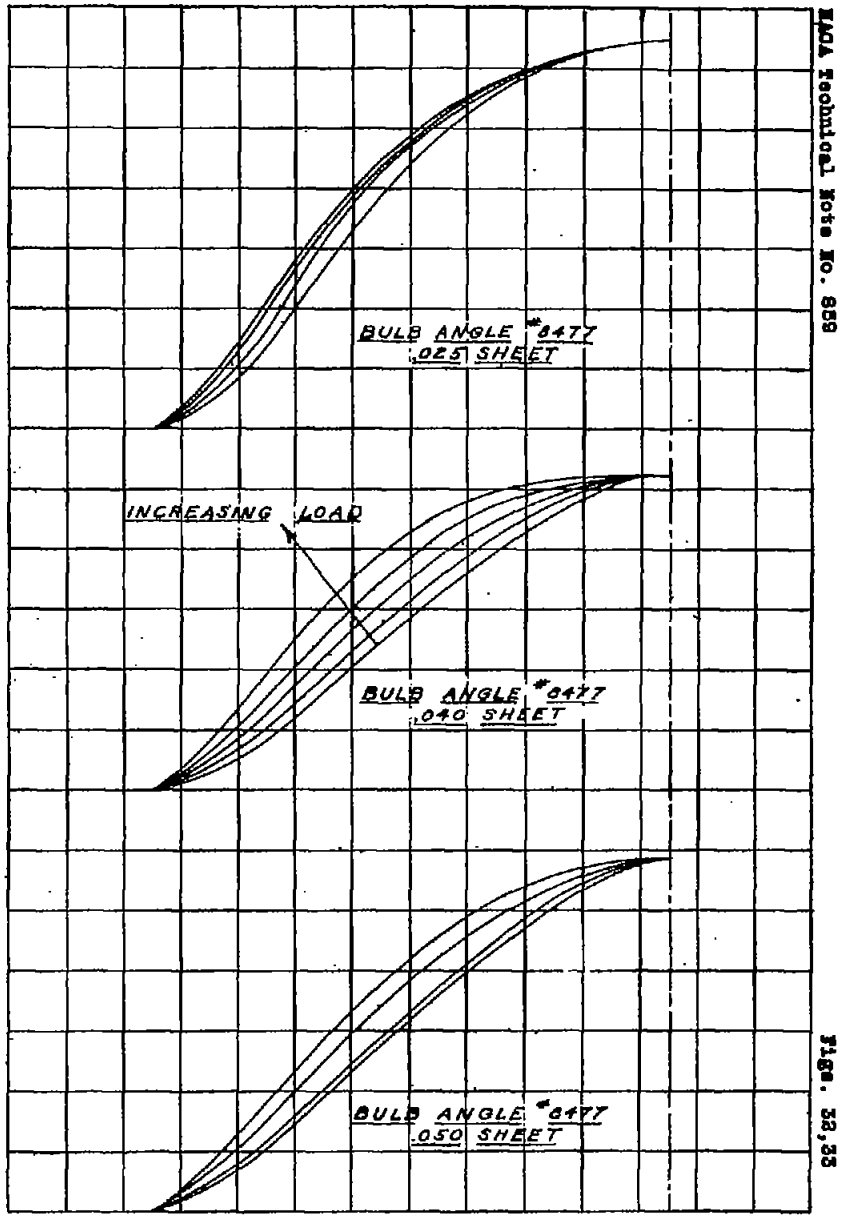
BULB ANGLE #6477
.025 SHEET
INCREASING LOAD
BULB ANGLE #6477
.040 SHEET
BULB ANGLE #6477
.050 SHEET

Fig. 33

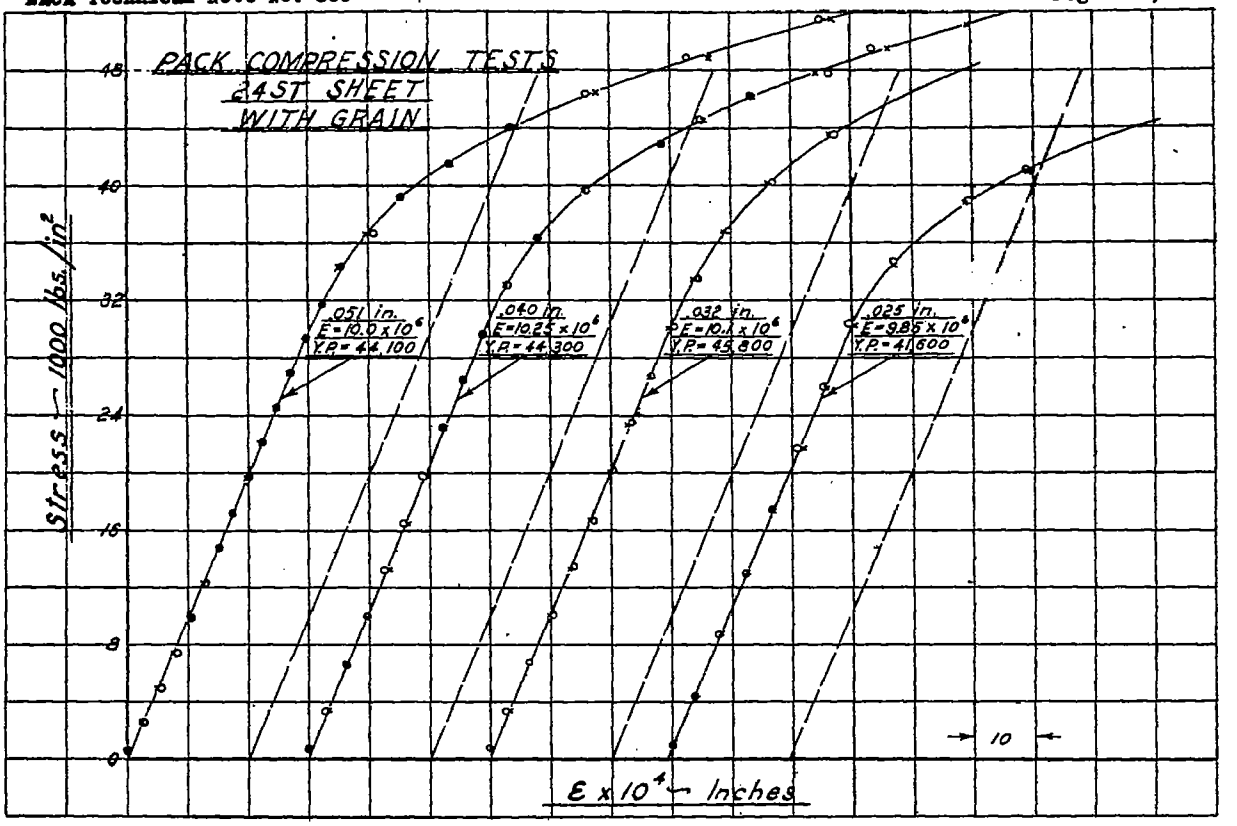
PACK COMPRESSION TESTS
24ST SHEET
WITH GRAIN
Stress — 1000 lbs./in.²
ε x 10⁴ — Inches
0
8
16
24
32
40
48
10
.051 in.
E=10.0 x 10⁶
Y.P.=44,100
.040 in.
E=10.25 x 10⁶
Y.P.=44,300
.032 in.
E=10.1 x 10⁶
Y.P.=45,800
.025 in.
E=9.85 x 10⁶
Y.P.=41,600

Fig.34

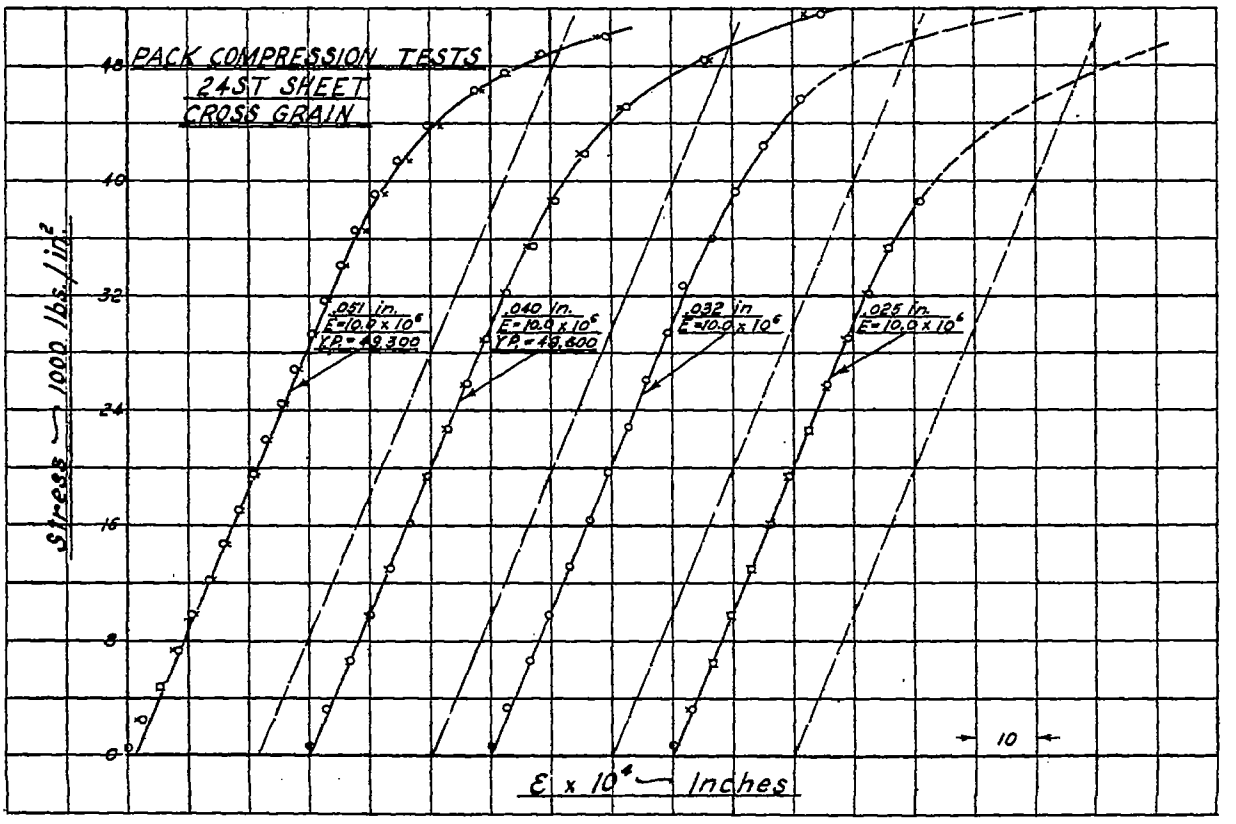
PACK COMPRESSION TESTS
24ST SHEET
CROSS GRAIN
Stress — 1000 lbs./in.²
ε x 10⁴ — Inches
0
8
16
24
32
40
48
10
.051 in.
E=10.0 x 10⁶
Y.P.=49,300
.040 in.
E=10.0 x 10⁶
Y.P.=48,600
.032 in.
E=10.0 x 10⁶
.025 in.
E=10.0 x 10⁶

Fig.35

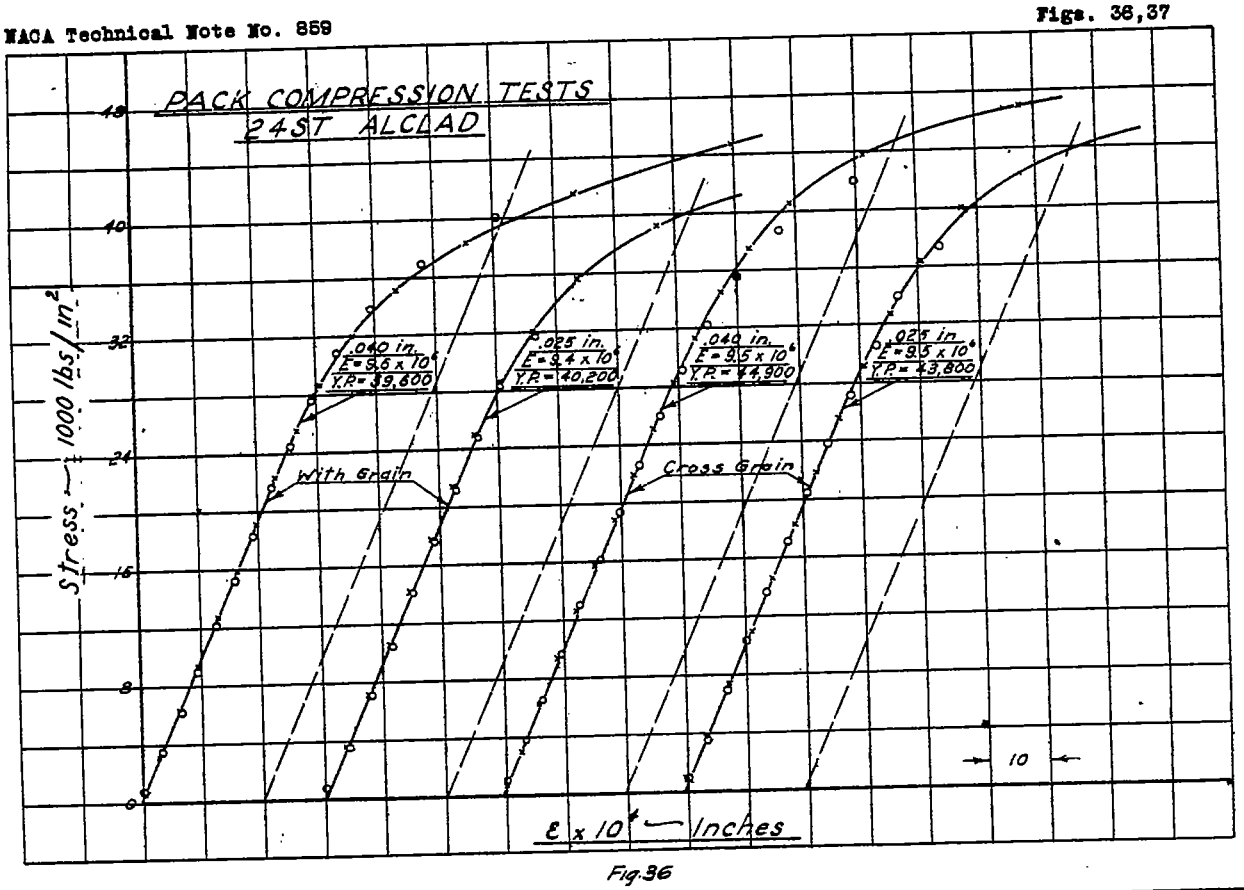
PACK COMPRESSION TESTS
24ST ALCLAD
Stress ~ 1000 lbs./in.²
48
40
32
24
16
8
0
.040 in.
E = 9.6 x 10⁶
Y.P. = 39,600
.025 in.
E = 9.4 x 10⁶
Y.P. = 40,200
.040 in.
E = 9.5 x 10⁶
Y.P. = 44,900
.025 in.
E = 9.5 x 10⁶
Y.P. = 43,800
With Grain
Cross Grain
10
ε x 10⁴ ~ Inches

Fig.36

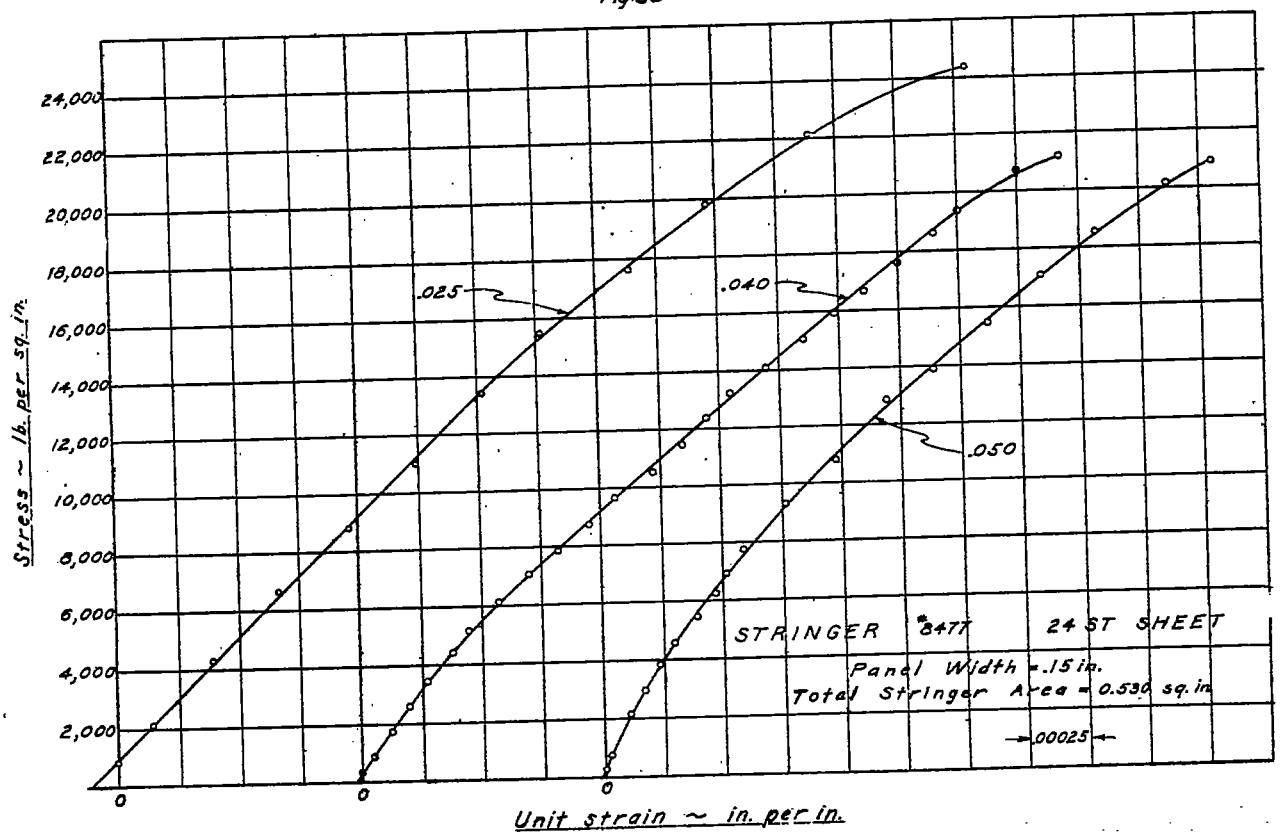
Stress ~ lb. per sq. in.
24,000
22,000
20,000
18,000
16,000
14,000
12,000
10,000
8,000
6,000
4,000
2,000
0
0
0
.025
.040
.050
STRINGER #477
24 ST SHEET
Panel Width = 15 in.
Total Stringer Area = 0.530 sq. in.
.00025
Unit strain ~ in. per in.

Fig. 37

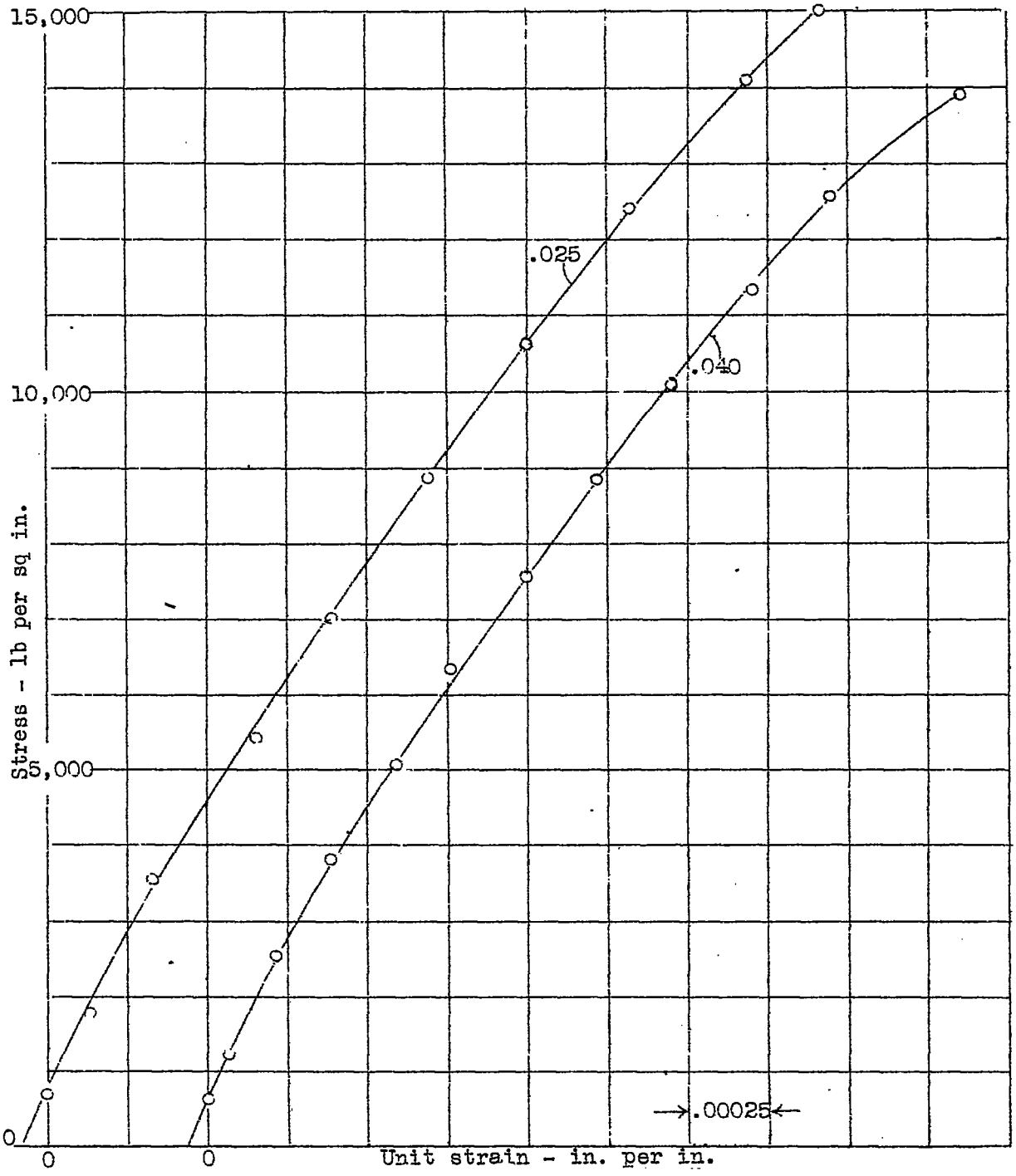

Figure 38.- Bulb angle 10265, 24ST sheet, panel width = 15 in., total stringer area = 0.1910 sq in.

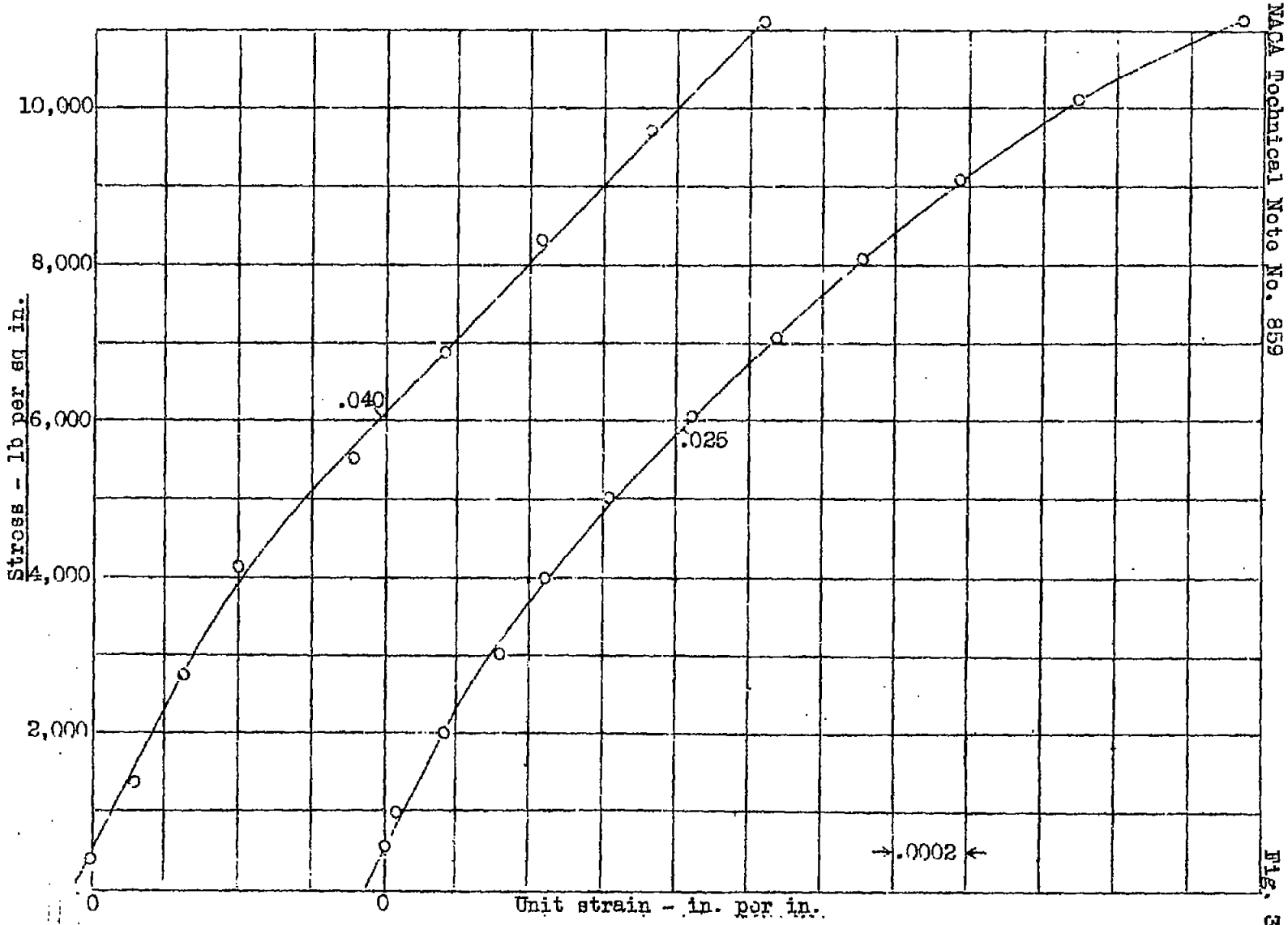

Ffgure 39.- Bulb angle 1, 24ST sheet, panel width = 15 in., total stringer area = 0.1150 sq in.

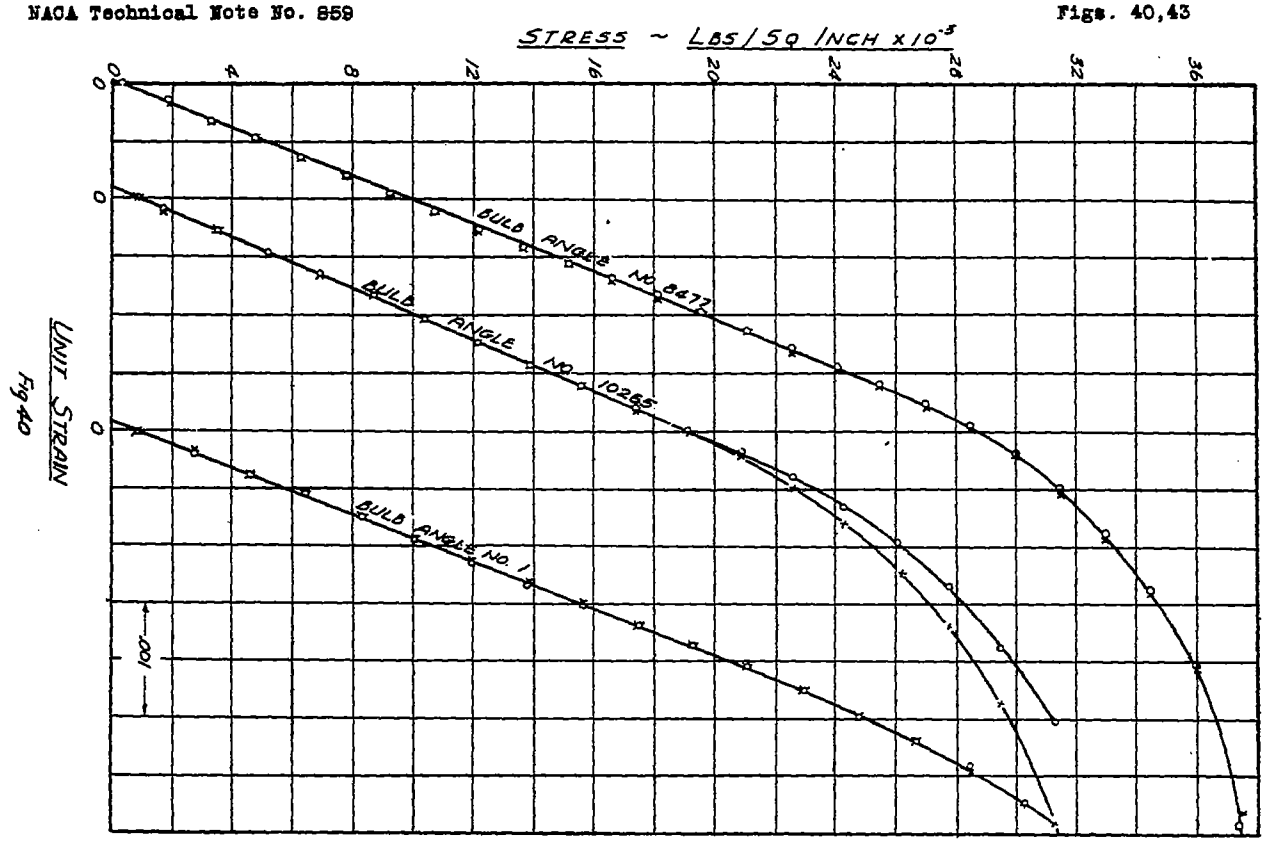

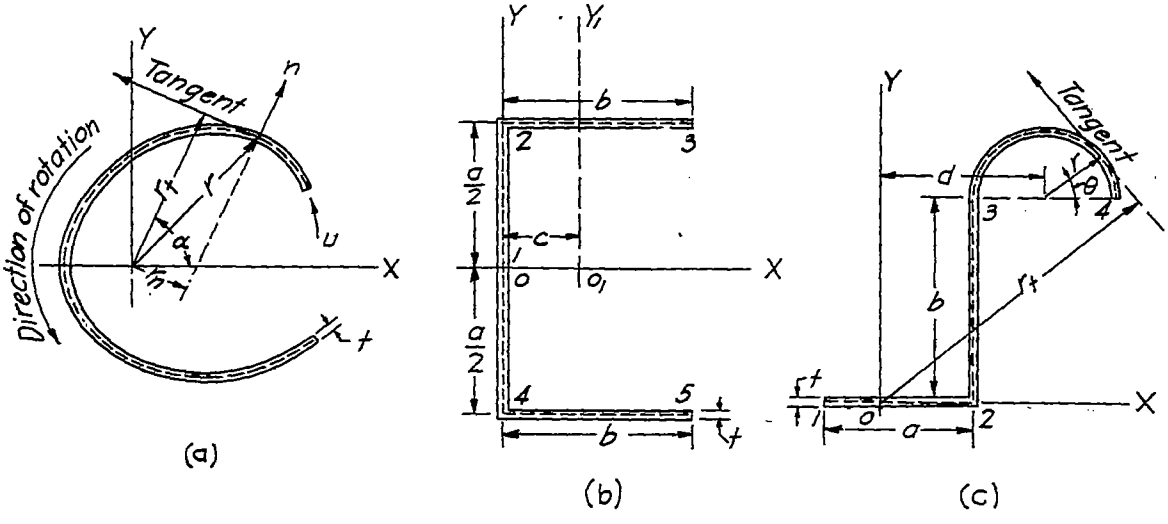

Notation for torsion column failure

Fig. 43

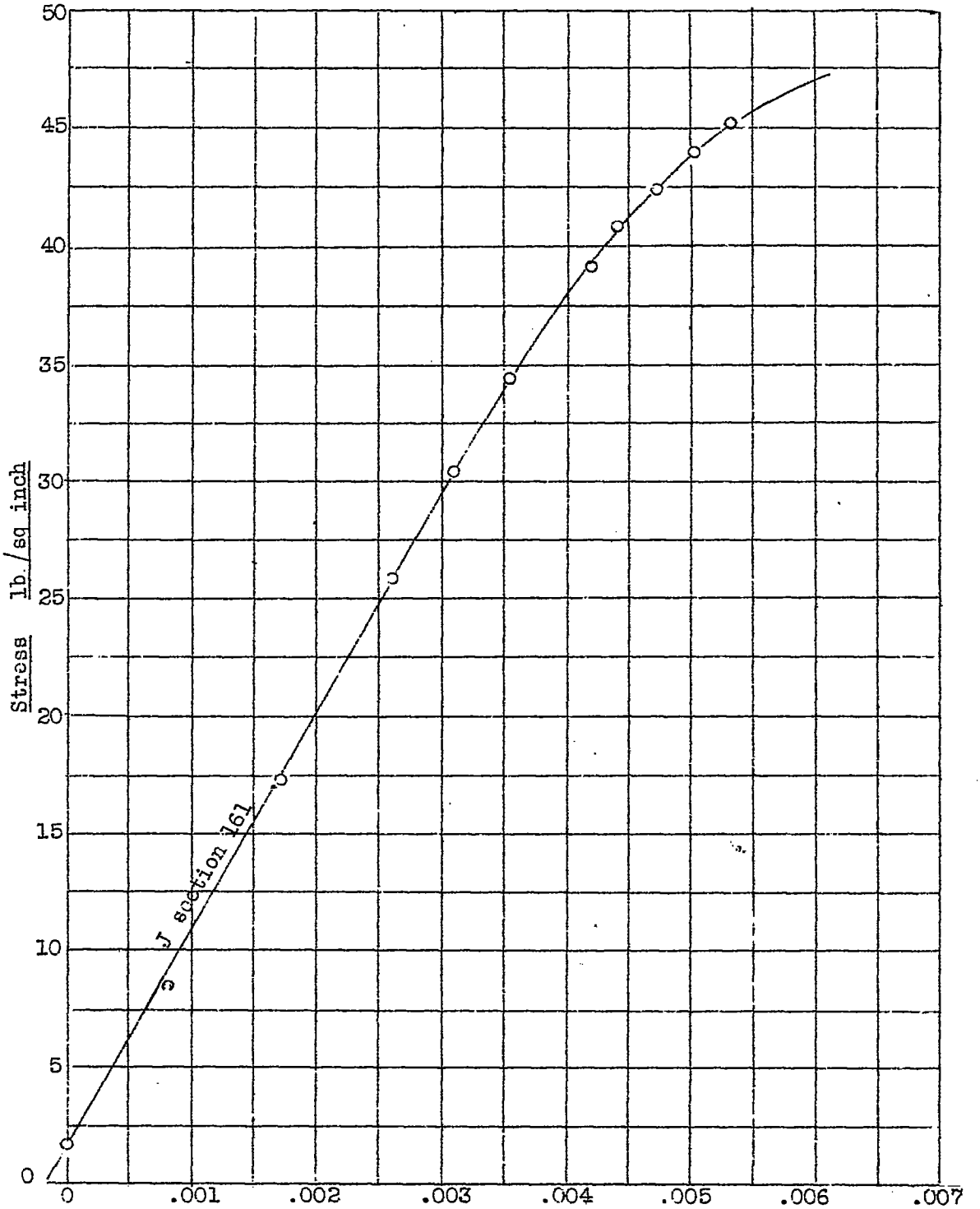
50
45
40
35
30
25
20
15
10
5
0
Stress lb./sq inch
0
.001
.002
.003
.004
.005
.006
.007
Unit strain
J section 161

Figure 41

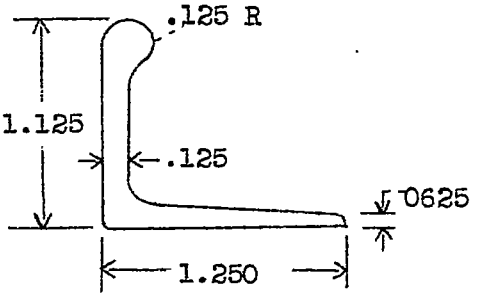

Bulb angle No. 8477

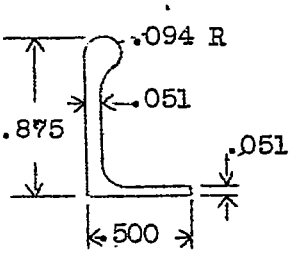

Bulb angle No. 10265

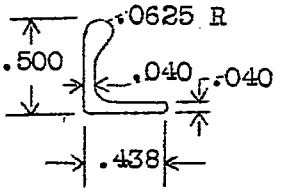

Bulb angle No. 1

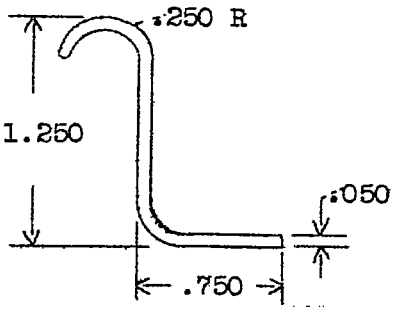

J section No. 161

Figure 42